e-Zine for meteor observers meteornews.net

MeteorNews

ISSN 2570-4745 VOL 8 / ISSUE 5 / SEPTEMBER 2023

The image was taken at the end of an all-night photo session at Bánd, Hungary
The tower in the foreground is the remnant of a 13. century castle, called Essegvár. (Esseg-castle).
A Nikon D5100 and a 10mm Sigma lens was used for capturing this image
(credit:Monika Landy-Gyebnar).

- Parent comet σ Hydrids
- 2023 Perseid surprises
- IAU Shower Database
- CAMS reports
- Radio meteor work
- Fireballs

Contents

The remarkable similarity of the orbit of C/2023 P1 Nishimura and the σ Hydrid meteor shower

John Greaves

Examination of meteor orbits from multiple publicly available databases when tested with D criteria reveal that many σ Hydrid meteors have orbits associated with that of the recently discovered C/2023 P1 Nishimura.

1 Introduction

CBET 5285[1] announced that a suspect comet had been confirmed as a true comet and gave particulars of its preliminary orbit. The orbit is a highly inclined one and thus suited for testing with D criteria with respect to orbital association with other objects as greatly inclined orbits usually follow a more random distribution such that "distance parameter" statistical testing is applicable. Meteor orbits from the following multiple publicly available databases, BRAMON, CAMS, CMN, EDMOND, GMN, SonotaCo and UKMON (in alphabetical order with source locations noted in the Acknowledgment section below) were tested against this preliminary orbit with both the Southworth and Hawkins (1963) and Jopek (1993) D criteria giving many matches to the meteor orbits with the orbit radiants and Solar Longitudes of the latter having a strong similarity to those of the σ Hydrid shower (McCrosky and Posen, 1961).

However, due to the then short orbital arc an elliptical orbit did not become available until later, and the present paper uses the currently latest updated elements based on 421 observations over a 17-day arc as published on August 28th 2023 in MPEC-Q150[2] and on August 29th 2023 in CBET 5290[3]. It should be noted that particulars of the shower noted in the latter are based on calculations of the current comet orbit as performed by Ye Quanzhi whilst the shower particulars in this paper are taken from the mean of the meteor orbits.

2 Results

The orbital elements for C/2023 P1 as per MPEC-Q150 as well as the mean elements derived from the analysis using both Jopek (D_J) and Southworth and Hawkins (D_{SH}) criteria are given in *Table 1*. For D_J 671 meteor orbits matched with values of 0.100 or less whilst 129 match for of 0.085 or less, the minimum value being 0.066. For D_{SH} a much larger number of 5456 meteors matched for their suggested threshold value of 0.150 or less with 2101 being of a value of 0.100 or less and the smallest value being 0.043. This discrepancy in scale can be explained in that Jopek (1993) states a tighter restriction upon assessing perihelia to make the search for new showers more rigorous relative to Southworth and Hawkins (1963). Here we have an established rather than new shower, albeit little mentioned in the literature.

It will be noted that the match with mean radiant positions and Solar Longitudes from the two criteria has an offset of a handful of degrees from literature values. The current orbital elements give the comet a period of about 500 years which is ample time for perturbational and YORP effects to have modified the orbits of the meteoroids somewhat, however such an analysis is beyond the remit of this paper. C/2023 P1 also has a quite small perihelion and at the time of writing it is also not clear whether nearer perihelion on 17th–18th September 2023 if there will be any outbursts or jets associated with the comet, however any dust ejected from the comet, which already sports a dust tail, will also be subject to fairly high levels of radiation pressure at perihelia.

The mean date of the meteors from these data from over the spread of the past 15 years is December 2nd (non-leap years).

Table 1 – Parameters for C/2023 P1 and for σ Hydrid meteors via both D_J and D_{SH}.

	RA (°)	DEC (°)	$\lambda_\odot$ (°).	v_g (km/s)	q (AU)	e	i (°)	ω (°)	Ω (°)
C/2023 P1	126-134	0-3	252.9	58–59	0.22516	0.99636	132.464	116.289	66.843
D_J mean	119.8	4.5	249.871	59.2	0.25426	0.98861	131.035	119.541	69.868
D_{SH} mean	121.2	3.8	251.111	59.1	0.26200	0.98383	130.390	118.791	71.109

[1] http://www.cbat.eps.harvard.edu/iau/cbet/005200/CBET005285.txt
[2] https://minorplanetcenter.net/mpec/K23/K23QF0.html
[3] http://www.cbat.eps.harvard.edu/iau/cbet/005200/CBET005290.txt

3 Conclusion

Examination of a large number of archival meteor orbits derived from multi-station surveys reveal that C/2023 P1 Nishimura is either the parent Comet for the σ Hydrid meteor shower or is at least strongly associated with any unknown parent comet that it has possibly disassociated from. When the mean orbital elements of the meteor orbits as seeded via the comet orbit are derived there is a slight offset in Solar Longitude and radiant position relative to the usual published values, however these are usually derived via radiant clustering algorithms, not D criteria between large numbers of orbits, which can be polluted via sporadic false positives. Nevertheless, there is a related very small but real offset in perihelion between meteor orbits and the comet orbit which may or may not be due to dispersion of meteoroids since the comet's last apparition roughly half a millennium ago.

Acknowledgment

The Minor Planet Center at the Harvard and Smithsonian Center for Astrophysics. The data sources and outline can be found online for the CAMS project[4], for GMN[5] , for SonotaCo[6], for UKMON[7]. Details of the EDMOND and some BRAMON data can be found online[8] . The URL of the orbital archives for the data from CMN, the Croatian Meteor Network, prior to its archiving its data with larger networks, could not be found.

References

Jopek T. J. (1993). "Remarks on the meteor orbital similarity D-criterion". *Icarus*, **106**, 603–607.

McCrosky R. E. and Posen A. (1961). "Orbital Elements of Photographic Meteors". *Smithson. Contrib. Astrophys.*, **4**,15–84.

Southworth R. R. and Hawkins G. S. (1963). "Statistics of meteor streams". *Smithson. Contrib. Astrophys.*, **7**, 261–286.

[4] http://cams.seti.org/
[5] https://globalmeteornetwork.org/data/
[6] https://www.astro.sk/iaumdcDB/home/PDA/SNMv3
[7] https://archive.ukmeteornetwork.co.uk/
[8] https://fmph.uniba.sk/en/microsites/daa/division-of-astronomy-and-astrophysics/research/meteors/edmond/

Unusual Perseid activity in 2023

Paul Roggemans

[1] **Pijnboomstraat 25, 2800 Mechelen, Belgium**
paul.roggemans@gmail.com

Two distinct peaks were observed before and after the annual Perseid maximum have been observed by video meteor cameras of the Global Meteor Network, at λ_O = 139.79 ± 0.04° and at λ_O = 140.69 ± 0.04°.

1 Introduction

In 2022 a paper has been published which describes how to compute meteor shower flux using Global Meteor Network data (Vida et al., 2022). Earlier this month (August 2023) a new tool was made available by Global Meteor Network to compute the real-time activity of meteor showers. Results are released on a new web page on the GMN site[9]. The data shown is produced by combining observations from all cameras that are added to the pipeline, regardless of whether they are paired with another camera or not.

In 2021 the Perseids displayed an unexpected outburst at solar longitude 141.474 ± 0.005° over the North American continent on August 14, 2021 (Jenniskens, 2021; Jenniskens & Miskotte, 2021; Miskotte et al., 2021). Strong Perseid activity had been noticed at this solar longitude by visual observers some years before like in 2018 (Gaarder, 2018; Miskotte, 2019), in 2019 (Vandeputte, 2019; Miskotte & Vandeputte, 2020) and in 2020 (Miskotte, 2020; 2021).

2 The 2023 Perseid surprise

According to preliminary 2023 data a secondary Perseid peak appeared about one day after the long term Perseid maximum at solar longitude 140° in the meteor shower flux monitoring (*Figure 1*). Initially it was not clear whether or not this was related to the dust trail that caused the 2021 peak. Radio observations reported online by the International Project for Radio Meteor Observations[10] website clearly show multiple peaks (see *Figure 2*).

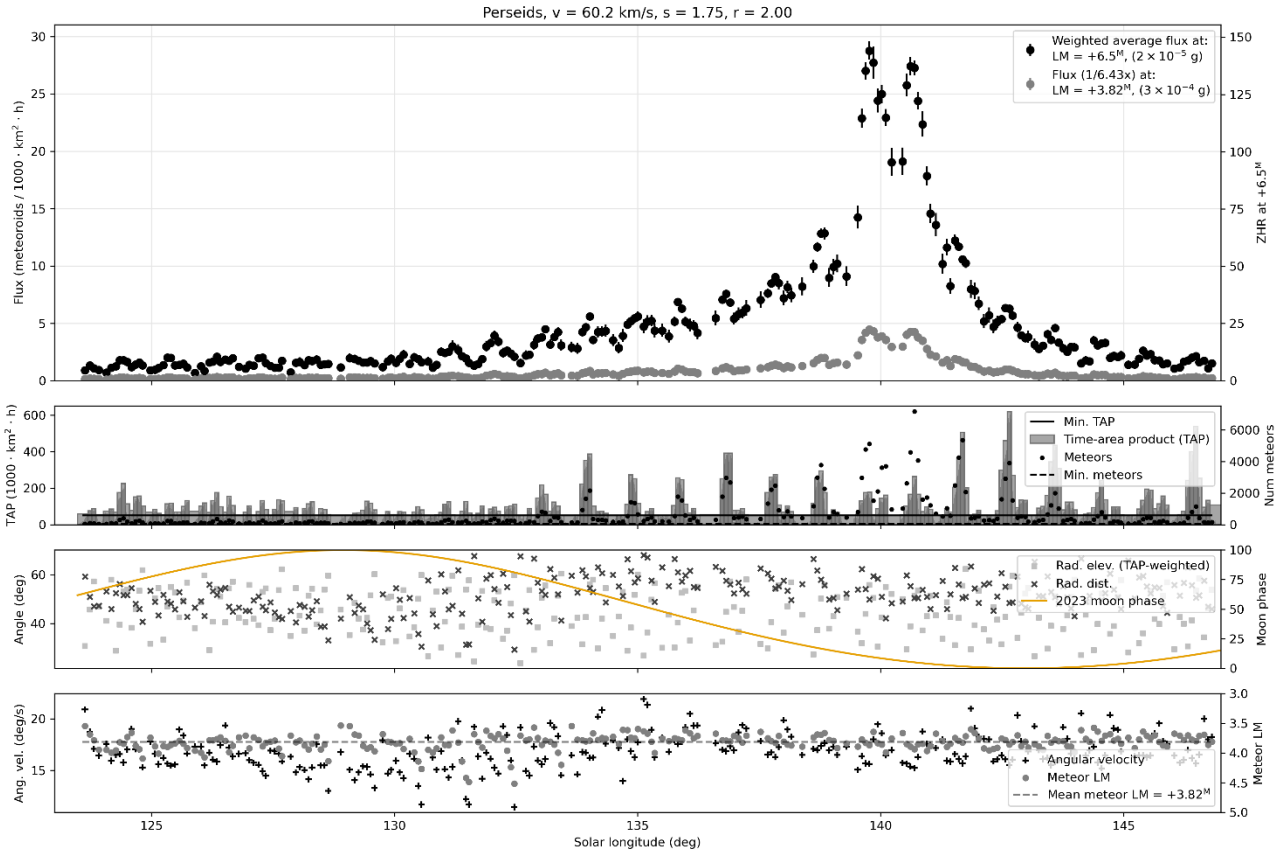

Figure 1 – The Perseids activity according to the meteor shower flux monitoring of the Global Meteor Network.

[9] https://globalmeteornetwork.org/flux/

[10] www.iprmo.org

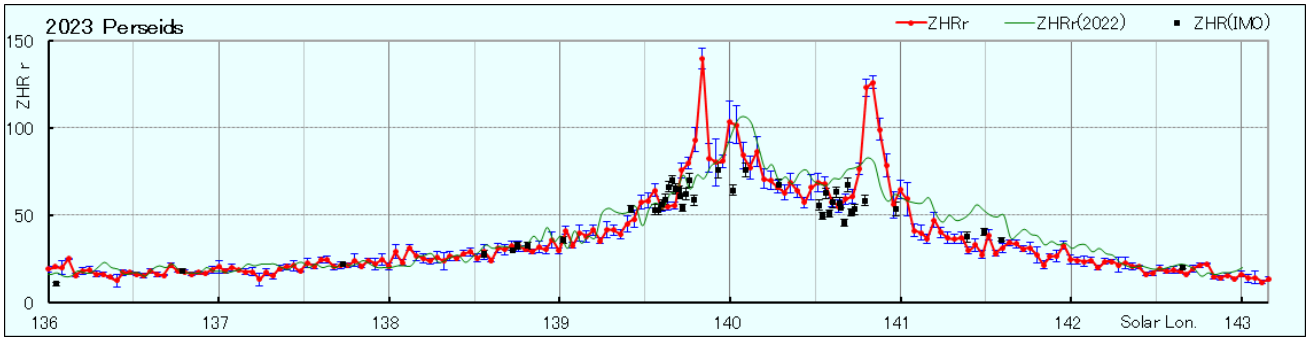

Figure 2 – Radio meteor activity according to The International Project for Radio Meteor Observations (Hirofumi Sugimoto).

3 A closer look at the flux profile

Hiroshi Ogawa published a more detailed radio activity profile revealing three maxima (Sugimoto and Ogawa, 2023). Meanwhile all camera data has been uploaded and reduced for the flux profile. The resolution of the video data flux profile is less detailed than that of the radio meteor observations but I could derive the following details from the graph:

- First peak at $\lambda_\odot = 139.79 \pm 0.04°$
- Second peak at $\lambda_\odot = 140.69 \pm 0.04°$

The theoretical annual Perseid maximum is rather broad and centered at $\lambda_\odot = 140°$, which is halfway at a dip between the above-mentioned peaks and does not emerge distinctly in the flux profile. It looks like Earth crossed additional dust trails before and after the main maximum which added extra activity on the ascending wing and on the descending wing of the broad annual Perseid activity, creating two extra peaks before and after the annual peak.

Peter Jenniskens (2006) predicted the crossing of a filament in 2023, 0.0074 AU from the Earth orbit at $\lambda_\odot = 139.83 \pm 0.2°$ which could explain the first peak. Jérémie Vaubaillon predicted a possible increased activity on August 14 between 1^h and 2^h45^m UTC ($\lambda_\odot = 140.74°$) when Earth was expected to cross a dust trail released by the parent comet Swift-Tuttle in the year 68 BC. This could explain the second peak. The flux profile shows a shoulder at about $\lambda_\odot = 141.54°$ which may be a trace of a concentration that caused the 2021 Perseid outburst at this solar longitude. This shoulder is not confirmed by the radio observations.

4 Conclusion

The 2023 Perseid activity profile was characterized by multiple peaks probably caused by the transit of a filament at $\lambda_\odot = 139.83 \pm 0.2°$ as predicted by Jenniskens (2006) and a dust trail at $\lambda_\odot = 140.74°$ as predicted by Vaubaillon.

References

Gaarder K. (2018). “2018 Perseid expedition to Crete”. *eMetN*, **3**, 263–266.

Jenniskens P. (2006). Meteor showers and their parent comets. Cambridge.

Jenniskens P. and Miskotte K. (2021). “Perseid meteor outburst 2021”. *eMetN*, **6**, 460–461.

Jenniskens P. (2021). “Perseid meteor shower outburst 2021”. CBET 5016, 2021 August 14, editor D.W.E. Green.

Miskotte K. (2019). “The Perseids in 2018: Analysis of the visual data”. *eMetN*, **4**, 135–142.

Miskotte K. and Vandeputte M. (2020). “Perseids 2019: another peak in activity around solar longitude 141.0?”. *eMetN*, **5**, 25–29.

Miskotte K. (2020). “Perseids 2020: again, enhanced Perseid activity around solar longitude 141?”. *eMetN*, **5**, 395–397.

Miskotte K. (2021). “Perseids 2020 revisited”. *eMetN*, **6**, 29–30.

Miskotte K., Sugimoto H. and Martin P. (2021). “The big surprise: a late Perseid outburst on August 14, 2021!”. *eMetN*, **6**, 517–525.

Sugimoto H. and Ogawa H. (2023). “Perseids 2023 by worldwide radio meteor observations”. *eMetN*, **8**, 285–287.

Vandeputte M. (2019). “Perseid campaign at Aubenas Les Alpes, Haute Provence”. *eMetN*, **4**, 83–88.

Vida D., Blaauw Erskine R.C., Brown P.G., Kambulow J., Campbell-Brown M., Mazur M.J. (2022). “Computing optical meteor flux using Global Meteor Network data”. *Monthly Notices of the Royal Astronomical Society*, **515**, 2322–2339.

Perseids 2023 by worldwide radio meteor observations

Hirofumi Sugimoto[1] **and Hiroshi Ogawa**[2]

[1] **The Nippon Meteor Society**
hiro-sugimoto@kbf.biglobe.ne.jp

[2] **The International Project for Radio Meteor Observations**
h-ogawa@amro-net.jp

Radio meteor observations in the world detected two unexpected peaks in the Perseid activity profile of 2023 before and after the annual peak around $\lambda_\odot = 140.00°$. One peak occurred at $\lambda_\odot = 139.84°$ (August 13, 3^h30^m UT) with an estimated $ZHR_r = 139$ (Activity Level Index (AL) = 1.9). Although this peak corresponds with a prediction for the encounter of a weak filament, it was so weak that it was not sure. Another peak was observed at $\lambda_\odot = 140.84°$ (August 14, 04^h30^m UT) with $ZHR_r = 126$ (AL = 1.6). It is possible that this peak was caused by an old dust trail which was released in 68BC, but it appeared later than expected in the prediction or it related to the secondary peak which was detected in previous years between $\lambda_\odot = 140.5°$ and 141.6°.

1 Introduction

The Perseids are one of the best meteor showers in a year. The shower reaches a maximum with a $ZHR = 100$ at $\lambda_\odot = 140.0°$ for visual observers (Rendtel 2022).

Radio Meteor Observation is also able to obtain a complete activity profile. In past research, activity profiles were derived from worldwide radio data from Radio Meteor Observation Bulletin (RMOB). As a result, The International Project for Radio Meteor Observations (IPRMO) which is organized to analyze a complete meteor shower activity without problems with radiant elevation and unstable weather, concluded that the peak of the Perseids occurred at $\lambda_\odot = 140.0°$ with FWHM (Full Width of Half Maximum) = –0.7°/+0.8° and a peak Activity Level of 1.2 (Ogawa, 2022).

Another peak was detected between $\lambda_\odot = 140.5°$ and $\lambda_\odot = 141.6°$ in recent years (Miskotte & Vandeputte, 2020; Miskotte, 2020; Miskotte et al., 2021). Besides, a surprisingly strong peak was observed at $\lambda_\odot = 141.5°$ in 2021 (Miskotte et al., 2021). The cause of this post maximum peak has not been clarified yet.

For 2023, the Meteor Shower Calendar published by the International Meteor Organization (IMO) described a possible encounter with a very old trail released in 68 BC at $\lambda_\odot = 140.74°$ and a weak filament at $\lambda_\odot = 139.83°$ (Rendtel, 2022). A secondary peak was observed around $\lambda_\odot = 141°$ using Global Meteor Network (GMN) data (Roggemans, 2023). This paper reports the result for the Perseids 2023 using worldwide radio meteor observations.

2 Method

For analyzing the worldwide radio meteor observation data, the meteor activity is calculated by the "Activity Level Index: AL(t)" (Ogawa et al., 2001) and the estimated Zenithal Hourly Rate: ZHR_r(t) (Sugimoto, 2017). The activity profile was estimated using the Lorentz activity profile (Jenniskens et al., 2000).

3 Results

Figure 1 shows the result of an estimated ZHR_r in 2023. Three significant peaks were observed in this year. The first peak occurred at $\lambda_\odot = 139.84°$ (August 13, 3^h30^m UT). The estimated peak reached $ZHR_r = 139$ ($AL = 1.9$). A secondary peak was observed at $\lambda_\odot = 140.00°$ (August 13, 07^h30^m UT) with $ZHR_r = 103$ ($AL = 1.4$). Finally, a third peak which had $ZHR_r = 126$ ($AL = 1.6$) at $\lambda_\odot = 140.84°$ (August 14, 04^h30^m UT) was detected. *Table 1* shows the three detected peaks in estimated ZHR_r and Activity Level Index.

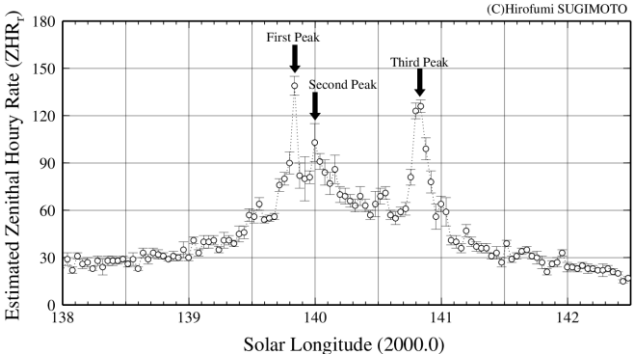

Figure 1 – Estimated ZHR_r using 39 datasets worldwide.

Table 1 – The three detected peaks.

Peak Time(UT)	$\lambda_\odot$(˚)	ZHR_r	Activity Level
Aug 13 03^h30^m	139.84	139±6	1.9±0.4
Aug 13 07^h30^m	140.00	103±12	1.4±0.4
Aug 14 04^h30^m	140.84	126±4	1.6±0.3

4 Discussion

4.1 Comparing with the average of the past

Figure 2 compares the results between the Activity Level in 2023 and the average in the past during the period 2001–2022. The first and third peaks are not visible in the average of the past, but the second peak was very similar to the maximum in the past. Therefore, the first and third peaks represent unusual activity in 2023.

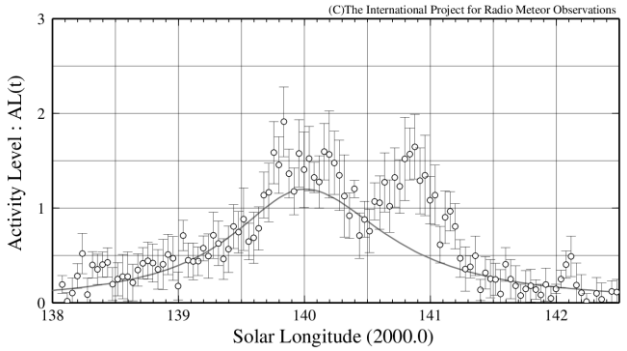

Figure 2 – The Activity Level Index: Comparing the average from the past (gray line) to the Activity Level Index in 2023. (circles with error: 2023).

4.2 How to explain the three peaks?

Figure 3 shows that the Activity Level Index of the Perseids 2023 displayed three components by using the Lorentz profile. *Table 2* shows the estimated components and some references.

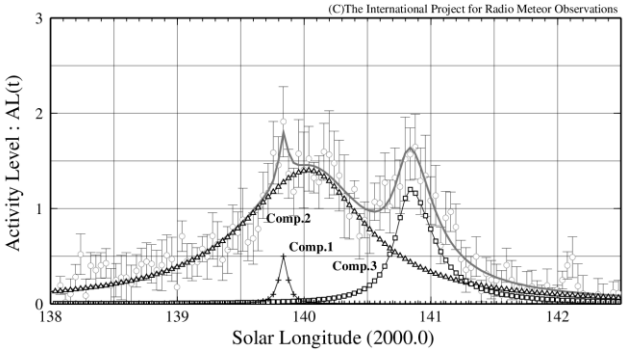

Figure 3 – The Activity Level Index: the estimated components using the Lorentz Profile (solid line: Comp1+Comp2+Comp3).

4.2.1 Component 1

The first peak represents a component (Comp.1) which had $AL(\max) = 0.5$ at $\lambda_\odot = 139.84°$ (August 13, 3^h30^m UT). Jenniskens (2006) described that a weak filament encountered the Earth at $\lambda_\odot = 139.83° \pm 0.2°$. Although the first peak seems to fit with the forecast, it was difficult to conclude that this was the encounter with the small filament because this peak had a very small activity level and a narrow FHWM.

4.2.2 Component 2

It is possible that the second peak (Comp.2) represents the main peak from the past activity. Using the Lorentz profile this component was estimated with $AL(\max) = 1.4$ at $\lambda_\odot = 140.04°$ (August 13, 8^h30^m UT).

4.2.3 Component 3

The third peak had its maximum with $AL(\max) = 1.2$ at $\lambda_\odot = 140.84°$ (August 14, 4^h30^m UT) (Comp.3). According to Vaubaillon as mentioned in the Meteor Shower Calendar published by IMO that a very old dust trail released in 68 BC may be encountered around $\lambda_\odot = 140.74°$ (between 01^h and 02^h45^m UT on August 14). Although the observed enhancement in activity was later than this prediction, it is possible that this activity was caused by this old trail.

However, on the other hand, it is also possible that this third peak is related to the secondary peak around $\lambda_\odot = 140.5°$–$141.6°$ which was observed in previous years.

It is very difficult to know whether or not an old dust trail and an unexpected peak activity are somehow related to the secondary peak observed in past years.

5 Conclusion

Radio meteor observations in the world observed three peaks during the Perseids 2023 and these could be identified as three different components. Comp.1 was the first peak with a modest and short activity at $\lambda_\odot = 139.84°$. Comp.2 represents the annual activity peak at $\lambda_\odot = 140.04°$. Comp.3 was the third peak at $\lambda_\odot = 140.84°$.

Although worldwide radio meteor observations succeeded to detect three peaks, it remains very difficult to explain the cause of these enhancements, except for Comp.2.

Table 2 – The estimated components using the Lorentz profile and some references.

	Radio Results by IPRMO				References		
	Peak Time (UT)	$\lambda_\odot$	FWHM (hours)	Peak Level (AL)	Peak Time (UT)	$\lambda_\odot$	Source
Comp.1	Aug 13 03^h30^m	139.84°	–1.0/+1.0	0.5 ($ZHR_r = 55$)	Aug 13, 03^h	139.83°	P.Jenniskens
					Aug 13, 7^h30^m	140.0°	annual
Comp.2	Aug 13 08^h30^m	140.04°	–16.0/+13.5	1.4 ($ZHR_r = 90$)			
					Aug 14, 1^h – 2^h45^m	140.74°	J. Vaubaillon
Comp.3	Aug 14 04^h30^m	140.84°	–3.5/+1.5	1.2 ($ZHR_r = 85$)			

Acknowledgment

The worldwide data were provided by the Radio Meteor Observation Bulletin (RMOB). The following observers provided data:

Chris Steyaert (Belgium), *Felix Verbelen* (Belgium), *Johan Coussens* (Belgium), *FLZ-R0* (Czech Republic), *SVAKOV-R12* (Czech Republic), *VALMEZ-R1* (Czech Republic), *ZEBRAK-R5* (Czech Republic), *Frederic Lucas* (France), *Jacques Molne* (France), *Philippe Rainard* (France), *DanielD SAT01_DD* (France), *Pierre Terrier* (France), *Istvan Tepliczky* (Hungary), *GABB.IT* (Italy), *Romano Serra* (Italy), *AAV Planetario di Venezia* (Italy), *Filzi School Observatory D12* (Italy), *Mario Bombardini* (Italy), *Hirofumi Sugimoto* (Japan), *Hironobu Shida* (Japan), *Hiroshi Ogawa* (Japan), *Kenji Fujito* (Japan), *Masaki Kano* (Japan), *Masaki Tsuboi* (Japan), *Minoru Harada* (Japan), *Nobuo Katsura* (Japan), *Norihiro Nakamura* (Japan), *Rainer Ehlert* (Mexico), *Salvador Aguirre* (Mexico), *MAR JEN* (Poland), *Rafael Martinez* (Puerto Rico), *Esteban Reina* (Spain), *Ian_Evans* (United Kingdom), *Philip Norton* (United Kingdom), *Philip NortonVert* (United Kingdom), *Philip Rourke* (United Kingdom), *Tracey Harty* (United Kingdom), *Eric Smestad_KC0RDD* (United States of America), *Stan Nelson* (United States of America).

We wish to thank *Pierre Terrier* for developing and hosting rmob.org. A very special thank you to Paul Roggemans for proofreading this article.

References

Jenniskens P., Crawford C., Butow S. J., Nugent D., Koop M., Holman D., Houston J., Jobse K., Kronk G., and Beatty K. (2000). “Lorentz shaped comet dust trail cross section from new hybrid visual and video meteor counting technique imprications for future Leonid storm encounters”. *Earth, Moon and Planets*, **82–83**, 191–208.

Miskotte K. and Vandeputte M. (2020). “Perseids 2019: another peak in activity around solar longitude 141.0?”. *eMetN*, **5**, 25–29.

Miskotte K. (2020). “Perseids 2020: again, enhanced Perseid activity around solar longitude 141?”. *eMetN*, **5**, 395–397.

Miskotte K., Sugimoto H. and Martin P. (2021). “The big surprise: a late Perseid outburst on August 14, 2021!”. *eMetN*, **6**, 517–525.

Ogawa H., Toyomasu S., Ohnishi K., and Maegawa K. (2001). “The Global Monitor of Meteor Streams by Radio Meteor Observation all over the world”. In, Warmbein Barbara, editor, Proceeding of the Meteoroids 2001 Conference, 6-10 August 2001, Swedish Institute of Space Physics, Kiruna, Sweden. ESA Publications Division, European Space Agency, Noordwijk, The Netherlands, 189–191.

Ogawa H. (2022). “Long-Term Studies of Major and Daytime Meteor Showers using Worldwide Radio Meteor Observations”. *WGN, Journal of the IMO*, **50**, 148–157.

Rendtel J. (2022). “2023 Meteor Shower Calendar”. International Meteor Organization

Roggemans P. (2023). “Second Perseid peak at S.L. 141° confirmed in 2023”. *eMetN*, **8**, 283–284.

Sugimoto H. (2017). “The new method of estimating ZHR using Radio Meteor Observations”. *eMetN*, **2**, 109–110.

Remaining problems in IAUMDC Shower Database (SD)

Masahiro Koseki

The Nippon Meteor Society, 4-3-5 Annaka Annaka-shi, Gunma-ken, 379-0116 Japan
geh04301@nifty.ne.jp

Although the Shower Database (SD) has improved, it still has many problems. #0340TPY has two different activities, #0165SZC also has two different activities and, moreover, one that is observed by video well should be classified as #0370MIC. Many other problems stem from the fact that meteor showers are not judged statistically, an example being the confusion of minor meteor showers near the ANT. Taurids are divided into small parts, and #0096NCC and #0097SCC have established status though they could not be distinguished from the background activity. MDC accepts generally requests based on peer-reviewed journals as they are, and reviewers and authors need to be careful not to cause further confusion in the SD. Even if published in a peer-reviewed journal, the MDC should not accept separate reports of radiant shifts and juxtaposition of possible interpretations.

1 Introduction

IAU Meteor Data Center[11] has improved the Shower Database (SD) in recent years (Hajduková et al., 2023; Jopek et al., 2023). Although simple typographic errors and entries without certain references or without enough data are rejected and provisional numbers have also been introduced to avoid further confusion, there remain several problematic entries. This paper outlines the remaining issues and points out what we should keep in mind to avoid further confusion in the SD; we use the version downloaded on March 29, 2023.

2 Simple double booking

We pointed out that theta-Pyxidids(#0340TPY), September Lyncids (#0081SLY), Microscopiids (#0370MIC) / Southern June Aquilids ((#0165SZC), and phi-Piscids (#0372PPS) have two different activities (Koseki, 2021). Here, we will reconfirm them and consider measures to prevent such problems from occurring. We use video data from Global Meteor Network (Vida et al., 2019; 2020; 2021) and CMOR radar view from 'Radar Meteor Radiants' (CMOR)[12].

2.1 theta-Pyxidids (#0340TPY)

Figure 1 shows the radiant distribution of #0340TPY centered at (λ–$\lambda_\odot$, β) = (261.2, –36.3) for the period of $\lambda_\odot$ = 248°~268°. Two concentrations on the inner circle are two TPY activities; the lower one is TPY00 and the upper TPY01/02. It is clear that TPY is a mixture of these two activities. We published details on the two TPYs before (Koseki, 2021) and to avoid duplication, no further discussion is given here.

Both TPY01 and TPY02 are based on CAMS' video observations (Jenniskens et al., 2016b) and the two activities were confused due to their careless identification. In principle, the MDC has a system in place to accept shower entrees for registration that have been published in peer-reviewed journals. Therefore, caution is required on the part of both authors and reviewers to avoid such confusion.

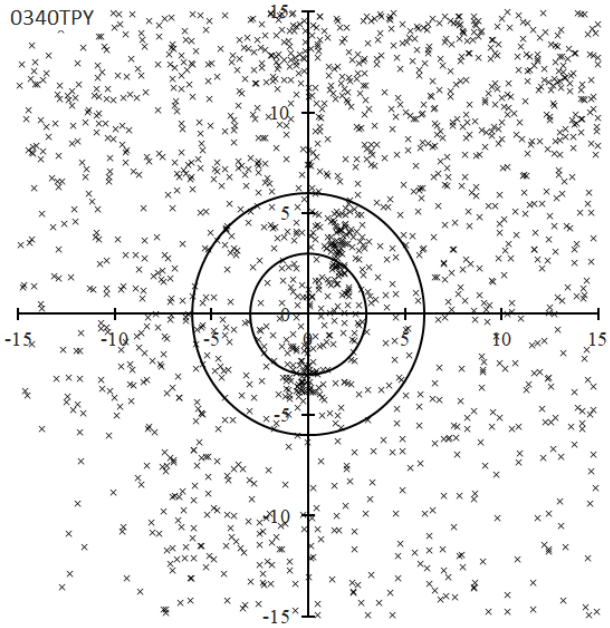

Figure 1 – Radiant distribution centered at (λ–$\lambda_\odot$, β) = (261.2, –36.3) for the period of $\lambda_\odot$ = 248~268°. The lower one is TPY00 and the upper TPY01/02.

2.2 September Lyncids (#0081SLY)

The book "*Meteor Showers and their parent comets*" (Jenniskens, 2006)[13], that is the prototype for the SD uses different observations for the September Lyncids and the SLY entry has been in its current form since 2015. *Figure 2* shows the radiant distribution of #0081SLY centered at (λ–$\lambda_\odot$, β) = (287, 29) for the period of $\lambda_\odot$ = 167°~187°. The concentration upper left is SLY00 and the lower right is SLY01. Though SLY01 is somewhat blurry, SLY00 is clearly distinct from it. Molau and Rendtel who reported

[11] IAU Meteor Data Center: https://www.ta3.sk/IAUC22DB/MDC2022/
[12] Radar Meteor Radiants (CMOR): https://fireballs.ndc.nasa.gov/cmor-radiants/
[13] http://www.astro.sk/~ne/IAUMDC/STREAMLIST/meteoroidstreamworkinglist.pdf

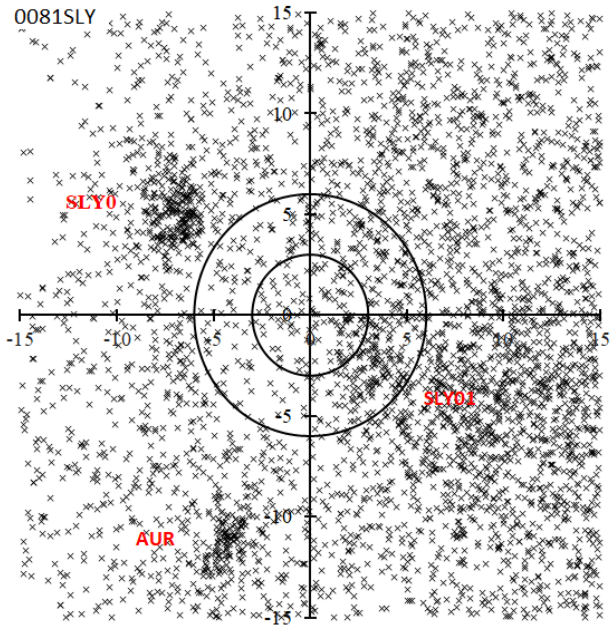

Figure 2 – Radiant distribution centered at (λ–$\lambda_\odot$, β) = (287, 29) for the period of $\lambda_\odot$ = 167~187. The concentration upper left is SLY00 and the lower right is SLY01.

both SLY00 and SLY 01 themselves wrote, "*81 SLY is found not only in the short interval listed in Table 6 (*SLY01) but was detected automatically by the standard procedure (*SLY00)*" (Molau and Rendtel, 2009); * is citation's note. They were not sure that there are two different activities then because they used single-station video observations and were cautious about making judgments in areas with high background activity. We showed that these are different activities by using multi-station video data (Koseki, 2021).

2.3 Microscopiids (#0370MIC) / Southern June Aquilids (#0165SZC)

#0165SZC should be divided into two showers; one is the original SZC detected by radar and the other one detected by video observations is the misidentification of #0370MIC. *Figure 3* shows CMOR observations in 2022 and the activity of SZC is short and clearly distinguished from MIC with an interruption. The radiant distribution for each corresponding period by video observations clearly shows that the original SZC is difficult to detect by video observations and MIC is compatible with video

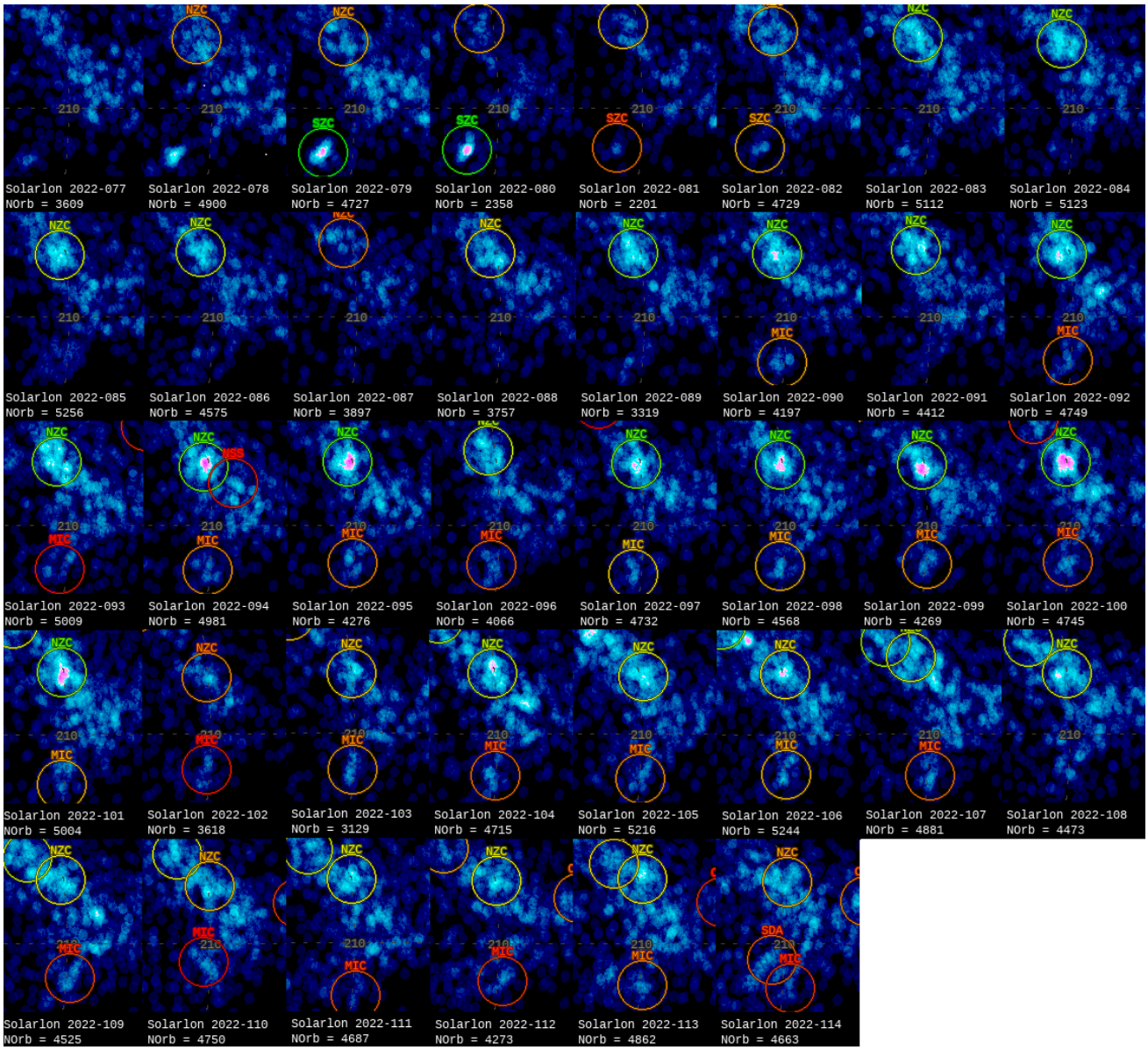

Figure 3 – CMOR radar plots from 'Radar Meteor Radiants' (CMOR) in 2022 for the period of $\lambda_\odot$ = 77°~114°.

observation. Jenniskens et al. (2016a) linked video observations to SZC and since then observations that should have been MIC have been registered as SZC following their example: SZC04 (Shiba, 2022). We listed this video activity as SZC in a previous paper (Koseki, 2021) considering the use by readers but added "*We should call this activity MIC instead of SZC*".

2.4 phi-Piscids (#0372PPS)

Although #372PPS is classified as established, the peak activity at the longitude of the Sun differs largely from $\lambda_\odot = 94°$ to $\lambda_\odot = 106°$. We hypothesized that PPS might consist of two activities (Koseki, 2021). We divide the activity into two periods shown in *Table 1* and study least square analysis. The estimated radiant drifts confirm the former conclusion; one moves upward-sloping and the other downward-sloping (*Figure 4a* to *4c*). PPS_A and PPS_B in *Figure 4a-c* are extrapolated ranges calculated based on *Table 1*. Both overlap around $\lambda_\odot = 100$~$105°$, but

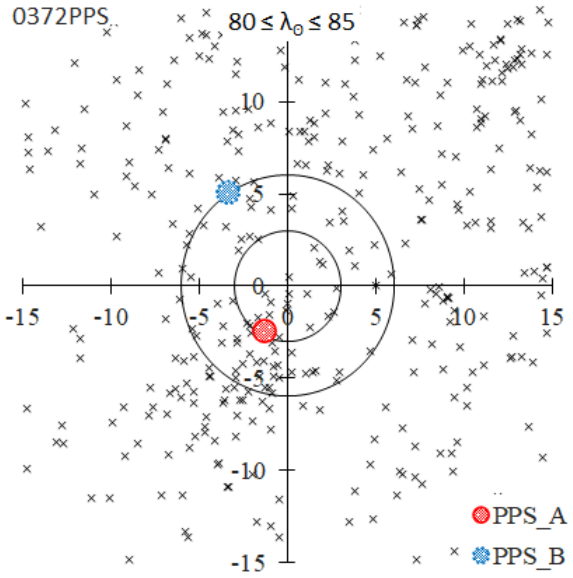

Figure 4a – Two possible PPS activities. Radiant distribution centered at (λ–$\lambda_\odot$, β) = (281.71°, 14.47°), for $\lambda_\odot$ = 80°–85°.

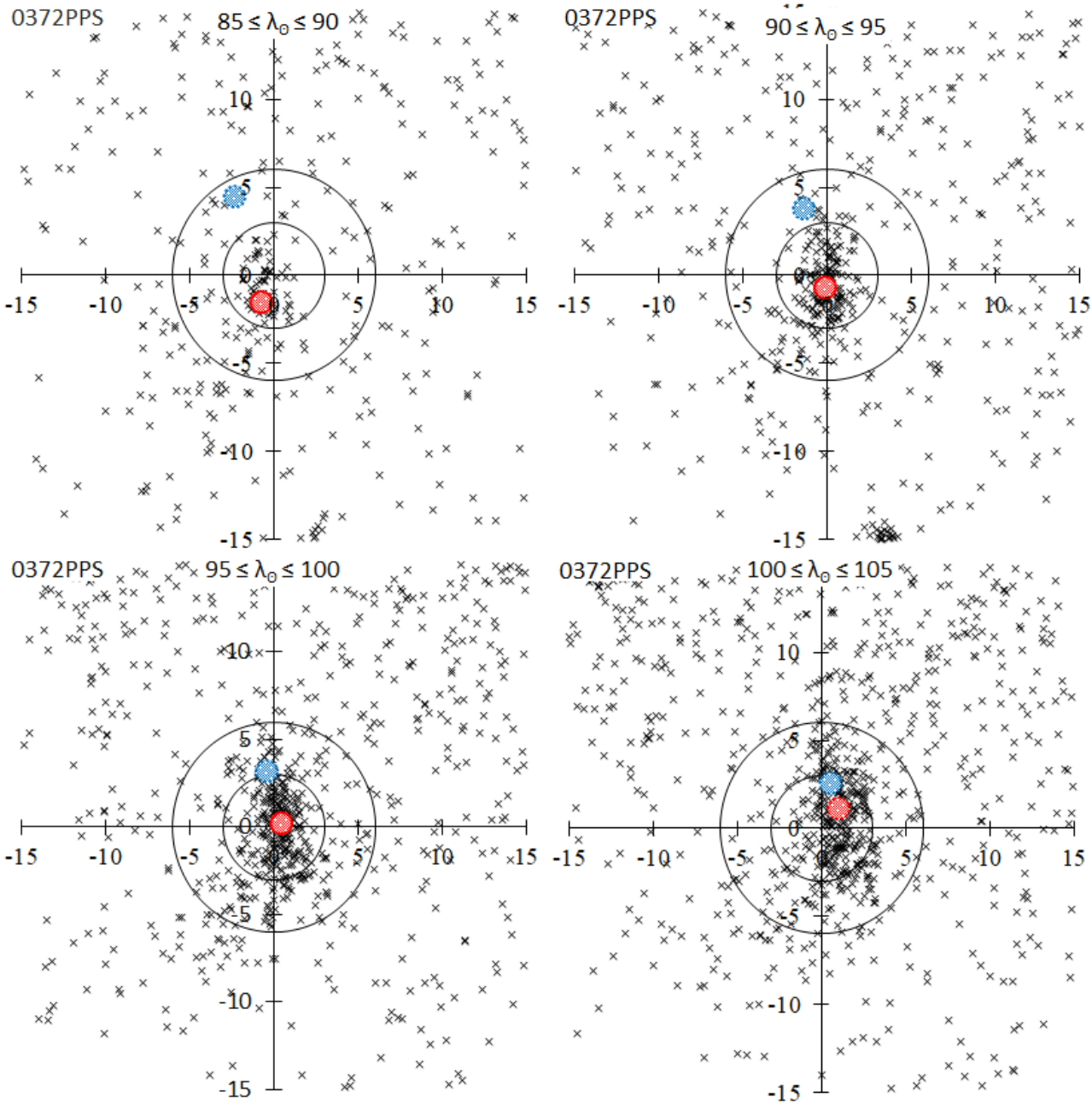

Figure 4b – Two possible PPS activities. Radiant distribution centered at (λ–$\lambda_\odot$, β) = (281.71°, 14.47°), for $\lambda_\odot$ = 85°–90° to 100°–105°.

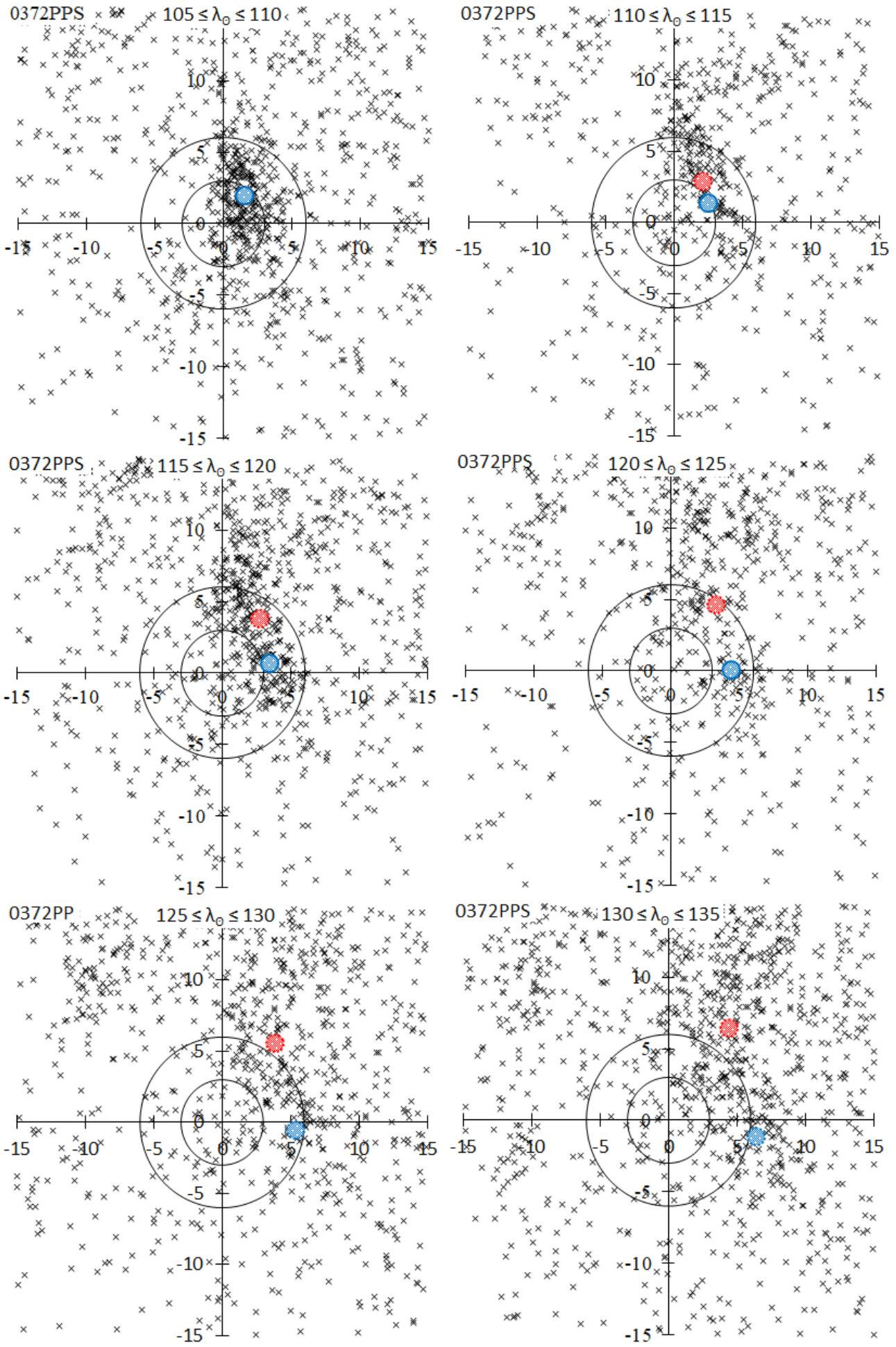

Figure 4c – Two possible PPS activities. Radiant distribution centered at (λ–λ_O, β) = (281.71°, 14.47°), for λ_O = 105°–110° to 130°–135°.

Table 1 – Search basis for two possible PPS activities.

$\lambda_\odot$	$\lambda-\lambda_\odot$	β	r	$\Delta\lambda_\odot$	N	
PPS_A	90	283.5	16	3	10	463
PPA_B	115	280	16	3	10	434

it should be noted that PPS_A and PPS_B represent the respective movements before and after this, and the extrapolated part is only an estimate. We could suggest that #0372PPS has two activities though not so clear because #0372PPS locates amid the apex meteor activity, and, therefore, we should be careful to study meteor activities that are surrounded by active sporadic backgrounds whether they are the established ones or not.

Brown et al. (2010) detected PPS firstly by radar, but their recent CMOR observations (2018–2022) scarcely marked its activity; one is at $\lambda_\odot = 106°$ in 2018 and the other is at $\lambda_\odot = 104°$ in 2019. #0382PPS might only stand out sometimes from Apex activity and may not be recognized every year by radar observations.

3 Segmentation of long-lived shower

3.1 Taurids

Figures 5a~5q show the meteor activities around ($\lambda-\lambda_\odot$, β) = (180°, 0°) from $\lambda_\odot = 160°$ to $\lambda_\odot = 320°$ with a step of $\Delta\lambda_\odot = 10°$, accompanied by the radiant distributions of the SD showers and with their reference tables. It can be seen from the figures that the start and end of the Taurids have not been clearly defined; boundaries between preceding and following activities are unclear.

Several researchers divided Taurids into sub-showers (see accompanying figures and tables). We pointed out that 'Taurids' would be clumsily decomposed (Koseki, 2018, 2023) if we applied the classification proposed by Jenniskens et al. (2016a). We revealed that #0002STA consists of two components; one is STA_SE the steady expression and the other is STA_SF the sharply fluctuating component (Koseki, 2020a); we could observe two peaks of #0002STA around $\lambda_\odot = 202.6°$ and $\lambda_\odot = 221.5°$.

On the other hand, there are also large differences within STA; 12 observations are listed in #0002STA, but there is an abnormal gap in the average value of the Sun's longitude $\lambda_\odot$ in the SD: averaged ecliptic longitude of the Sun at the shower activity, (J2000, deg). It used to be the value at the maximum, but now it is expressed as the average value. In general, even the average value does not deviate greatly from the value at the maximum, and the difference in the values posted in the SD, $\lambda_\odot = 196°$~$265.1°$, is too large. We will discuss this issue later.

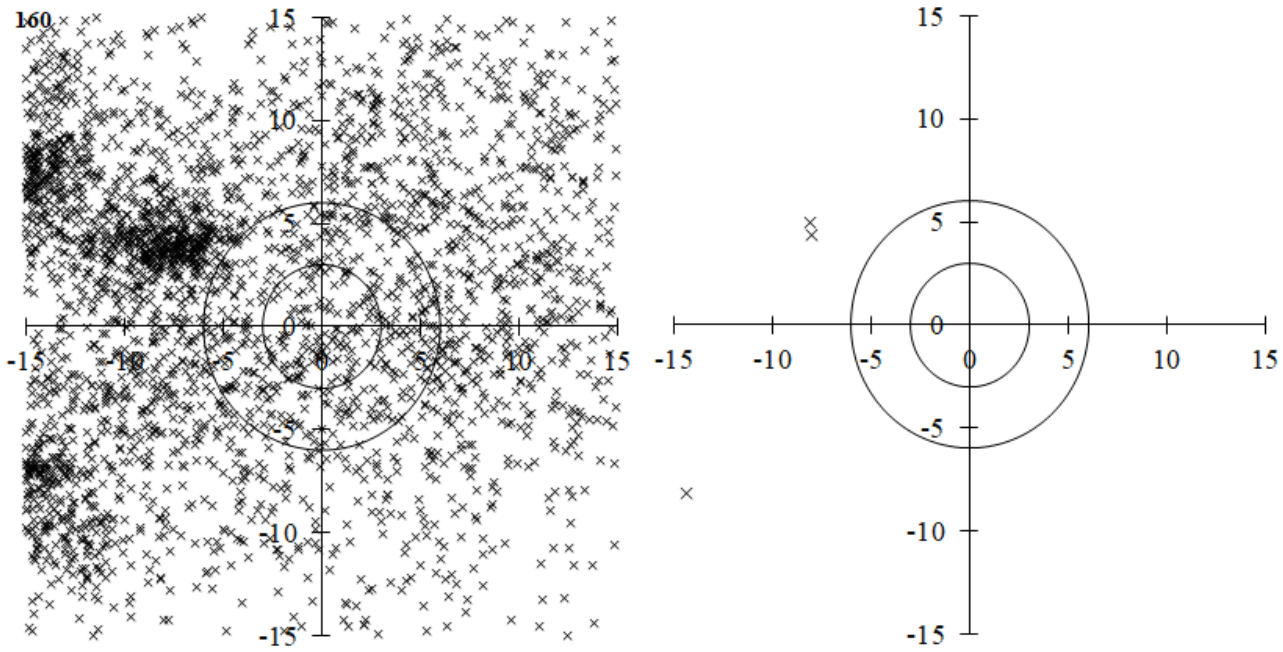

Figure 5a – Meteor activities around ($\lambda-\lambda_\odot$, $\lambda_\odot$) = (180°, 0°) at $\lambda_\odot = 160°$, radiant distribution of video meteors left, radiant distribution according to the SD reference.

Table 2a – Explanation of the SD radiants listed around ($\lambda-\lambda_\odot$, $\lambda_\odot$) = (180°, 0°) at $\lambda_\odot = 160°$.

Code	$\lambda_\odot$	$\lambda-\lambda_\odot$	β	v_g	*Distance*	*Angle*	x	y
0033NIA03	159	198.1	5.0	28.7	9.51	59	-8.11	4.97
0033NIA02	159.5	198.0	4.3	28.6	9.11	61	-8.00	4.35
0642PCE00	161	204.4	-8.1	36.5	16.51	120	-14.32	-8.21

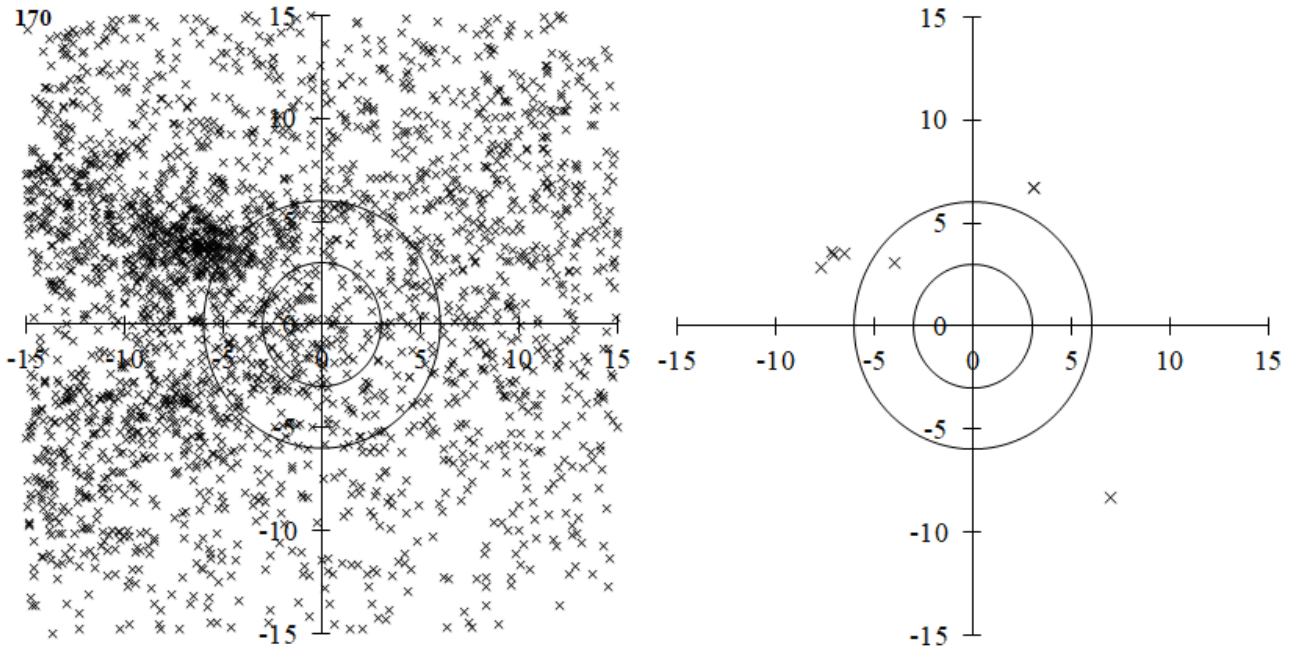

Figure 5b – Meteor activities around (λ–$\lambda_\odot$, $\lambda_\odot$) = (180°, 0°) at $\lambda_\odot$ = 170°, radiant distribution of video meteors left, radiant distribution according to the SD reference.

Table 2b – Explanation of the SD radiants listed around (λ–$\lambda_\odot$, $\lambda_\odot$) = (180°, 0°) at $\lambda_\odot$ = 170°.

Code	$\lambda_\odot$	λ–$\lambda_\odot$	β	v_g	*Distance*	*Angle*	*x*	*y*
0033NIA07	166.9	197.2	3.6	29.7	8.00	63	-7.15	3.59
0898SGP00	166.9	186.9	6.7	32.1	7.43	335	3.14	6.73
0898SGP00	166.9	186.9	6.7	32.1	7.43	335	3.13	6.73
0215NPI00	168.3	194.0	3.1	27.4	5.03	52	-3.96	3.10
0215NPI02	173.3	196.5	3.5	30.4	7.43	62	-6.53	3.54
0215NPI01	173.5	197.7	2.9	25.6	8.18	70	-7.66	2.86
0217OPC00	174	182.9	-8.3	21.4	10.86	220	7.02	-8.29
0215NPI03	174.4	197.1	3.4	31.2	7.86	64	-7.07	3.44

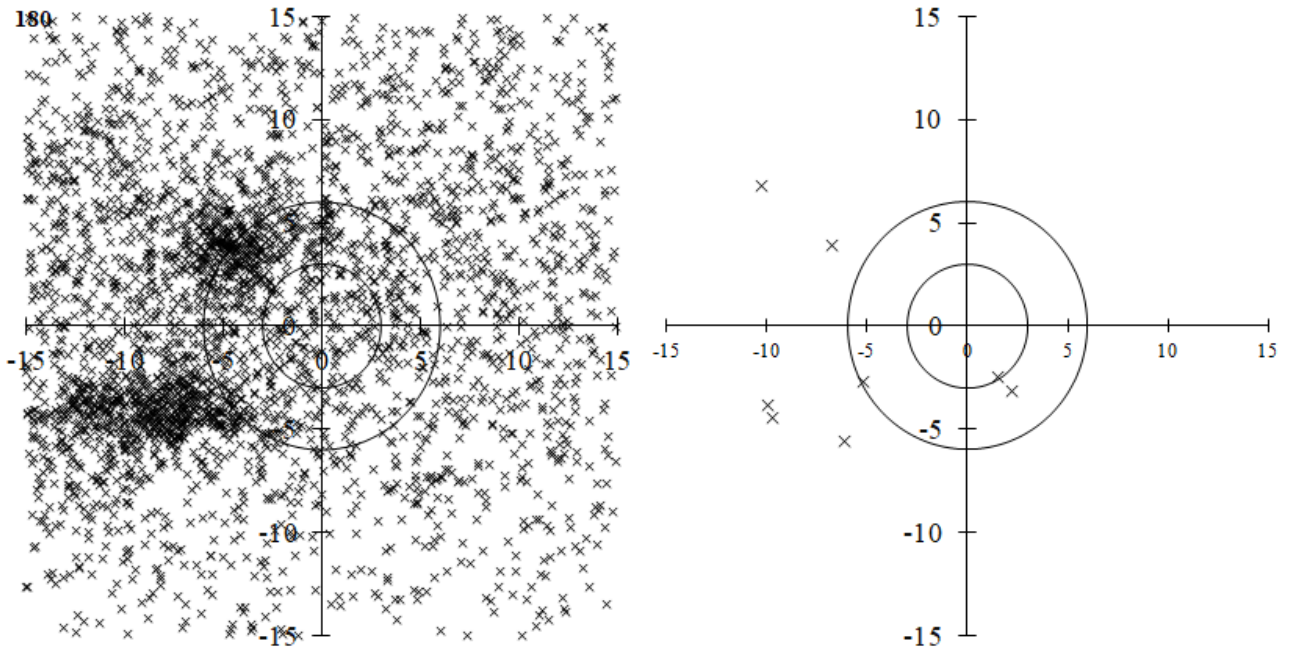

Figure 5c – Meteor activities around (λ–$\lambda_\odot$, $\lambda_\odot$) = (180°, 0°) at $\lambda_\odot$ = 180°, radiant distribution of video meteors left, radiant distribution according to the SD reference.

Table 2c – Explanation of the SD radiants listed around ($\lambda–\lambda_\odot$, $\lambda_\odot$) = (180°, 0°) at $\lambda_\odot$ = 180°.

Code	$\lambda_\odot$	$\lambda–\lambda_\odot$	β	v_g	*Distance*	*Angle*	*x*	*y*
0476ICE01	175.5	188.4	-2.5	26.23	2.92	212	1.56	-2.47
0215NPI04	176	196.8	3.9	28	7.78	60	-6.74	3.88
0216SPI04	176	200.0	-3.8	28.6	10.69	111	-9.99	-3.81
0476ICE00	176.1	187.8	-3.2	26.9	3.90	215	2.25	-3.19
0219SAR00	183.3	200.3	6.8	36.7	12.30	57	-10.26	6.79
0216SPI02	183.6	196.2	-5.6	31.9	8.31	132	-6.13	-5.61
0216SPI00	184	199.7	-4.4	26.5	10.68	115	-9.71	-4.44
0216SPI01	184	195.2	-2.7	28.6	5.86	117	-5.21	-2.69

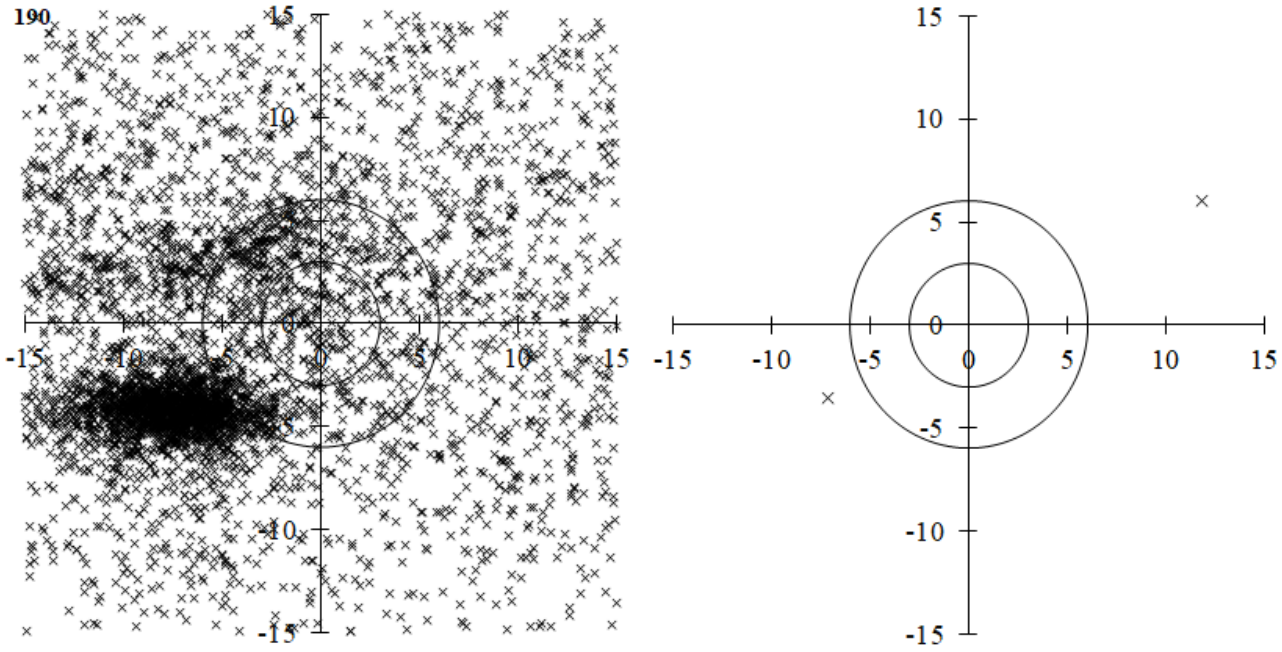

Figure 5d – Meteor activities around ($\lambda–\lambda_\odot$, $\lambda_\odot$) = (180°, 0°) at $\lambda_\odot$ = 190°, radiant distribution of video meteors left, radiant distribution according to the SD reference.

Table 2d – Explanation of the SD radiants listed around ($\lambda–\lambda_\odot$, $\lambda_\odot$) = (180°, 0°) at $\lambda_\odot$ = 190°.

Code	$\lambda_\odot$	$\lambda–\lambda_\odot$	β	v_g	*Distance*	*Angle*	*x*	*y*
0234EPC00	188.9	178.1	6.0	21.7	13.29	297	11.87	5.99
0627NPS00	189	197.1	-3.5	29.4	7.93	116	-7.10	-3.53

Table 2e – Explanation of the SD radiants listed around ($\lambda–\lambda_\odot$, $\lambda_\odot$) = (180°, 0°) at $\lambda_\odot$ = 200°.

Code	$\lambda_\odot$	$\lambda–\lambda_\odot$	β	v_g	*Distance*	*Angle*	*x*	*y*
0002STA05	196	195.6	-4.2	28.2	6.98	127	-5.58	-4.19
0028SOA01	196	196.8	-4.2	29	7.94	122	-6.75	-4.19
0002STA03	196.5	195.2	-4.3	27.92	6.71	130	-5.14	-4.32
0028SOA00	198.5	195.8	-2.8	25.6	6.41	116	-5.77	-2.79
0946TEA00	199.3	203.2	-3.2	34.95	13.53	104	-13.14	-3.23
0025NOA00	201.7	197.4	5.9	36.32	9.45	51	-7.36	5.93
0902DCT00	202.1	194.4	-13.2	32.7	13.91	162	-4.34	-13.21
0902DCT00	202.1	194.4	-13.2	32.7	13.91	162	-4.34	-13.21
0002STA09	202.4	195.2	-4.6	28.6	6.97	131	-5.23	-4.61
0237SSA00	202.7	203.7	-2.7	40.48	13.92	101	-13.64	-2.77

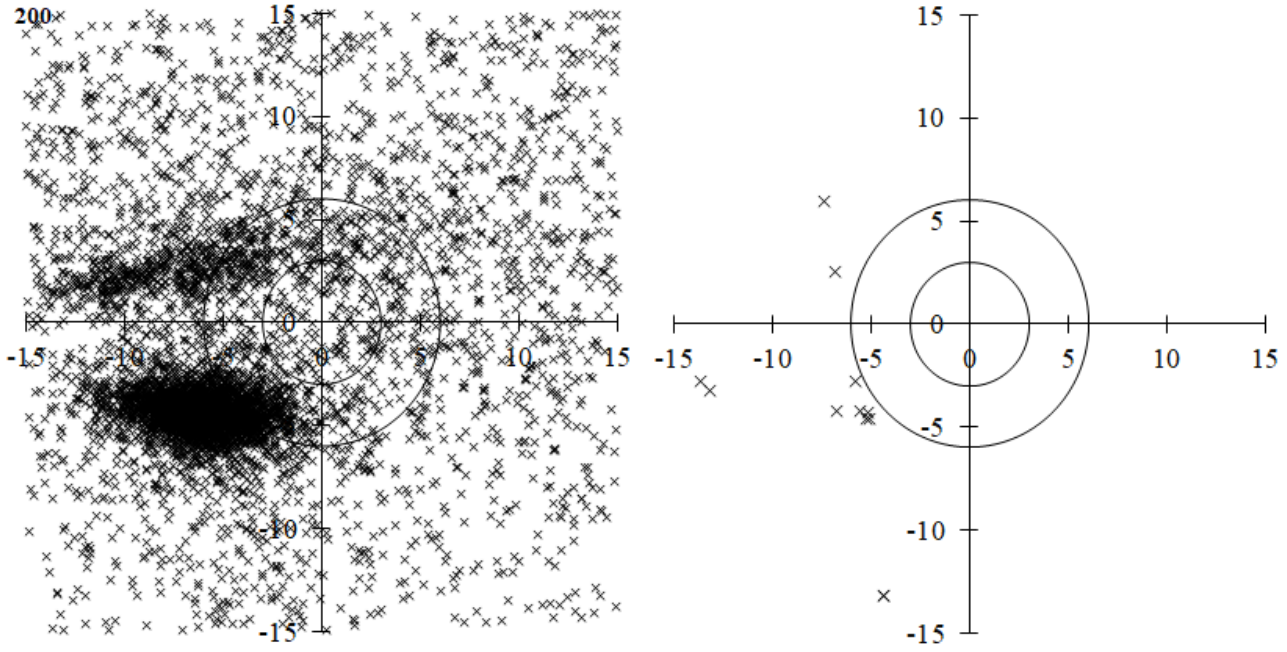

Figure 5e – Meteor activities around (λ–$\lambda_\odot$, $\lambda_\odot$) = (180°, 0°) at $\lambda_\odot$ = 200°, radiant distribution of video meteors left, radiant distribution according to the SD reference.

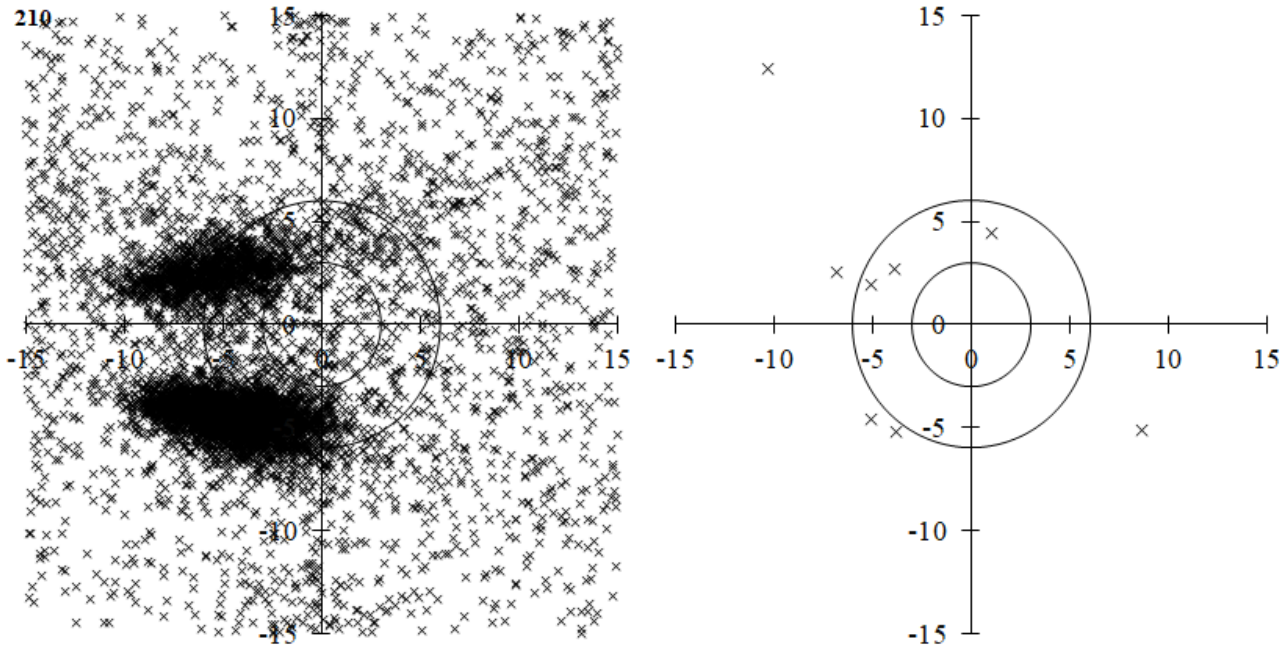

Figure 5f – Meteor activities around (λ–$\lambda_\odot$, $\lambda_\odot$) = (180°, 0°) at $\lambda_\odot$ = 210°, radiant distribution of video meteors left, radiant distribution according to the SD reference.

Table 2f – Explanation of the SD radiants listed around (λ–$\lambda_\odot$, $\lambda_\odot$) = (180°, 0°) at $\lambda_\odot$ = 210°.

Code	$\lambda_\odot$	λ–$\lambda_\odot$	β	v_g	*Distance*	*Angle*	*x*	*y*
0025NOA01	205	196.9	2.5	30.1	7.30	70	-6.85	2.54
0624XAR00	205	195.1	-4.6	28.5	6.80	132	-5.04	-4.57
0002STA01	207.6	193.8	-5.2	27.8	6.44	144	-3.79	-5.20
1195SCD00	212.036	181.3	-5.1	23.839	10.08	239	8.68	-5.14
0017NTA01	212.7	195.1	2.0	30.69	5.41	69	-5.05	1.95
0538FFA00	214	200.5	12.3	36.9	16.11	40	-10.29	12.40
0017NTA02	214.1	193.9	2.7	29.6	4.73	55	-3.87	2.72
1194MAR00	214.93	188.9	4.4	25.58	4.55	346	1.07	4.42

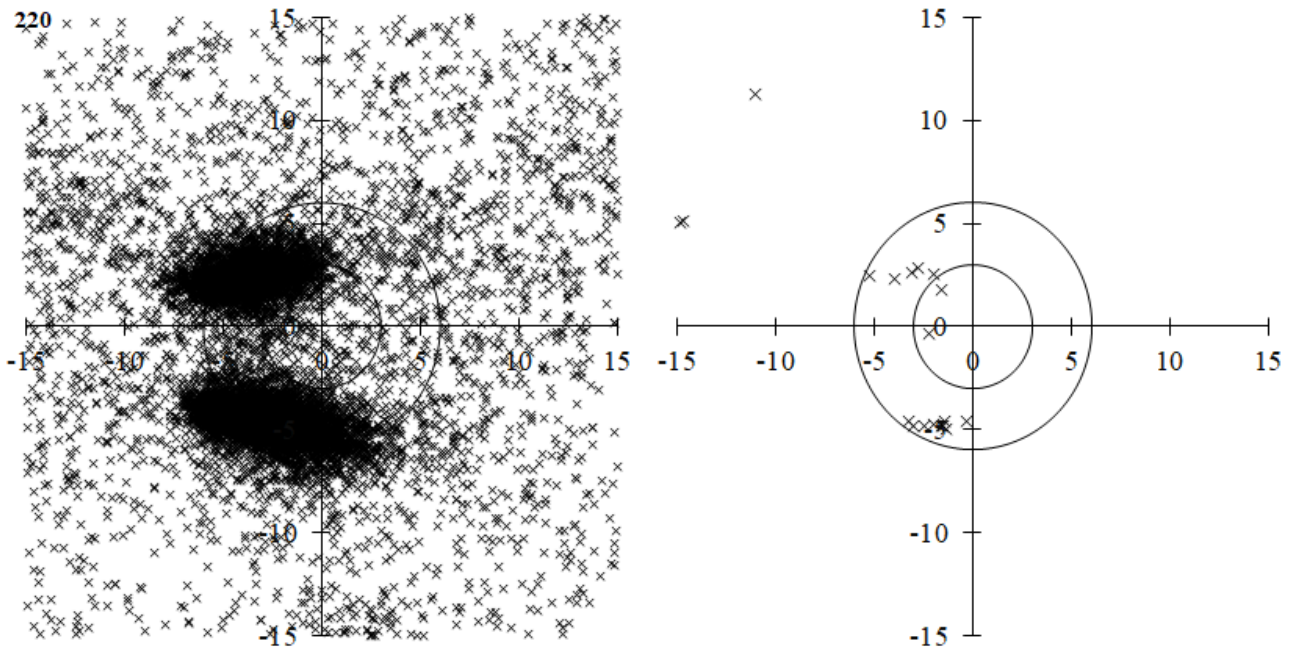

Figure 5g – Meteor activities around ($\lambda–\lambda_\odot$, $\lambda_\odot$) = (180°, 0°) at $\lambda_\odot$ = 220°, radiant distribution of video meteors left, radiant distribution according to the SD reference.

Table 2g – Explanation of the SD radiants listed around ($\lambda–\lambda_\odot$, $\lambda_\odot$) = (180°, 0°) at $\lambda_\odot$ = 220°.

Code	$\lambda_\odot$	$\lambda–\lambda_\odot$	β	v_g	*Distance*	*Angle*	*x*	*y*
0538FFA01	215.1	201.1	11.2	38.12	15.77	44	-11.00	11.30
0002STA06	216	193.0	-4.9	26.6	5.70	148	-2.99	-4.85
0626LCT00	216	193.3	-4.6	27.9	5.64	145	-3.25	-4.61
0631DAT00	216	195.2	2.4	29.3	5.74	65	-5.21	2.42
0002STA00	217.3	192.5	-4.9	28	5.46	153	-2.49	-4.86
0017NTA09	218.8	193.9	2.3	29.1	4.56	59	-3.93	2.32
0017NTA06	219	192.2	-0.4	28.1	2.25	100	-2.22	-0.38
0002STA04	219.7	191.5	-4.8	27.2	5.07	162	-1.53	-4.83
0017NTA07	220	192.0	2.5	28	3.22	39	-2.01	2.52
0630TAR00	220	193.1	2.6	28.1	4.08	50	-3.11	2.64
0388CTA01	221	204.9	5.0	41.1	15.66	71	-14.82	5.05
0002STA02	221.5	191.4	-4.6	28.2	4.84	163	-1.39	-4.64
0002STA10	221.6	191.3	-5.0	27.4	5.13	165	-1.31	-4.96
0017NTA03	222.7	192.8	2.9	28.8	3.97	44	-2.77	2.85
0388CTA02	223	204.7	5.1	39.4	15.54	71	-14.67	5.14
0628STS00	223	192.0	-4.8	28.2	5.14	158	-1.97	-4.75
0002STA08	224.5	191.6	-4.8	28	5.05	162	-1.56	-4.80
0017NTA04	224.5	191.6	1.8	28.1	2.37	41	-1.57	1.78

Table 2h – Explanation of the SD radiants listed around ($\lambda–\lambda_\odot$, $\lambda_\odot$) = (180°, 0°) at $\lambda_\odot$ = 230°.

Code	$\lambda_\odot$	$\lambda–\lambda_\odot$	β	v_g	*Distance*	*Angle*	*x*	*y*
0637FTR00	225	190.3	-4.62	27.4	4.629709	176.2928	-0.29935	-4.62002
0017NTA00	226.2	194.82	1.26	28.3	4.981591	75.33128	-4.81922	1.261487
0632NET00	227	191.9	2.45	28	3.100048	37.77194	-1.89884	2.450449
0625LTA00	231	187.85	-5.22	25.7	5.644298	202.3251	2.144047	-5.22122
0635ATU00	231	190.54	2.38	27.4	2.440457	12.77616	-0.53969	2.380035
0285GTA00	232.8	188.68	-3.02	14.1	3.295631	203.5881	1.318777	-3.02027
0629ATS00	233	190.24	2.44	27.5	2.451768	5.61419	-0.23985	2.440007
0017NTA05	234.4	190.17	3	26.7	3.004808	3.240329	-0.16984	3.000004

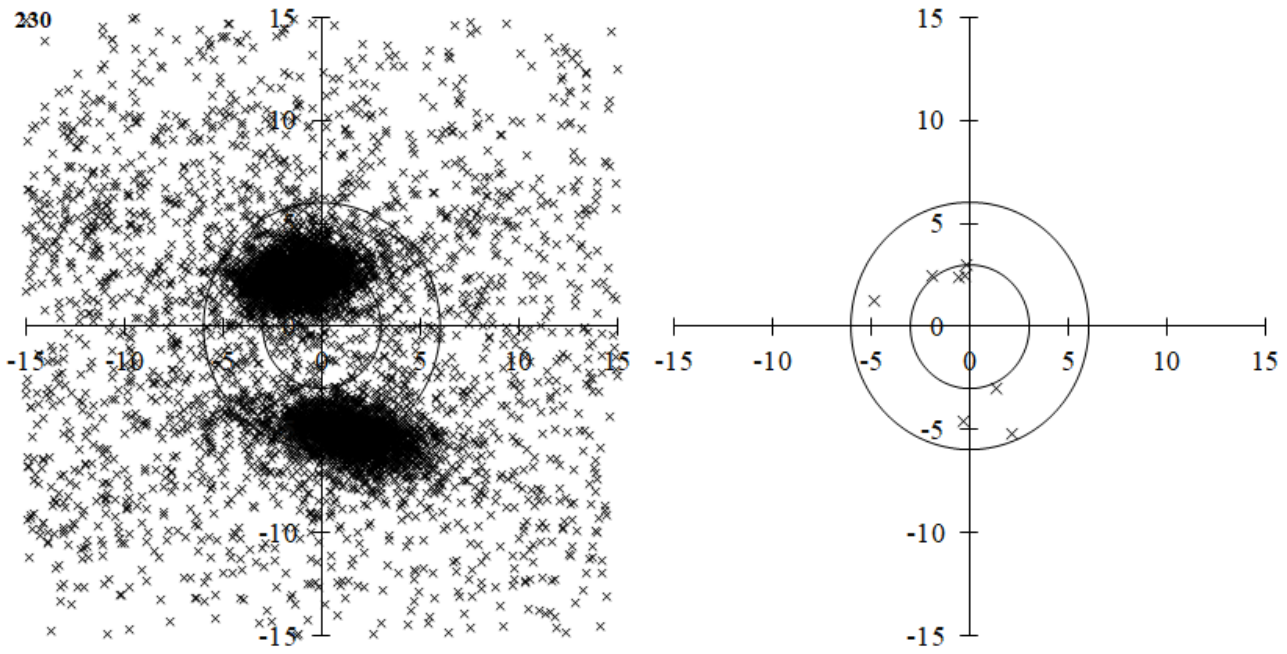

Figure 5h – Meteor activities around (λ–$\lambda_\odot$, $\lambda_\odot$) = (180°, 0°) at $\lambda_\odot$ = 230°, radiant distribution of video meteors left, radiant distribution according to the SD reference.

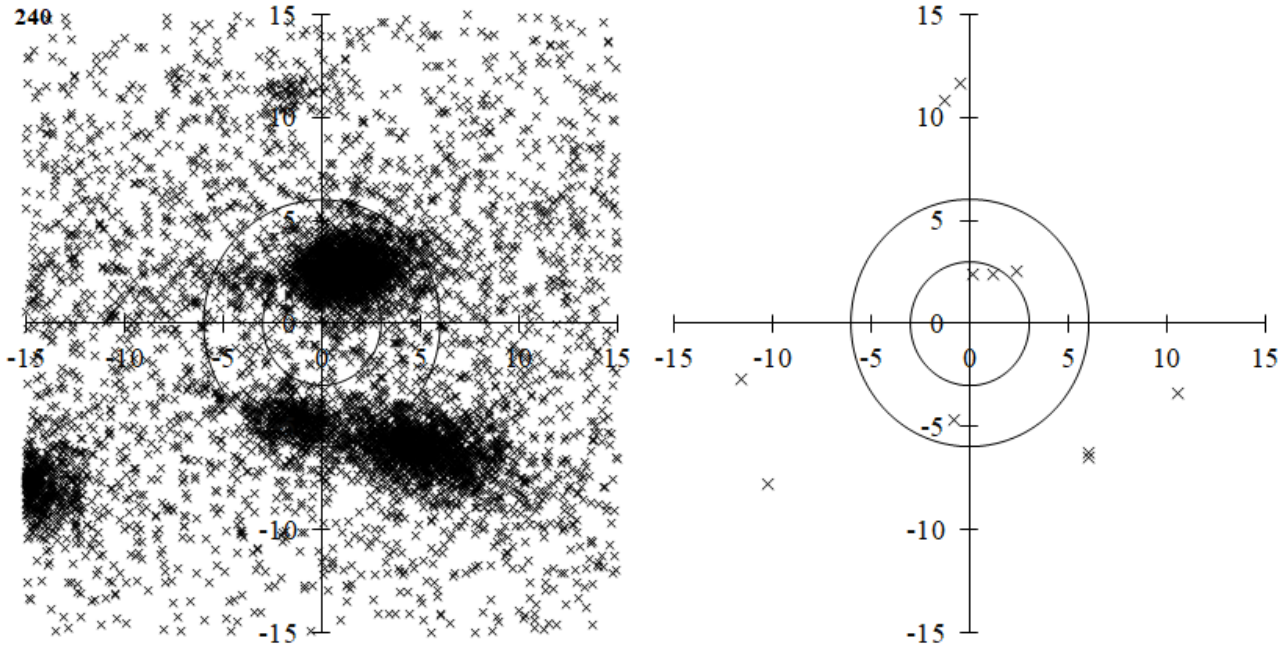

Figure 5i – Meteor activities around (λ–$\lambda_\odot$, $\lambda_\odot$) = (180°, 0°) at $\lambda_\odot$ = 240°, radiant distribution of video meteors left, radiant distribution according to the SD reference.

Table 2i – Explanation of the SD radiants listed around (λ–$\lambda_\odot$, $\lambda_\odot$) = (180°, 0°) at $\lambda_\odot$ = 240°.

Code	$\lambda_\odot$	λ–$\lambda_\odot$	β	v_g	*Distance*	*Angle*	*x*	*y*
0017NTA10	236.2	189.8	2.4	27.1	2.43	356	0.16	2.42
0485NZT00	240	201.6	-2.7	35.5	11.86	103	-11.55	-2.70
0486NZP01	240	191.3	10.8	29.5	10.86	7	-1.28	10.78
0633PTS00	240	188.8	2.4	26.7	2.64	333	1.18	2.36
0286FTA01	240.2	179.5	-3.4	21.7	11.06	252	10.54	-3.37
0486NZP00	240.4	190.4	11.7	29.4	11.67	2	-0.43	11.66
0286FTA00	242	184.0	-6.3	23.3	8.71	224	6.02	-6.30
0002STA11	242.1	183.9	-6.5	23.4	8.90	223	6.05	-6.52
0257ORS03	243	190.8	-4.7	27.9	4.75	171	-0.78	-4.69
0634TAT00	244	187.6	2.6	25.8	3.49	317	2.39	2.55

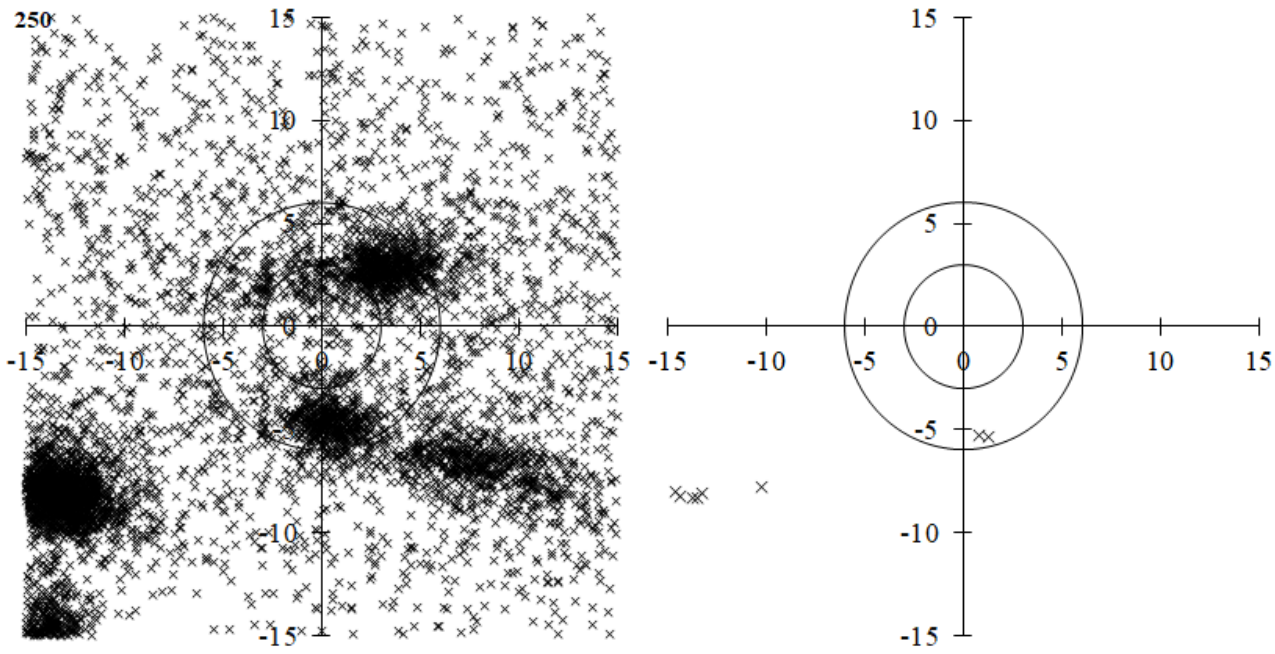

Figure 5j – Meteor activities around (λ–$\lambda_\odot$, $\lambda_\odot$) = (180°, 0°) at $\lambda_\odot$ = 250°, radiant distribution of video meteors left, radiant distribution according to the SD reference.

Table 2j – Explanation of the SD radiants listed around (λ–$\lambda_\odot$, $\lambda_\odot$) = (180°, 0°) at $\lambda_\odot$ = 250°.

Code	$\lambda_\odot$	λ–$\lambda_\odot$	β	v_g	*Distance*	*Angle*	*x*	*y*
0250NOO02	245	200.3	-7.8	43.3	12.89	127	-10.27	-7.80
0250NOO00	245.5	204.7	-7.9	43.5	16.66	119	-14.60	-8.03
0250NOO05	246	204.5	-8.1	43.1	16.58	120	-14.39	-8.23
0250NOO06	247	203.6	-8.2	42.5	15.85	122	-13.50	-8.32
0250NOO04	248	203.9	-8.2	42.66	16.07	121	-13.75	-8.31
0250NOO03	249.2	203.3	-8.0	42	15.52	121	-13.24	-8.09
0257ORS05	250.1	189.2	-5.3	26.8	5.38	189	0.81	-5.32
0636MTA00	252	188.7	-5.3	27.4	5.48	193	1.27	-5.33

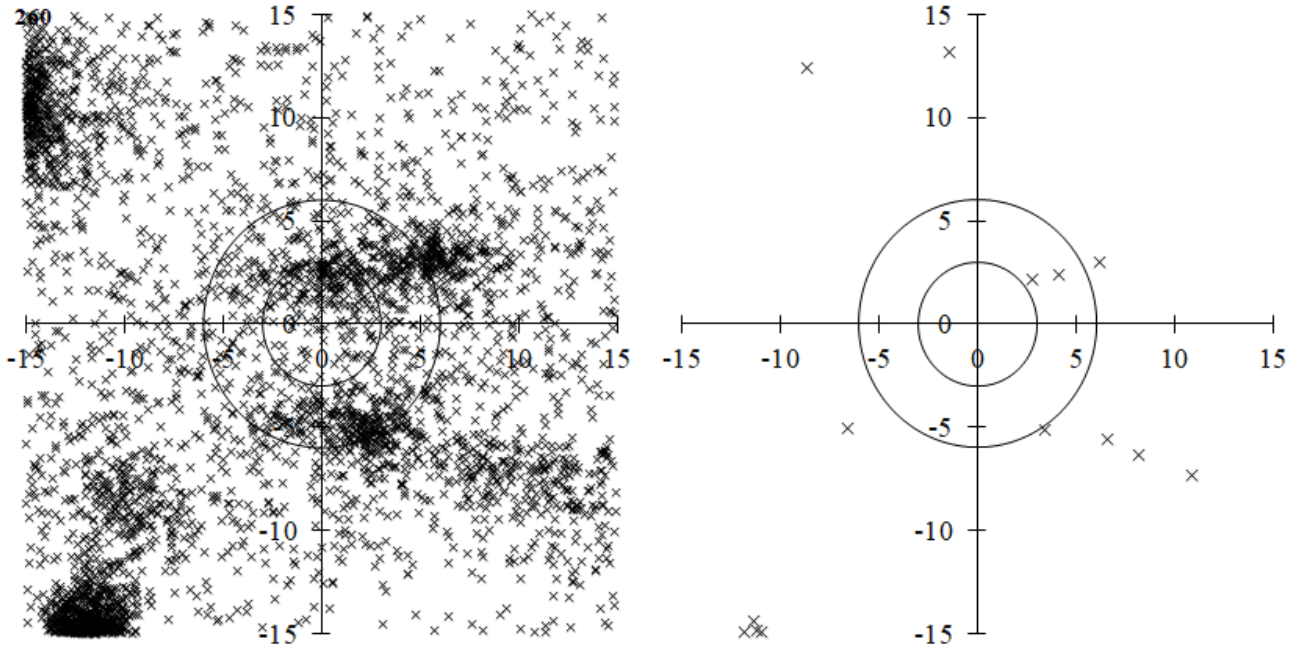

Figure 5k – Meteor activities around (λ–$\lambda_\odot$, $\lambda_\odot$) = (180°, 0°) at $\lambda_\odot$ = 260°, radiant distribution of video meteors left, radiant distribution according to the SD reference.

Table 2k – Explanation of the SD radiants listed around ($\lambda–\lambda_\odot$, $\lambda_\odot$) = (180°, 0°) at $\lambda_\odot$ = 260°.

Code	$\lambda_\odot$	$\lambda–\lambda_\odot$	β	v_g	*Distance*	*Angle*	*x*	*y*
0256ORN00	257.3	187.2	2.2	24.9	3.56	308	2.81	2.18
0257ORS02	257.9	183.4	-5.6	24.6	8.63	230	6.59	-5.57
0256ORN02	258	185.9	2.4	24.7	4.78	300	4.13	2.41
0257ORS01	259.3	181.8	-6.3	21.5	10.37	232	8.20	-6.35
0257ORS00	260	179.0	-7.3	21.5	13.15	236	10.90	-7.35
0638DZT00	260	186.6	-5.1	25.8	6.14	214	3.42	-5.10
0019MON00	260.9	201.2	-14.9	42	18.52	144	-10.94	-14.94
0019MON04	261	201.6	-14.3	40.6	18.31	142	-11.31	-14.40
0396DTA00	261	191.5	13.2	58.9	13.27	6	-1.44	13.19
0019MON01	261.5	202.1	-14.8	42.3	19.06	142	-11.86	-14.92
0019MON02	261.5	201.4	-14.8	41.5	18.59	143	-11.15	-14.88
0397NGM00	262	196.6	-5.1	65.8	8.31	128	-6.57	-5.08
0944TGD00	262.8	198.8	12.3	35.91	15.10	35	-8.64	12.39
0017NTA11	263.9	183.8	3.0	23.8	6.90	296	6.22	2.99

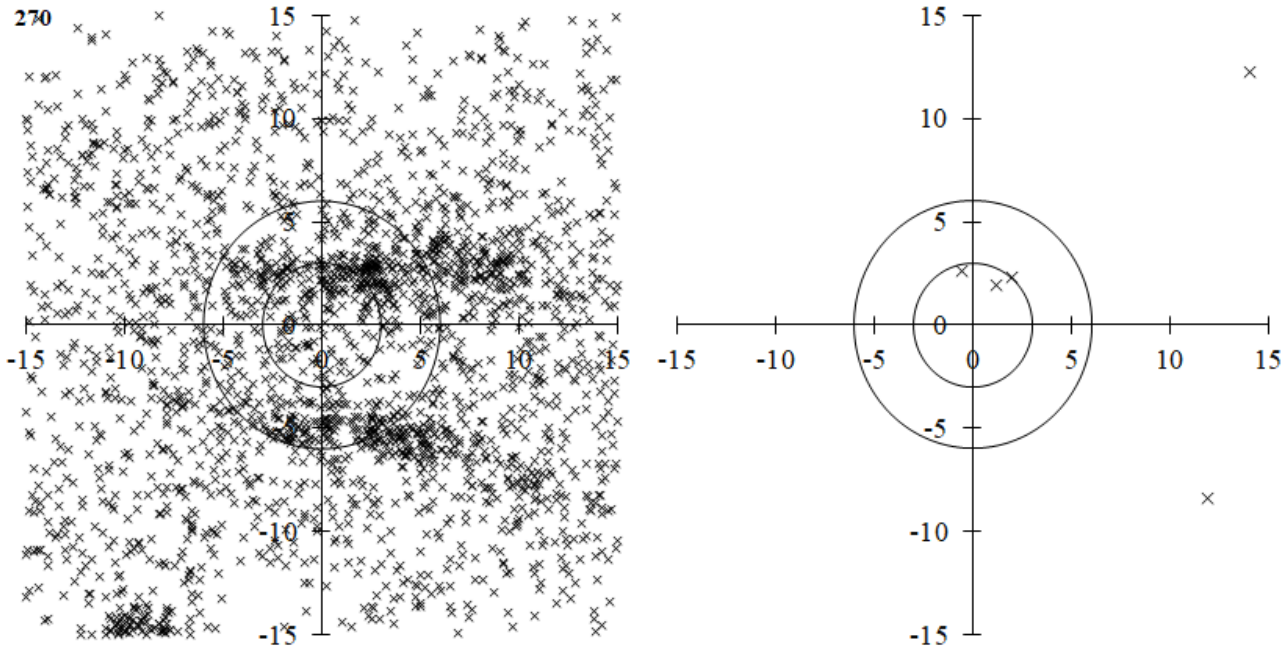

Figure 5l – Meteor activities around ($\lambda–\lambda_\odot$, $\lambda_\odot$) = (180°, 0°) at $\lambda_\odot$ = 270°, radiant distribution of video meteors left, radiant distribution according to the SD reference.

Table 2l – Explanation of the SD radiants listed around ($\lambda–\lambda_\odot$, $\lambda_\odot$) = (180°, 0°) at $\lambda_\odot$ = 270°.

Code	$\lambda_\odot$	$\lambda–\lambda_\odot$	β	v_g	*Distance*	*Angle*	*x*	*y*
0002STA12	265.1	178.0	-8.4	20.6	14.62	235	11.94	-8.43
0256ORN01	266	190.6	2.6	28.2	2.69	12	-0.57	2.63
0256ORN04	267.9	188.8	1.9	26.9	2.27	328	1.20	1.93
0726DEG00	268	188.0	2.3	26.8	3.02	320	1.96	2.30
0258DAR00	270.7	175.8	12.1	19.5	18.63	311	14.04	12.24

Table 2m – Explanation of the SD radiants listed around ($\lambda–\lambda_\odot$, $\lambda_\odot$) = (180°, 0°) at $\lambda_\odot$ = 280°.

Code	$\lambda_\odot$	$\lambda–\lambda_\odot$	β	v_g	*Distance*	*Angle*	*x*	*y*
0728PGE00	276.5	199.8	2.0	37.7	9.98	78	-9.77	2.05
0604ACZ00	282	199.6	-3.0	33.8	10.08	107	-9.63	-2.98
1179OGE00	284.2	179.7	3.9	22	11.04	291	10.32	3.92

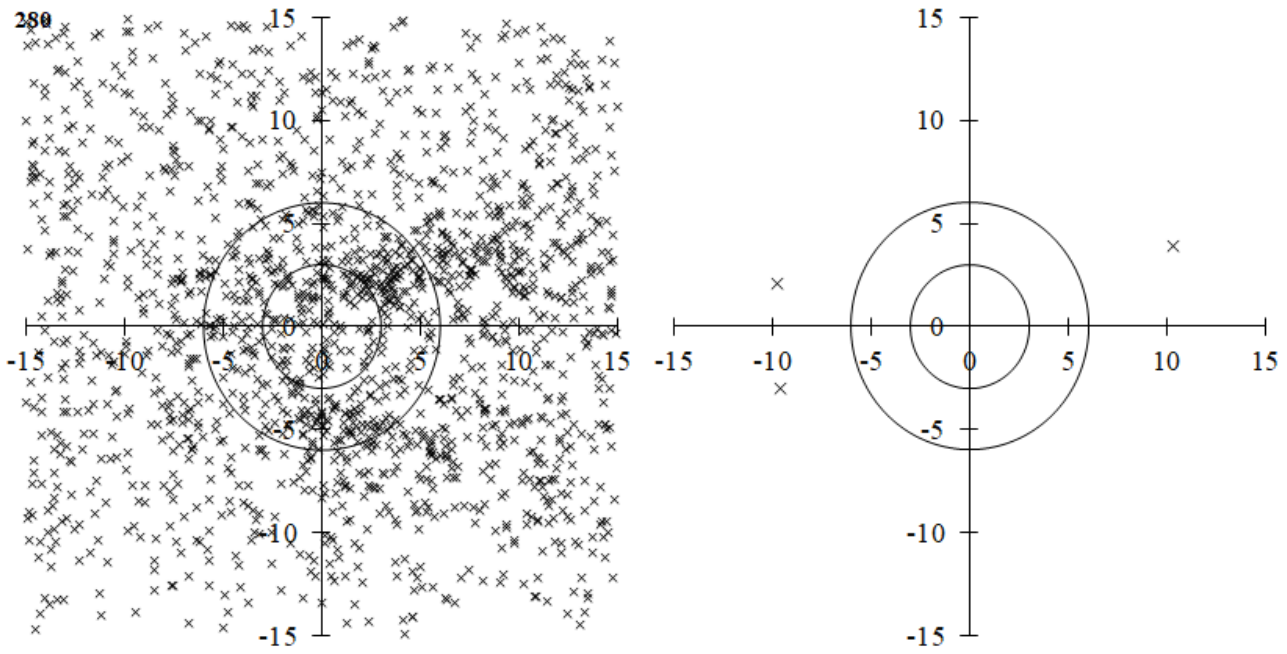

Figure 5m – Meteor activities around (λ–$\lambda_\odot$, $\lambda_\odot$) = (180°, 0°) at $\lambda_\odot$ = 280°, radiant distribution of video meteors left, radiant distribution according to the SD reference.

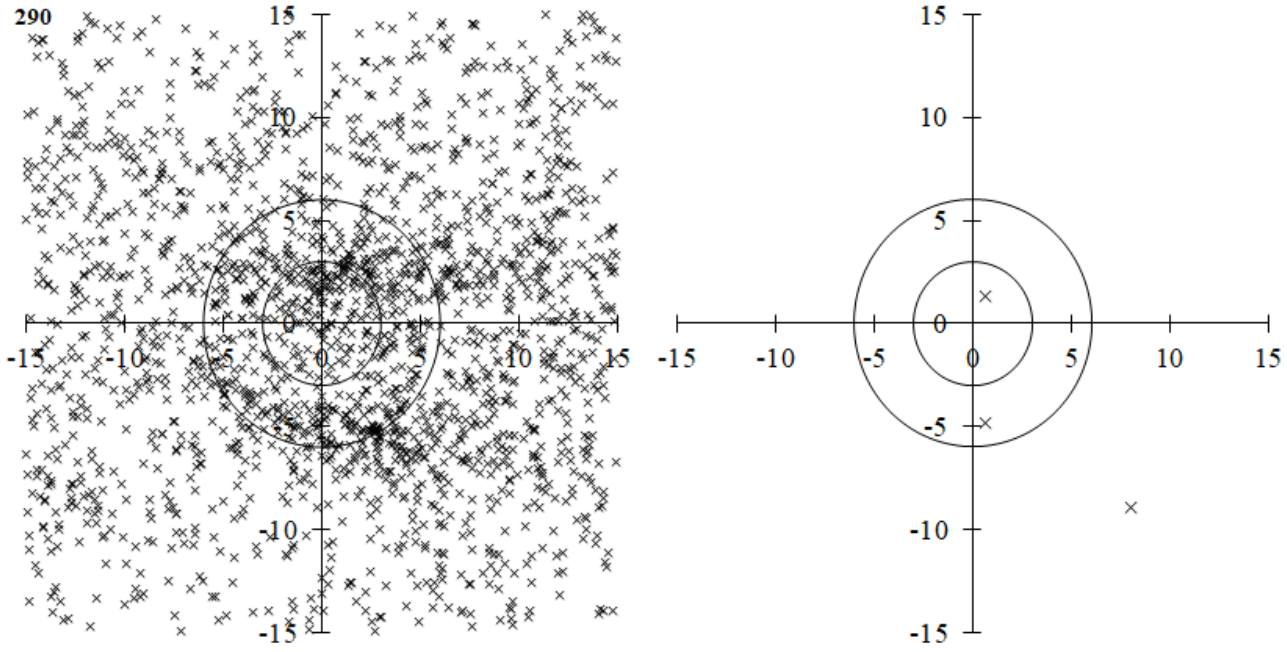

Figure 5n – Meteor activities around (λ–$\lambda_\odot$, $\lambda_\odot$) = (180°, 0°) at $\lambda_\odot$ = 290°, radiant distribution of video meteors left, radiant distribution according to the SD reference.

Table 2n – Explanation of the SD radiants listed around (λ–$\lambda_\odot$, $\lambda_\odot$) = (180°, 0°) at $\lambda_\odot$ = 290°.

Code	$\lambda_\odot$	λ–$\lambda_\odot$	β	v_g	*Distance*	*Angle*	*x*	*y*
1193JLG00	286.927	181.9	-8.9	23.201	12.03	222	8.05	-8.94
0097SCC05	287.1	189.3	-4.9	27.9	4.89	188	0.66	-4.85
0096NCC03	292.9	189.4	1.3	25.8	1.45	333	0.65	1.30

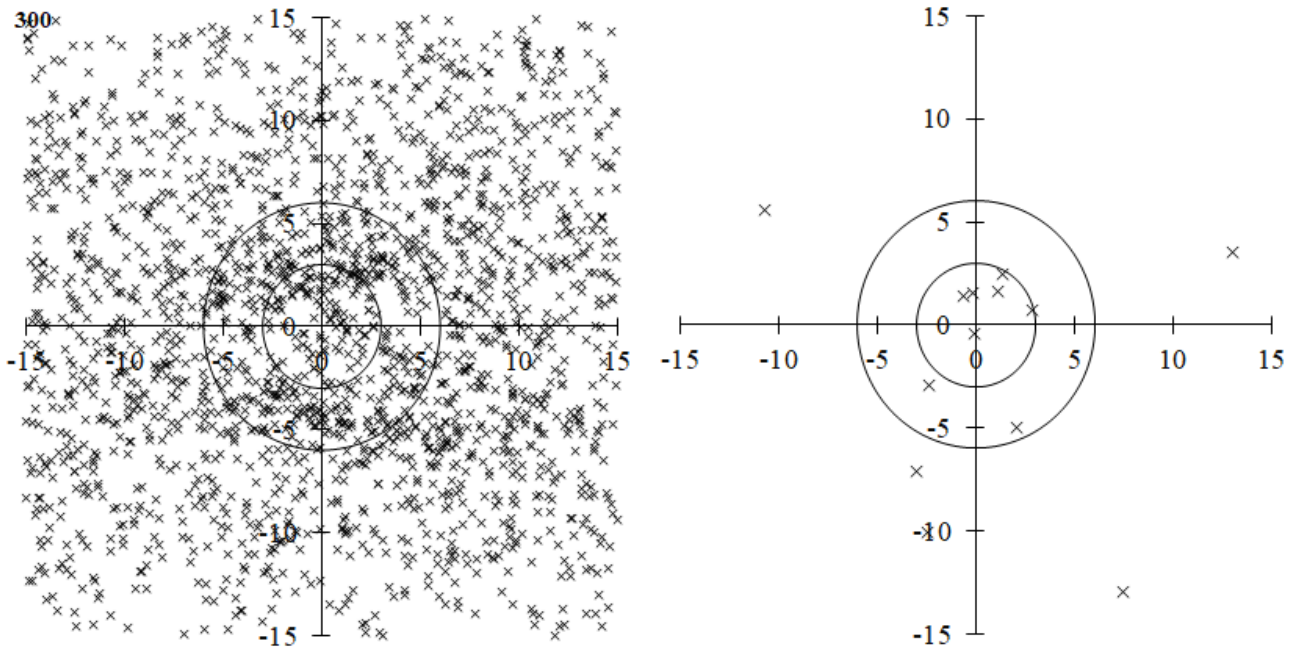

Figure 5o – Meteor activities around (λ–$\lambda_\odot$, $\lambda_\odot$) = (180°, 0°) at $\lambda_\odot$ = 300°, radiant distribution of video meteors left, radiant distribution according to the SD reference.

Table 2o – Explanation of the SD radiants listed around (λ–$\lambda_\odot$, $\lambda_\odot$) = (180°, 0°) at $\lambda_\odot$ = 300°.

Code	$\lambda_\odot$	λ–$\lambda_\odot$	β	v_g	*Distance*	*Angle*	*x*	*y*
0945SNC00	295.2	200.8	5.5	34.19	12.09	63	-10.73	5.57
0096NCC06	296	188.6	2.5	27.2	2.82	331	1.37	2.47
0097SCC03	296	187.9	-5.0	27	5.44	203	2.09	-5.02
0094RGE02	296.3	177.0	3.5	23	13.46	285	12.98	3.55
0096NCC08	296.9	188.9	1.6	28.2	1.97	326	1.10	1.63
0096NCC00	297	190.2	1.6	25.67	1.58	6	-0.17	1.57
0097SCC01	297	182.4	-12.9	24	14.94	210	7.46	-12.95
0096NCC02	297.1	187.1	0.7	28	2.98	284	2.89	0.73
0096NCC04	297.1	190.6	1.4	26.4	1.55	24	-0.62	1.42
0097SCC02	298	193.0	-7.1	26.43	7.74	157	-3.00	-7.13
0096NCC05	299	190.1	-0.4	27.73	0.41	169	-0.08	-0.40
0096NCC01	300.2	192.4	-2.9	26.7	3.78	141	-2.38	-2.94
0266ACC00	304.2	192.5	-10.1	19.3	10.39	167	-2.42	-10.10

Table 2p – Explanation of the SD radiants listed around (λ–$\lambda_\odot$, $\lambda_\odot$) = (180°, 0°) at $\lambda_\odot$ = 310°.

Code	$\lambda_\odot$	λ–$\lambda_\odot$	β	v_g	*Distance*	*Angle*	*x*	*y*
0097SCC00	305.7	185.2	-5.8	24.36	7.57	220	4.83	-5.83
0113SDL01	314.5	181.6	-9.0	20.9	12.28	223	8.32	-9.03

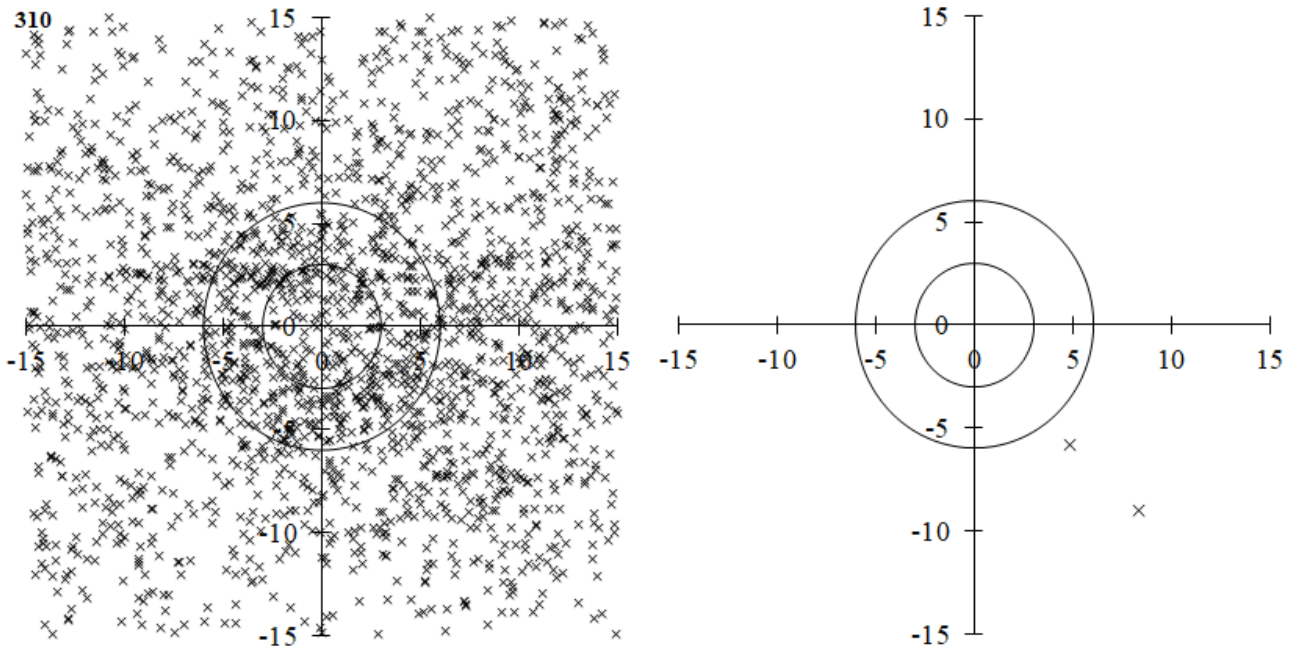

Figure 5p – Meteor activities around (λ–$\lambda_\odot$, $\lambda_\odot$) = (180°, 0°) at $\lambda_\odot$ = 310°, radiant distribution of video meteors left, radiant distribution according to the SD reference.

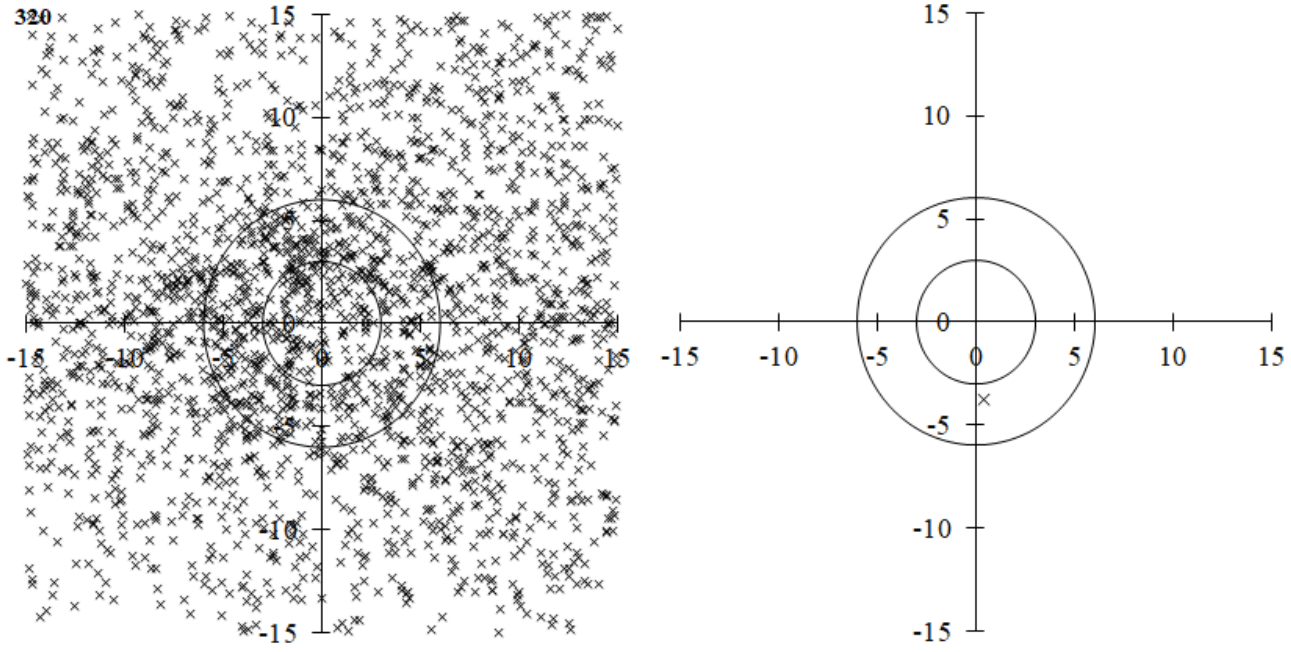

Figure 5q – Meteor activities around (λ–$\lambda_\odot$, $\lambda_\odot$) = (180°, 0°) at $\lambda_\odot$ = 320°, radiant distribution of video meteors left, radiant distribution according to the SD reference.

Table 2q – Explanation of the SD radiants listed around (λ–$\lambda_\odot$, $\lambda_\odot$) = (180°, 0°) at $\lambda_\odot$ = 320°.

Code	$\lambda_\odot$	λ–$\lambda_\odot$	β	v_g	*Distance*	*Angle*	*x*	*y*
0501FPL00	317.3	189.6	-3.8	28.3	3.79	186	0.41	-3.77

3.2 Comae Berenicids

Figure 6a represents the radiant distribution around (λ–$\lambda_\odot$, β) = (242.3°, 20.1°) from $\lambda_\odot$ = 240° to $\lambda_\odot$ = 320°, accompanied by the radiant distribution of the SD showers and with their reference table. They are compensated for radiant drift; the observed radiants are concentrated within 3 degrees, indicating effective compensation. The SD showers are also concentrated within 3 degrees; #0032DLM, #0020COM, #0499DDL, #0090JCO, and #0506FEV. It seems a too long activity period for the retrograde shower but the radiant distribution compensated for the radiant drift indicates they represent a single activity.

The activity profile is smooth reaching its maximum at $\lambda_\odot$ = 268° (*Figure 6b*) and the radiant locates then near the border of Ursa Major and Leo Minor, not in Coma Berenices. We understood that a new meteor shower (and a meteoroid stream) should be named after the constellation that contains the star nearest to the shower radiant. If so, #0032DLM (December Leonis Minorids) is the most proper name among above mentioned five.

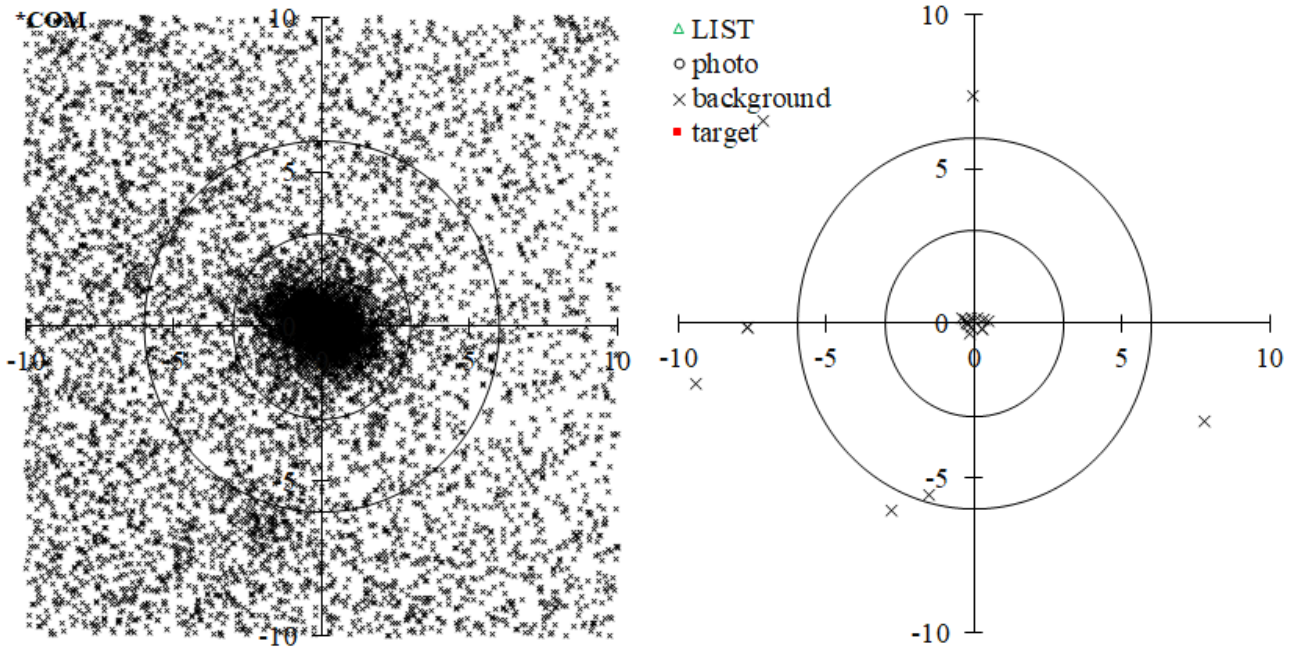

Figure 6a – Comae Berenicids complex. Radiant distribution around ($\lambda-\lambda_\odot$, $\lambda_\odot$) = (242.3°, 20.1°) from $\lambda_\odot$ = = 240° to $\lambda_\odot$ = = 320°, accompanied by the radiant distribution of the SD showers and with their reference table. For explanations, see *Figure 5a*.

Table 3a – Explanation of the SD radiants listed around ($\lambda-\lambda_\odot$, $\lambda_\odot$) = (242.3°, 20.1°) from $\lambda_\odot$ = = 240° to $\lambda_\odot$ = = 320°.

Code	$\lambda_\odot$	$\lambda-\lambda_\odot$	β	v_g	*Distance*	*Angle*	*x*	*y*
0722FLE00	250.1	246.7	16.1	66.3	6.67	155	-2.81	-6.05
1118MLT00	258.88	245.0	16.1	65.3	5.75	164	-1.54	-5.54
0619SLM00	260	235.1	18.2	60.4	8.40	248	7.78	-3.16
0020COM06	261.7	251.4	21.1	63.02	7.67	91	-7.67	-0.15
0032DLM01	261.7	251.4	21.1	63.02	7.67	91	-7.67	-0.15
0032DLM00	262.2	243.4	21.1	62.3	0.35	154	-0.15	-0.31
0020COM00	265.7	243.3	21.3	63	0.31	68	-0.29	0.12
0032DLM02	268	243.0	20.9	63.02	0.16	138	-0.11	-0.12
0020COM01	274	252.5	18.4	63.7	9.61	102	-9.41	-1.94
0020COM08	274	242.8	20.6	63.3	0.19	102	-0.19	-0.04
0020COM03	275.9	242.8	20.5	67	0.28	85	-0.28	0.03
0499DDL00	275.9	242.8	20.5	67	0.28	85	-0.28	0.03
0020COM04	277.4	242.2	20.2	63.06	0.29	236	0.24	-0.16
0499DDL01	277.4	242.2	20.2	63.06	0.29	236	0.24	-0.16
0615TOR00	292	249.6	25.8	63.6	9.68	48	-7.14	6.54
0616TOB00	300	241.4	26.2	61.2	7.34	1	-0.07	7.34
0090JCO01	300.5	240.8	18.9	63.9	0.48	276	0.47	0.05
0090JCO00	304	241.6	18.8	64.74	0.47	71	-0.45	0.15
0506FEV02	314	240.5	18.1	62.9	0.20	331	0.10	0.17
0506FEV01	315	240.2	18.0	64.03	0.32	288	0.31	0.10
0506FEV00	315.3	240.7	18.1	63.02	0.22	30	-0.11	0.19

The activity profile drawn with the original shower classification of GMN decreases to zero after $\lambda_\odot$ = 300° because they classified meteors of #020COM after $\lambda_\odot$ = 300° into #0506FEV; #506FEV has an established status. It is written in line #0506FEV00 as a remark that this a component of shower #0020COM, after solar longitude 300° (different radiant drift). #0506FEV is an extension of #0020COM and can be considered as a part of rather than an independent entity; the radiant drift and the activity profile both indicate the inclusion may be proper. #506FEV should be moved to the working list.

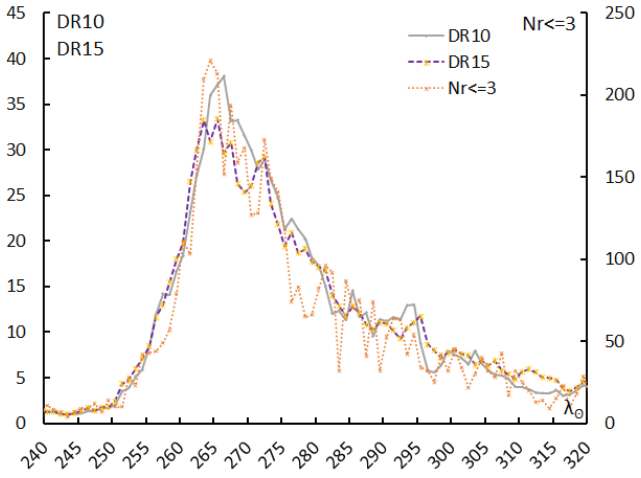

Figure 6b – Activity profiles of the Comae Bereniceds complex. Raw observed meteor number (*Nr* <= 3) fluctuates but profiles for different DR become much smoother. *Nr* <= 3 is the number of meteors within 3 degrees from the estimated radiant and *DR*s are the radiant density ratios (for details, see Koseki, 2019).

3.3 DSV complex

DSV has a retrograde orbit, and it seems a too long activity but the radiant distribution compensating for the radiant drift indicates they represent one single activity (Koseki, 2020b). *Figure 7a* represents the radiant distribution around $(\lambda-\lambda_\odot, \beta) = (293.7°, 14.8°)$ from $\lambda_\odot = 240°$ to $\lambda_\odot = 300°$, accompanied by the radiant distribution of the SD showers and with their reference table. Compensated radiants are concentrated well within 3 degrees in both video and the SD. Activity profile based on GMN observations clearly shows three components, #0428DSV, #0513EPV00, and #0500JPV which are continual activities (*Figure 7b*); GMN combines these three activities into one DSV. #0428DSV is the established one but #0513EPV00 and #0500JPV are in the working list; they should have a remark stating, 'component of #0428DSV'.

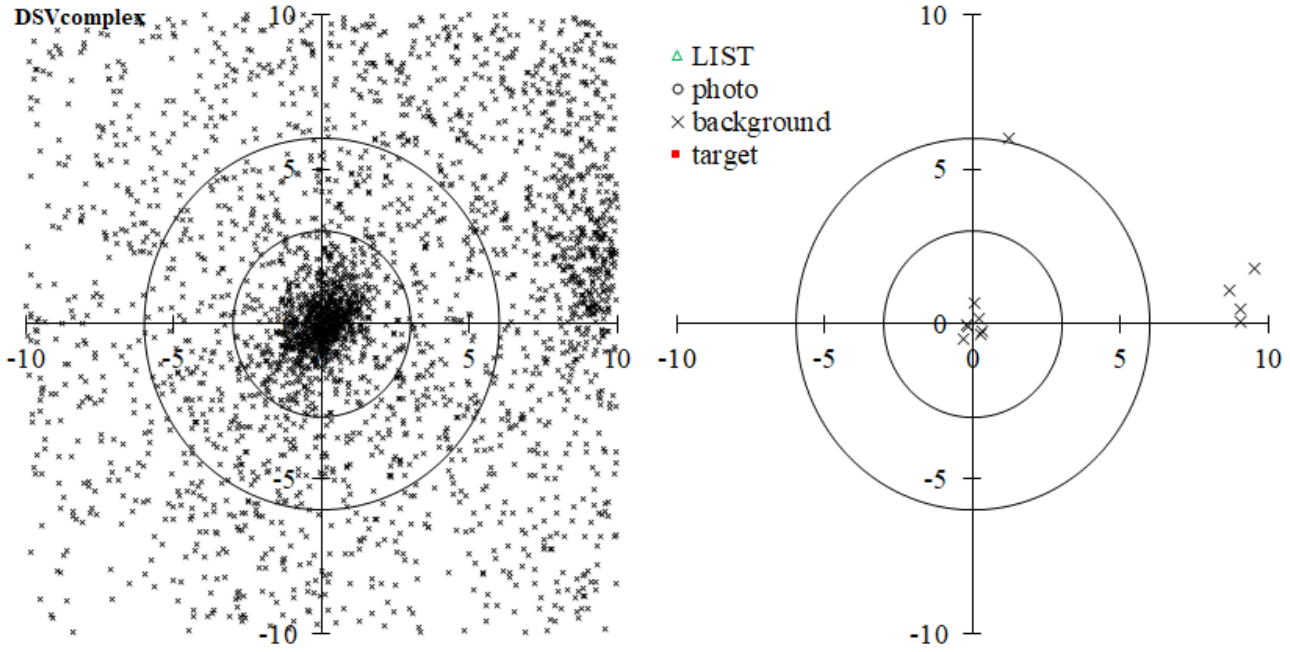

Figure 7a – DSV complex. Radiant distribution around $(\lambda-\lambda_\odot, \lambda_\odot) = (293.7°, 14.8°)$ from $\lambda_\odot = 240°$ to $\lambda_\odot = 300°$, accompanied by the radiant distribution of the SD showers and with their reference table. For explanations, see Figure 5a.

Table 4a – Explanation of the SD radiants listed around $(\lambda-\lambda_\odot, \lambda_\odot) = (293.7°, 14.8°)$ from $\lambda_\odot = 240°$ to $\lambda_\odot = 300°$.

Code	$\lambda_\odot$	$\lambda-\lambda_\odot$	β	v_g	*Distance*	*Angle*	*x*	*y*
1116NFL00	247.07	287.4	12.2	68.24	9.07	270	9.07	0.06
0502DRV00	252.5	287.0	13.8	68.1	8.77	277	8.70	1.08
0502DRV01	253.2	286.5	13.3	68.18	9.08	273	9.07	0.47
0502DRV02	256	285.6	14.9	68.3	9.68	281	9.51	1.77
0513EPV00	258	294.8	13.3	66.4	0.40	238	0.34	-0.22
0428DSV01	262	295.0	13.5	66.2	0.58	148	-0.31	-0.49
0428DSV00	267.414	293.7	14.8	66	0.29	312	0.22	0.20
0731JZB00	282	290.7	22.2	64.8	6.13	349	1.21	6.01
0500JPV00	285.6	291.5	17.3	66.2	0.69	357	0.03	0.69
0500JPV01	288.2	290.9	16.6	65.05	0.41	218	0.25	-0.33
0500JPV02	289	291.3	16.9	66.5	0.23	103	-0.23	-0.05
1124HTV00	293.06	290.6	17.3	65.88	0.17	124	-0.14	-0.10

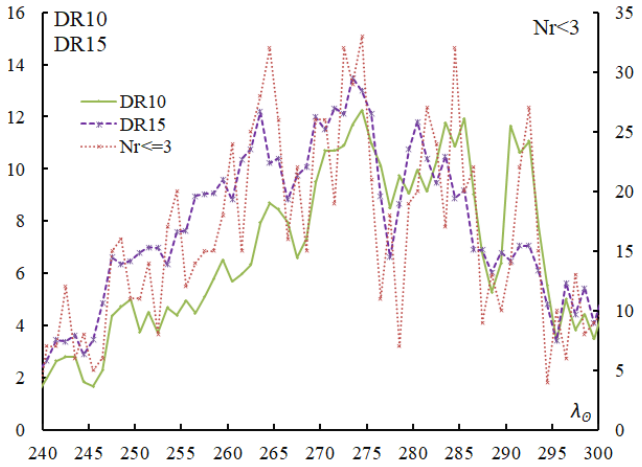

Figure 7b – Activity profiles of DSV complex. For explanations, see *Figure 6b*.

4 Minor shower in the active sporadic backgrounds

After the activity of the Taurids, the activity seems to decline once around $\lambda_\odot = 280°$, and then becomes somewhat active (*Figures 5m~5q*). Two established showers, #0096NCC and #0097SCC, during this period are listed in the SD as established. They are not distinct from the sporadic background unlike the three Virginids, #0011EVI, #0021AVI, and #0343HVI (Koseki, 2020c). Here we examine whether minor showers in the active sporadic background might be classified as established in the case of #0096NCC and #0097SCC (*Table 5*).

Table 5 – Summaries of #0096NCC and #0097SCC in the SD. All entries have the status as single established shower. Explanation: (α_g, δ_g), the geocentric coordinates of the shower radiant (J2000, deg), v_g: geocentric velocity (Km/sec), λ_g: ecliptic longitude of the shower radiant (J2000, deg), λ_g–$\lambda_\odot$: Sun centered ecliptic longitude of the shower radiant (deg), β_g: ecliptic latitude of the radiant (J2000, deg), *T*: observation technique: C-CCD, P-photo, R-radar, T-TV, V-visual.

CODE	Remark	α_g	δ_g	v_g	λ_g	λ_g–$\lambda_\odot$	β_g	*T*	Reference
0096NCC00	(1)	130	20	25.67	297	190.17	1.57	V	Arlt R., 1995
0096NCC01	(2)	134.19	14.2	26.7	300.2	192.38	-2.94	R	Nilsson, 1964
0096NCC02	–	126.72	19.92	28	297.1	187.11	0.73	P	Lindblad, 1971
0096NCC03	(3)	124.83	20.92	25.8	292.9	189.35	1.3	R	Sekanina, 1973
0096NCC04	(4)	130.52	19.71	26.4	297.1	190.62	1.42	R	Sekanina, 1976
0096NCC05	(5)	131.4	17.6	27.73	299	190.08	-0.4	V	Molau et al., 2013
0096NCC06	(6)	127.6	21.5	27.2	296	188.63	2.47	T	Jenniskens et al., 2016
0096NCC08	–	128.6	20.4	28.2	296.9	188.9	1.63	T	Shiba, 2022
0097SCC00	(7)	131.68	11.91	24.36	305.7	185.15	-5.82	P	Terentjeva, 1989
0097SCC01	(8)	118.87	7.63	24	297	182.41	-12.91	R	Nilsson, 1964
0097SCC02	(9)	131.5	10.6	26.43	298	193.02	-7.13	T	Molau & Rendtel, 2009
0097SCC03	(10)	125	14.4	27	296	187.9	-5.02	T	Jenniskens et al., 2016
0097SCC05	–	117.5	16.1	27.9	287.1	189.34	-4.85	T	Shiba, 2022

Remarks:

(1) In Arlt 1995 the shower name is delta-Cancrids, member of delta-Cancsrids group (#95 in 2006 PJ).
(2) In Nilsson 1964, Table 4 radiant 61.1.1, member of delta-Cancrids group (#95 in 2006 PJ).
(3) In Sekanina 1973, the shower name is delta-Cancrids (p. 255 & 258) member of delta-Cancrids group (#95 in PJ 2006).
(4) In Sekanina 1976, the shower name is delta-Cancrids (Tab. VI, p. 274) member of delta-Cancrids group (#95 in PJ 2006).
(5) Member of 95/DCA group.
(6) Ecliptic antihelion source, member of delta-Cancrids group (#95 in PJ2006).
(7) In Terentjeva 1989 in Table 1 alpha-Cnc(a), member of delta-Cancrids group (#95 in PJ2006).
(8) In Nilsson 1964, Table 4 radiant 61.1.2 member of delta-Cancrids group (#95 in PJ2006).
(9) Ecliptic antihelion source, twin of 204/DXL, member of delta-Cancrids group (#95 in PJ2006).
(10) Ecliptic antihelion source, twin of 204/DXL, member of delta-Cancrids group (#95 in PJ2006).

The description of "member of delta-Cancrids group (#95 in PJ2006)" in the remarks under *Table 5* for the NCC and SCC is used repeatedly, but there is actually a paper by Lindblad (1971). Prior studies were assigned to NCC or SCC by Jenniskens (2006). Lindblad detected 7 delta-Cancrids photographic orbits using a computerized stream search based on the Southworth-Hawkins D-criterion (Southworth and Hawkins, 1963). According to his method, the radiant points are mixed without distinguishing whether they are north or south of the ecliptic (*Table 6*). Jenniskens classified Lindblad's delta-Cancrids to NCC according to the average radiant points; it is now #0096NCC02.

Figure 8a represents the radiant distribution around NCC08 from $\lambda_\odot = 286.9°$ to $\lambda_\odot = 306.9°$, accompanied by the radiant distribution of the SD showers and their reference *Table 6*. Photographic radiants show no concentration.

Activity profiles Nr ≤ 3 and both activity levels DR are reasonably high, but both peaks occur earlier than the center of activity (*Figure 8b*). *Figure 9a* shows the radiant distribution around SCC05 from $\lambda_\odot$ = 277.1° to $\lambda_\odot$ = 297.1°, accompanied by the radiant distribution of the SD showers and their reference Table 7. The activity profile is similar to NCC08 (*Figure 9b*). This indicates that the active background fluctuates and gradually converges to serenity. There seem to be too many problems to consider them as established.

Table 6 – Delta-Cancrids by Lindblad (1971). For abbreviations in code, see Koseki (2009).

Code	α_g	δ_g	v_g	$\lambda_\odot$	λ_g–$\lambda_\odot$	β_g
H2-6069	119.1	22	23	293.5	183.3	1.2
H1-6081	124.7	19.8	28.5	293.7	188.7	0.2
H2-6179	112.4	34.5	19.6	295.6	173.2	12.5
H1-6189	123.7	16.8	26.7	295.7	186.4	-2.9
H1-6254	127.7	20.8	24.6	299.7	185.2	1.8
H1-6258	128.7	13.8	27.8	299.7	187.8	-4.7
H1-6292	131.7	23.8	25	301.7	186	5.7

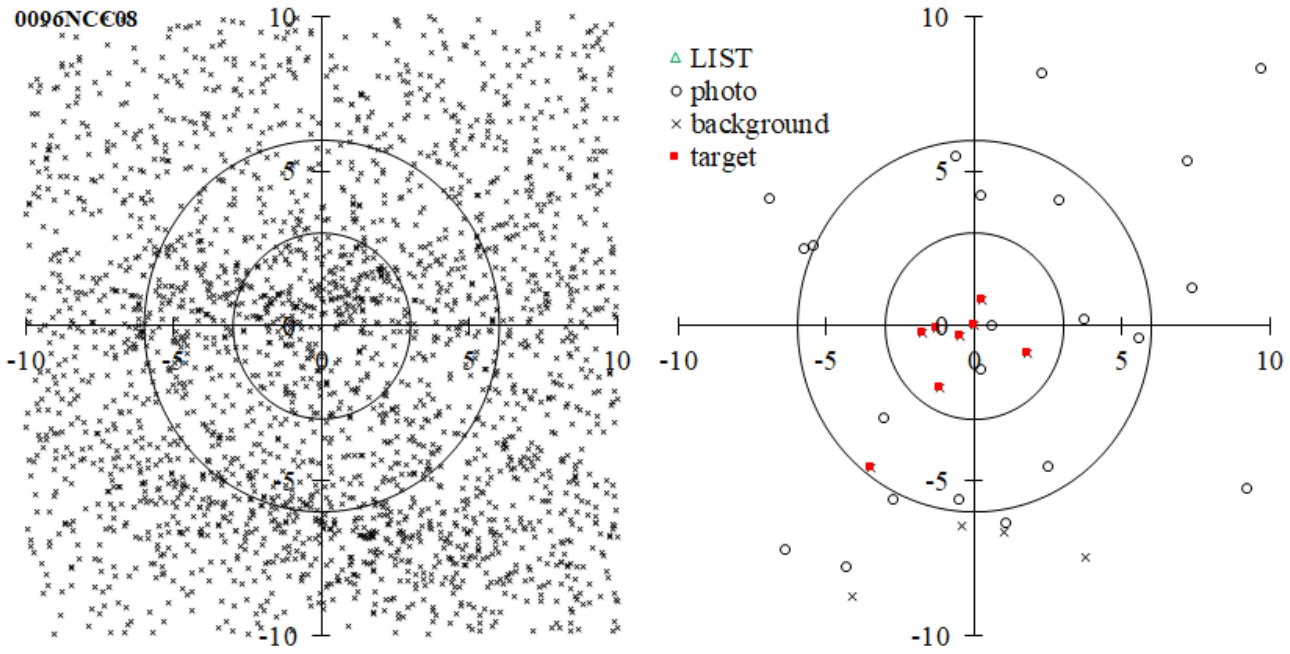

Figure 8a – Radiant distribution around NCC08 from $\lambda_\odot$ = 286.9° to $\lambda_\odot$ = 306.9°, accompanied by the radiant distribution of the SD showers and with their reference *Table 7*. For explanations, see *Figure 5a*.

Table 7 – Summaries of #0096NCC and #0097SCC in the SD.

Code	$\lambda_\odot$	λ–$\lambda_\odot$	β	v_g	*Distance*	*Angle*	*x*	*y*
0097SCC05	287.1	189.3	-4.9	27.9	6.49	176	-0.44	-6.48
0096NCC03	292.9	189.4	1.3	25.8	0.56	126	-0.45	-0.33
0096NCC06	296	188.6	2.5	27.2	0.88	342	0.27	0.84
0097SCC03	296	187.9	-5.0	27	6.72	189	1.00	-6.65
0096NCC08	296.9	188.9	1.6	28.2	0.00		0.00	0.00
0096NCC00	297	190.2	1.6	25.67	1.27	93	-1.27	-0.06
0096NCC02	297.1	187.1	0.7	28	2.00	243	1.79	-0.90
0096NCC04	297.1	190.6	1.4	26.4	1.73	97	-1.72	-0.21
0097SCC02	298	193.0	-7.1	26.43	9.68	155	-4.10	-8.76
0096NCC05	299	190.1	-0.4	27.73	2.35	150	-1.18	-2.03
0096NCC01	300.2	192.4	-2.9	26.7	5.74	143	-3.48	-4.57
0097SCC00	305.7	185.2	-5.8	24.36	8.34	207	3.74	-7.45

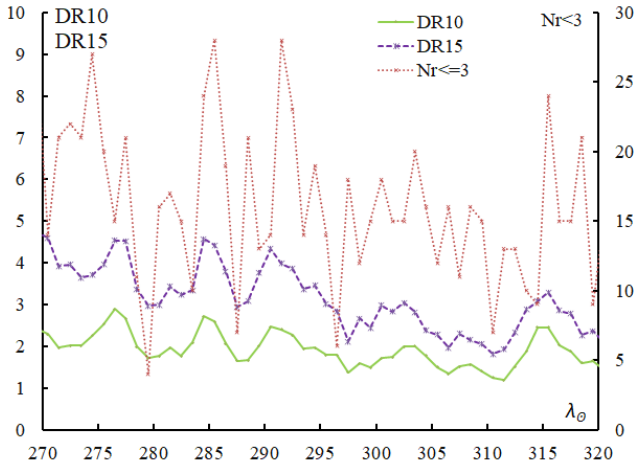

Figure 8b – Activity profiles of the NCC complex. For explanations, see *Figure 6b*.

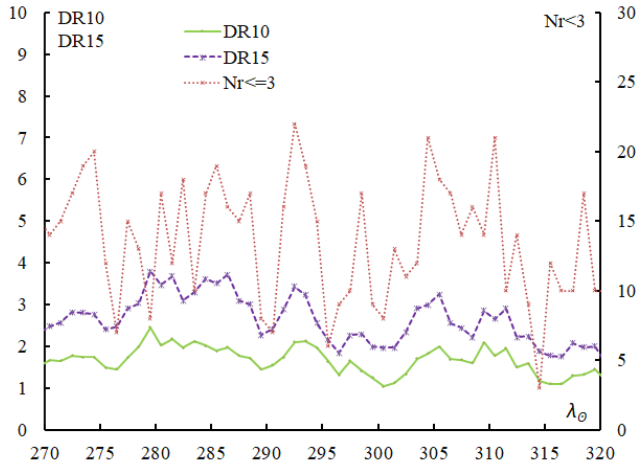

Figure 9b – Activity profiles of SCC complex. For explanations, see *Figure 6b*.

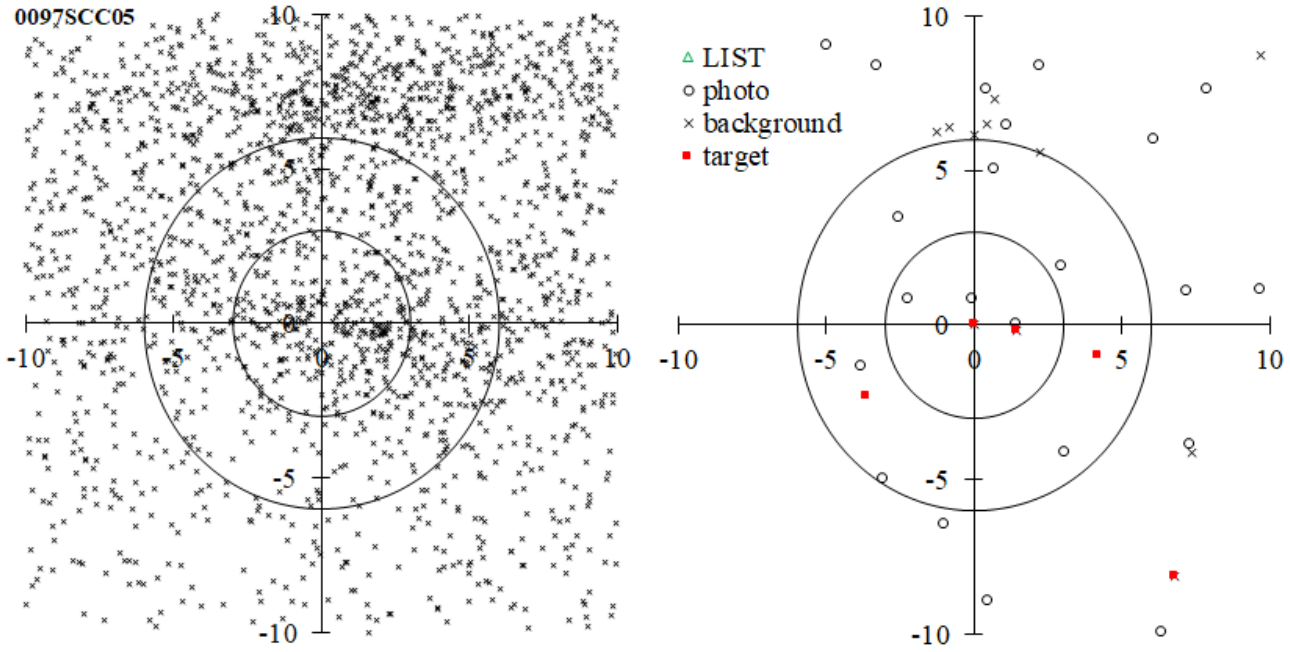

Figure 9a – Radiant distribution around SCC05 from $\lambda_{\odot}$ = 277.1° to $\lambda_{\odot}$ = 297.1°, accompanied by the radiant distribution of the SD showers and with their reference *Table 8*. For explanations, see *Figure 5a*.

Table 8 – Summaries of #0096NCC and #0097SCC in the SD.

Code	$\lambda_{\odot}$	λ–$\lambda_{\odot}$	β	v_g	*Distance*	*Angle*	*x*	*y*
1179OGE00	284.2	179.7	3.9	22	13.04	312	9.70	8.72
1193JLG00	286.927	181.9	-8.9	23.201	8.44	241	7.38	-4.11
0097SCC05	287.1	189.3	-4.9	27.9	0.00		0.00	0.00
0096NCC03	292.9	189.4	1.3	25.8	6.15	0	-0.01	6.15
0096NCC06	296	188.6	2.5	27.2	7.35	354	0.71	7.32
0097SCC03	296	187.9	-5.0	27	1.44	263	1.43	-0.17
0096NCC08	296.9	188.9	1.6	28.2	6.49	356	0.44	6.48
0096NCC00	297	190.2	1.6	25.67	6.47	7	-0.83	6.42
0097SCC01	297	182.4	-12.9	24	10.57	220	6.78	-8.11

5 Discussions

Although MDC has combined multiple reports into one, it has no experience in splitting what was considered as the same. First, it is necessary for the WG to consider the validity of the report that different activities are mixed. As a matter of common sense, the name given by the preceding report will be given priority, and the subsequent reporter will be asked to give a new name. However, the paper that raised the issue is not enough, if a member of WG does not raise issues, things will not move. There are other cases where different codes are given to the same meteor shower, but this is also left untouched unless a problem is raised by the members of the working group. WG members have not read the articles published in amateur journals and are unaware of the problems that have been pointed out, which is one of the reasons for the lingering SD confusion.

However, the most serious problem is the lack of a definition of a meteor shower. The major difference is that asteroids and comets are independent individual bodies, while a meteor shower consists of clusters of particles. Statistical treatment is essential when dealing with a meteor shower as a group of particles. For asteroids and comets, there are two options, whether they exist or not, but in the case of meteor showers, the boundary between existence and non-existence can only be expressed in a statistical sense. Meteor shower activity should be represented statistically, and we should use DR (Koseki, 2019) or Sekanina's method (Sekanina, 1970, Koseki, 2020d). Since we must consider the background activities, the current Lookup Table is a list of meteors that have been judged to belong, and it is difficult to use.

The break-point method (Neslušan et al., 1995) does not work for surveying minor meteor showers in areas with high background activity (Koseki, 2020d). When investigating meteor showers based on orbital elements, using Sekanina's method properly is desirable depending on the situation, because the breakpoint is often unclear in minor meteor showers.

Shiba divided STA into five parts in his work (2022) and reported them in the SD as they are. This is inconvenient for readers because one who reads the paper can understand what they mean but the other who did not would be confused about when and where the observers can catch the maximum of STA. There was an implicit understanding in the SD that only representative values were shown, so it is not appropriate to list several data separately. Even if the authors request that the individual data presented in the paper be published verbatim, the SD should ask the authors to provide only representative values.

References

Arlt R. (1995). "The new working list of visual meteor showers". *WGN, Journal of the International Meteor Organization*, **23**, 105–109.

Brown P., Wong D. K., Weryk R. J., and Wiegert P. (2010). "A meteoroid stream survey using the Canadian Meteor Orbit Radar. II. Identification of minor showers using a 3D wavelet transform". *Icarus*, **207**, 66–81.

Hajduková M., Rudawska R., Jopek T., Koseki M., Kokhirova G., Neslušan L. (2023). "Modification of the Shower Database of the IAU Meteor. Data Center". *Astronomy and Astrophysics*, **671**, A155. doi:10.1051/0004-6361/202244964.

Jenniskens P. (2006). Meteor Showers and their parent comets. Cambridge, Table 7, 'Working list of cometary meteor showers', 691–746.

Jenniskens P., Nénon Q., Albers J., Gural P. S., Haberman B., Holman D., Morales R., Grigsby B. J., Samuels D., Johannink C. (2016a). "The established meteor showers as observed by CAMS". *Icarus*, **266**, 331–354.

Jenniskens P., Nénon Q., Gural P. S., Albers J., Haberman B., Johnson B., Holman D., Morales R., Grigsby B. J., Samuels D., Johannink C. (2016b). "CAMS confirmation of previously reported meteor showers". *Icarus*, **266**, 355–370.

Jopek T. J., Hajduková M., Rudawska R., Koseki M., Kokhirova G., Neslušan L. (2023). "New nomenclature rules for meteor showers adopted". *New Astronomy Reviews*, **96**, 101671. doi:10.1016/j.newar.2022.101671.

Koseki M. (2009). "Meteor Shower Records: A Reference Table of Observations from Previous Centuries". *WGN, Journal of the International Meteor Organization*, **37**, 139–160.

Koseki M. (2016). "Research on the IAU meteor shower database". *WGN, Journal of the International Meteor Organization*, **44**, 151–169.

Koseki M. (2018). "Different definitions make a meteor shower distorted. The views from SonotaCo net and CAMS". *WGN, Journal of the International Meteor Organization*, **46**, 119–135.

Koseki M. (2019). "Profiles of meteor shower activities inferred from the radiant Density Ratios (DR)". *WGN, Journal of the International Meteor Organization*, **47**, 168–179.

Koseki M. (2020a). "Three components of 'Taurids' II". *WGN, Journal of the International Meteor Organization*, **48**, 36–46.

Koseki M. (2020b). "December sigma Virginids (DSV) complex". *eMetN*, **5**, 121–126.

Koseki M. (2020c). "Three Virginid showers". *eMetN*, **5**, 245–251.

Koseki M. (2020d). “Problems in searching for meteor showers”. *WGN, Journal of the International Meteor Organization*, **48**, 99–107.

Koseki M. (2021). “The activity of meteor showers recorded by SonotaCo Net video observations 2007–2018”. *eMetN*, **6**, 91–246.

Koseki M. (2023). “Major meteor showers based on Global Meteor Network data”. *eMetN*, **8**, 231–245.

Lindblad B. A. (1971). “A Computerized Stream Search among 2401 Photographic Meteor Orbits”. *Smithsonian Contributions to Astrophysics*, **12**, 14–24.

Molau S. and Rendtel J. (2009). “A Comprehensive List of Meteor Showers Obtained from 10 Years of Observations with IMO Video Meteor Network”. *WGN, Journal of the International Meteor Organization*, **37**, 98–121.

Molau S., Kac J., Berko E., Crivello S., Stomeo E., Igaz A., Barentsen G., Goncalves R. (2013). “Results of the IMO Video Meteor Network - January 2013”. *WGN, Journal of the International Meteor Organization*, **41**, 61–66.

Neslušan L., Svoreň J., Porubčan V. (1995). “A Procedure of Selection of Meteors from Major Streams for Determination of Mean Orbits”. *Earth Moon Planets*, **68**, 427–433.

Nilsson C.–S. (1964). “A southern hemisphere radio survey of meteor streams”. *Australian Journal of Physics*, **17**, 205–256.

Sekanina Z. (1970). “Statistical model of meteor streams. I. analysis of the model”. *Icarus*, **13**, 459–474.

Sekanina Z. (1973). “Statistical Model of Meteor Streams. III. Stream Search Among 19303 Radio Meteors”. *Icarus*, **18**, 253–284.

Sekanina Z. (1976). “Statistical Model of Meteor Streams. IV. A Study of Radio Streams from the Synoptic Year”. *Icarus*, **27**, 265–321.

Shiba Y. (2022). “Jupiter family meteor showers explored in SonotaCo data”. *WGN, Journal of the International Meteor Organization*, **50**, 38–61.

SonotaCo (2009). “A meteor shower catalog based on video observations in 2007–2008”. *WGN, Journal of the International Meteor Organization*, **37**, 55–62.

SonotaCo, Uehara S., Sekiguchi T., Fujiwara Y., Maeda K., and Ueda M. (2021). “J14: A Meteor Shower and Cluster Catalog”. *WGN, Journal of the International Meteor Organization*, 49:4, 76–97.

Southworth R. B. and Hawkins G. S. (1963). “Statistics of meteor streams”. *Smithsonian Contributions to Astrophysics*, **7**, 261–285.

Terentjeva A. K. (1989). “Fireball streams”. *WGN, Journal of the International Meteor Organization*, **17**, 242–245.

Vida D., Gural P., Brown P., Campbell-Brown M., Wiegert P. (2019). “Estimating trajectories of meteors: an observational Monte Carlo approach - I. Theory”. *Monthly Notices of the Royal Astronomical Society*, **491**, 2688–2705.

Vida D., Gural P., Brown P., Campbell-Brown M., Wiegert P. (2020). “Estimating trajectories of meteors: an observational Monte Carlo approach - II. Results”. *Monthly Notices of the Royal Astronomical Society*, **491**, 3996–4011.

Vida D., Šegon D., Gural P. S., Brown P. G., McIntyre M. J., Dijkema T. J., Pavletić L., Kukić P., Mazur M. J., Eschman P., Roggemans P., Merlak A., Zubrović D. (2021). “The Global Meteor Network – Methodology and first results”. *Monthly Notices of the Royal Astronomical Society*, **506**, 5046–5074.

2023: Winter, Spring and Midsummer night visual meteor observations

Koen Miskotte

Dutch Meteor Society
k.miskotte@upcmail.nl

In June, after a very cloudy and rainy spring, visual observations could be done more often again. Unfortunately, regular hay fever attacks also prevented doing visual meteor observations during several clear nights in June. This report also describes some earlier sessions from 2023.

1 Introduction

As written, the period January–May 2023 was characterized by many cloudy days and a lot of rain. The night 21–22 January was partly clear, but the observations were also ended by clouds. Two sporadic magnitude 0 and +1 meteors were the most beautiful ones. Observations were done from the flat roof of the dormer (my so called "meteor platform"), the temperature dropped to –4 degrees Celsius. Two nights with clear skies followed at the end of February: February 25–26 and February 26–27. During both nights observations were done from the Groevenbeekse Heide (a heath). Very low temperatures were recorded at ground level: on February 26 –8 degrees Celsius and on February 27 even –12 degrees Celsius! Due to the low meteor activity season only a few meteors were seen, I counted between 5 and 9 meteors an hour. No bright meteors in the first night, the second yielded a few more meteors of +1 and –1. Table 1 provides an overview of all observations until July 1st, 2023.

Table 1 – Overview of the author's observations at Ermelo. T_{min} is the effective time in minutes N_d is the number of meteors per night.

Date	T_{min}	Lm	SQM_{mx}	N_d	Fireball
21–22/01	105	6.2	20.28	15	~
25–26/02	180	6.4	20.45	21	~
26–27/02	135	6.3	20.38	17	~
18–19/04	140	6.2	20.23	13	~
09–10/06	120	6.1	20.12	14	~
10–11/06	120	6.2	20.14	12	~
14–15/06	125	6.3	20.15	20	~
16–17/06	123	6.3	20.15	16	-3 SPO

In April the Lyrids made their appearance. Also, this month had many cloudy nights, only 18–19 and 21–22 April were partly clear. The night April 18–19 observations were done during two hours from the heath under a very hazy sky with a limiting magnitude maximum 6.2 and very low meteor activity. Only 2 Lyrids, 1 ANT and 9 SPO. April 21–22 it cleared unexpectedly around 23^h UT, I just came home from a concert and was too tired to do anything. It also seemed to be cloudy again. That indeed happened, but soon after that it cleared up again and it remained clear until the morning twilight. The all-sky camera captured 2 not too bright Lyrid fireballs. The maximum night April 22–23 had also a "clear" sky, but due to fog and very hazy conditions the limiting magnitude got no better than 4.0. So, no visual observations were possible, but again the all-sky camera captured a Lyrid fireball.

Figure 1 – The fireball of May 7, 2023 photographed through the clouds by all-sky camera EN908. Camera: Canon 6D, Sigma 8 mm F 4.0 with Lyquid Crystal Shutter set at 16 br/s.

2 Midsummer nights in June 2023

In June, in the Netherlands, it gets no longer astronomical dark. The Sun does not get lower than 18 degrees below the horizon, this results in a twilight starry sky in a northerly direction, while the sky background in other directions remains somewhat brighter than in other months. Each night there is a period of about two hours when de limiting magnitude is increasing from lm 5.8 to 6.2 sometimes 6.3 at 23^h30^m UT, and then slowly decreasing again to 5.8 at the end of the session. Despite the lesser viewing conditions, there is still quite a bit to see, and the permanent twilight in northern direction, the possible Noctilucent clouds (NLC), the sounds of birds, frogs and foxes, adds something special to the night sky. And there are nice numbers of meteors to see when the transparency is good. This year in June I had another two weeks of vacation and finally a period of warm and stable summer weather started. No vacation in northern France this year, we stayed at home for several reasons.

Lots of clear nights, but some of these nights I could not observe due to very hazy conditions or severe hay fever attacks.

In total I was able to do four short sessions. All observations were done at the Groevenbeekse Heide. During all sessions frogs could be heard on the heath, I had never heard that before from that location! A number of times I was also visited by a large owl.

June 9–10, 2023
Very hazy conditions this night. At the zenith, the limiting magnitude still reached 6.2, but the transparency quickly decreases towards the horizon. For example, of the constellation Scorpio only the stars Antares and β and δ were (barely) visible. The first hour only 5 and the second hour still 9 meteors were counted. An Antihelion meteor of +2 was the highlight. Of course, many dozens of satellites were visible again, but I didn't get the impression that it was much more than in previous years. More often visible are those short bright flashes of light caused by rapidly rotating or spinning satellites. With the disappearance of the Iridium satellites, the associated very bright "Iridium" flares have disappeared. No NLCs were visible this night.

June 10–11, 2023
This night the conditions were slightly better. The Milky Way was a little easier to see and more stars could be seen in the Scorpio region. However, this had no positive effect on the meteors, with hourly counts of only 6 meteors in both hours, one of which was a +3 Antihelion. No meteors from the gamma Delphinid radiant were seen. Again, no NLCs were visible this night.

June 14–15, 2023
Finally, a beautiful night with great transparency and a beautiful Milky Way was visible despite the gray nights. The limiting magnitude briefly touched 6.3 around 23^h40^m UT. In total 8 and 12 meteors were seen respectively; these are good numbers for a June night! A possible June Lyrid of +1 was seen moving from Hercules to Corona Borealis. Three Antihelions (+3, +4, +4) were counted. A beautiful +4 APEX meteor moved along a long trajectory across the sky. No NLCs were seen this night.

June 15–16, 2023
Again, a nice clear night, but it was just a little less than the previous night, the limiting magnitude briefly touched 6.3. With hourly counts of 7 and 9 the activity was nice. This night I saw a striking number of bright meteors. First a beautiful short, orange and fast –2 sporadic meteor appeared above the star β Scorpio. At 23^h44^m UT a fast +1 sporadic meteor in Cygnus and at 23^h48^m UT a magnitude 0 sporadic meteor in Cassiopeia. The most beautiful meteor was at 00^h27^m UT, just before the end of the session: a fast yellow sporadic meteor of –2 with a short flash of -3 again in Cygnus leaving a persistent train of 3 seconds.

During the last minutes of this session, sharply defined fog banks formed over the heath. What a beautiful sight! Because of the clean and dry air, it was a relatively cold night. Around 00^h22^m UT the temperature was +2 degrees Celsius at ground level.

Figure 2 – The big fireball of May 27, 2023: 10 seconds of fireworks. According to many eye witness accounts the fireball showed fragmentation during a large part of the traject. Camera: Canon 6D, Sigma 8 mm F 4.0 with Lyquid Crystal Shutter set at 16 br/s.

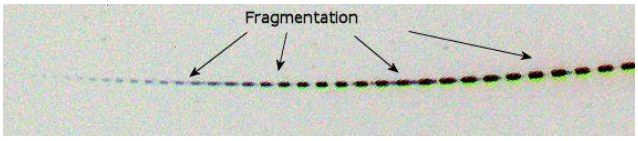

Figure 3 – Fragmentation is also clearly visible of the image! A sonic boom was heard by an observer from the Bussloo Public Observatory.

3 Conclusion

The first half of 2023 was not a very good one for visual meteor observations. In total, only 128 meteors were counted. My all-sky camera EN908 recorded several nice fireballs during this period. On May 7, 2023 at $20^h27^m05^s$ UT, a bright fireball was obtained through many clouds. This turned out to be simultaneous with all-sky cameras at Dwingeloo (operator Felix Bettonvil) and Oostkapelle (operator Klaas Jobse). The brilliant fireball of May 27, 2023, $01^h09^m08^s$ UT was also beautifully captured from Ermelo, including some fragmentation. This fireball was captured by 11 other stations of the BeNeLux European Network[14]. The results of these fireballs can be found in the newest issue of Radiant 2023-2[15] and on the website of the Dutch Meteor Society[16].

[14] https://www.dutch-meteor-society.nl/2023/05/27/tatsu-3993/
[15] https://www.dutch-meteor-society.nl/2023/07/01/radiant-2023-2/
[16] https://www.dutch-meteor-society.nl/

The meteorite-dropping-Pinkster-fireball, 2023 May 27, over Belgium and the Netherlands

Kees Habraken[1], Denis Vida[2,3], Hervé Lamy[2,4], Pierre de Ponthiere[2], Roel Gloudemans[2], Jacques Masson[2], Uwe Glässner[2], Jürgen Dörr[2], Tammo Jan Dijkema[2], Steve Rau[2], Damir Šegon[2]

[1] **Global Meteor Network, Grindweg 3, 4474NN Kattendijke, the Netherlands**
meteorkees@gmail.com

[2] **Global Meteor Network**

[3] **Department of Physics and Astronomy, University of Western Ontario, London, Ontario, N6A 3K7, Canada**
dvida@uwo.ca

[4] **Royal Belgian Institute for Space Aeronomy, Brussels, Belgium**

On May 27, 2023, a fireball dropped ~200 g of meteorites Northeast of Deventer in the Netherlands. Its fall has been observed by 13 cameras of the Global Meteor Network. We report its trajectory, strewn field, and orbit.

1 Introduction

This article is written from the perspective of the lead author, Kees Habraken.

What has the track of a fireball to do with the track of a ship? Well, they both started in Antwerp. On May 26 at 21^h30^m UTC while asleep I got a phone call, "work to do". They called me to pilot the vessel Quetzal Arrow (*Figure 1*) from Antwerp (BE) to Flushing (NL). I knew it would be a long night work. On the way to the pilot station, I saw clear skies. Finally perfect weather for the RMS cameras to observe meteors. I boarded the vessel at Kallo-Lock around 23^h30^m and started piloting the vessel down the river Westerscheldt. At 01^h09^m UTC the vessel was heading NW when we left the light polluted terminals of the port of Antwerp, Belgium. A nice calm dark river with a crescent moon lying ahead.

Figure 1 – The ship Quetzal Arrow.

The Quetzal Arrow is not the fasted vessel. Plenty time to stare out of the window and watch the sky, of course, hoping to see a nice fireball or other nice event on the night sky. Nothing seen! After 4 hours sailing, together with the officer on watch, we watched the sunrise. We counted the sunspots (6) which were easy to identify. That was the most exciting event of the night…. I thought! We talked a bit about the destination of the vessel. She was on the way to the West coast USA via the Panama Canal, and final destination Canada the mate told me. That will a take a few weeks. My job was done, the vessel reached safely deep water and she was on the way to Canada, I wished them a safe voyage.

2 Fireball reduction

Back at home at around 07^h30^m local time, I checked the GMN weblog[17] to see the captures of the night from the 4 RMS cameras. Hey, what is that? Camera NL000K captured a bright event (*Figure 2*). Hmmm, due to the reflections it looked like a re-entry of a piece space junk. I checked the weblog of the Belgian cameras. Yup, they captured the event too. Okay, this could be nice, but I was also disappointed that I missed the event while at work all night! It happened behind me at 01^h09^m UTC when the vessel was just leaving Antwerp. The fireball's track started above Antwerp, and I did not see it! That's why they say, "*it is a once in a lifetime event to see a fireball with the naked eye*". I was excited, disappointed, and tired at the same time. What to do? Stay awake and check in detail the captured data or take a rest and check the data when awake again. Nature took over, the man with the hammer came along and I took a good sleep.

Figure 2 – The FF file for NL000K.

[17] https://globalmeteornetwork.org/weblog/

Awake again at 12^h30^m a bit early after an all-night job, but too excited about the event, I wanted to warn other observers that maybe a nice event had been captured by the RMS cameras. I pushed out a mail to the GMN mailing list, and I started checking the timelapse of other cameras than mine. For sure this was a nice event. Work to do, cool.

Figure 3 – The captured stack for NL000K.

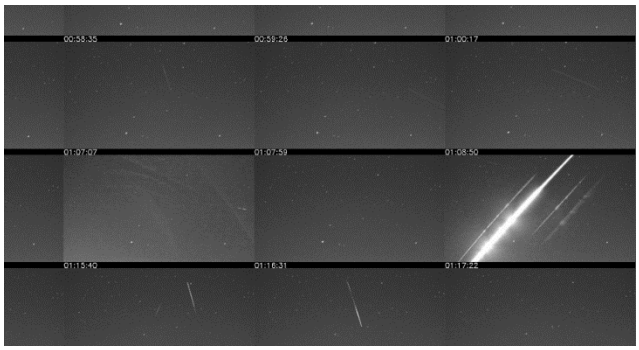

Figure 4 – The captured thumbnails for NL000K.

Soon it became clear via the incoming messages that it was a nice fireball. Saving and collecting data was the first job. Via mail some other observers from Belgium and Germany reported back with the datafiles. A daily check on the GMN weblog gives a good impression about what happened during the night. Check also the captured thumbnails, they give a good impression of the events. For example, the mentioned fireball was not in the stack image with meteor detections, but those only usually contain fainter meteors. (*Figure 3*). But the fireball was clearly visible in the captured thumbnails *(Figure 4*).

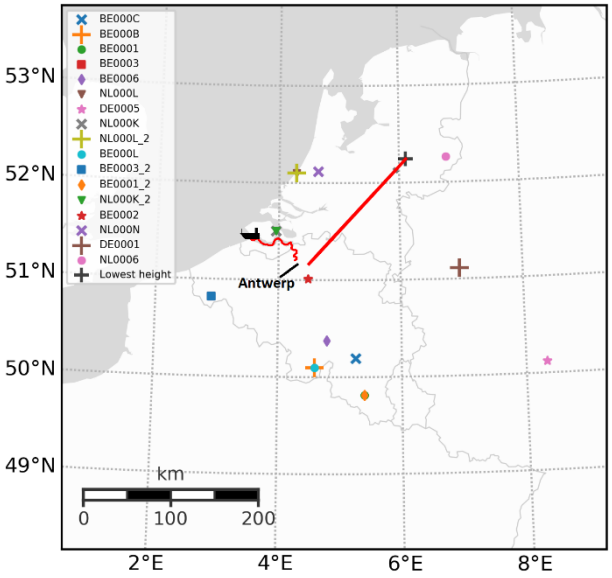

Figure 5 – Ground track of the fireball on 2023, May 27, $01^h09^m07^s$ UTC and the route of the vessel Quetzal Arrow.

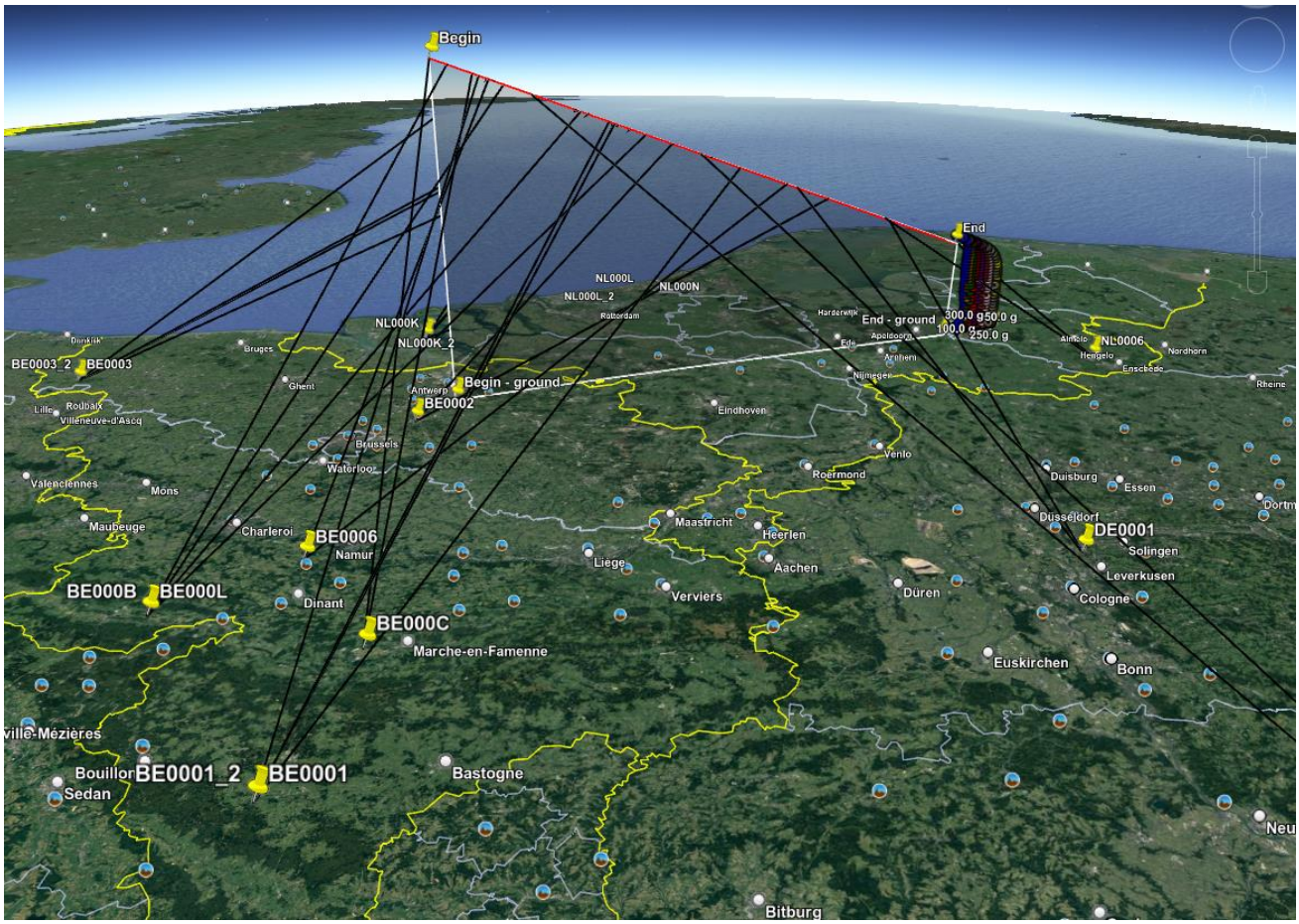

Figure 6 – 3D plot of the trajectory and the camera locations involved in the solution.

I was gently motivated to reduce this event. I watched the SkyFit2 software (Vida et al., 2021) tutorial a few times and started feeding it with the data I received from stations in Germany, Belgium, and The Netherlands (*Figure 5*). With some help I got the WMPL (Western Meteor Python Library) software to work (Vida et al., 2020), but I was missing data from the middle of the track as Denis told me later. Denis Vida collected all necessary data together to get a nice reduction of this Pinkster-fireball and came with the happy message that a small number of meteorites were dropped.

3 Trajectory

Denis improved my initial trajectory solution by adding GMN cameras that observed the fireball, a total of 13! The full trajectory and the positions of cameras are shown in *Figure 6*. The average measurement scatter from all cameras was well within 100 meters (*Figure 7*). NL0006 was the only one to capture the end of the fireball and showed an interesting deviation after the final fragmentation, something that has been observed for other meteorite-dropping fireballs too (e.g., Winchcombe; King et al., 2022).

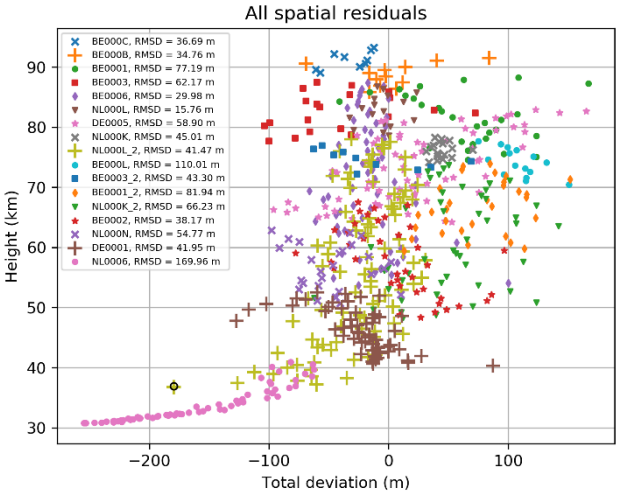

Figure 7 – All spatial residuals expressed in meters in function of the height for the fireball on 2023, May 27, $01^h09^m07^s$ UTC.

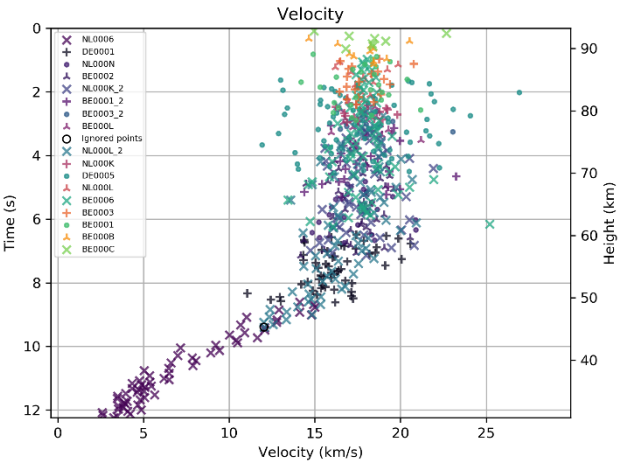

Figure 8 – Velocity and deceleration in function of time for the fireball on 2023, May 27, $01^h09^m07^s$ UTC.

The fireball first became visible at the height of ~93 km over Antwerp and it flew about 175 km NE, ending just near Apeldoorn. The terminal height was ~30.5 km and it was last observed at a speed of ~3 km/s (*Figure 8*), indicating that some meteorites might have survived!

4 Strewn field

Running the dynamic mass script in WMPL produced *Figure 9*. Assuming a meteorite density of 3500 kg/m^3 it predicts a meteorite on the ground between 140 – 380 g, with a nominal mass of about 200 g. Denis used wind measurements made in Essen (Germany, about 100 km SE) to predict the strewn field shown in *Figure 10*.

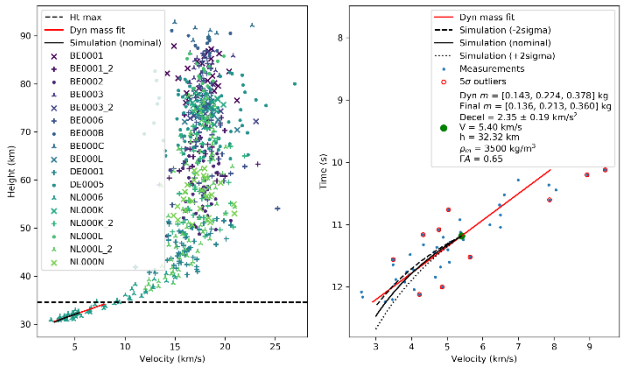

Figure 9 – The dynamic mass fit for the fireball on 2023, May 27, $01^h09^m07^s$ UTC.

Figure 10 – The strewn field for the fireball on 2023, May 27, $01^h09^m07^s$ UTC.

Due to the low elevation of the fireball of only ~21.3° the strewn field is long, the distance between the main mass and potential 10 g fragments of ~10 km. The strewn field was located NE of Deventer. Brick-shaped meteorites were assumed. As the strewn field was so big and the search zone for the main mass (1500 × 500 m) was on private land, we chose to make the strewn field public so local residents can check their properties.

5 Orbit

The orbit is nothing extraordinary, with an inclination around zero and coming from the asteroid belt (T_J = 3.4). A top-down orbit is shown in *Figure 11*. A parent body search returned a few potential candidates (2020 RG10 and 2022 KK) with Southworth-Hawkins D criterion values of < 0.05 (Southworth & Hawkins, 1963) but this is a dense part of the asteroid belt, so this correlation is most probably spurious. The radiant and full orbital elements with 1 sigma uncertainties and a 95% confidence interval are given in *Table 1*.

Table 1 – The ground fixed radiant and initial velocity, the geocentric radiant and velocity and the orbital elements.

Name	Value	1σ	95% CI lower	95% CI upper
Az. (°)	222.40	0.01	222.388	222.429
Elev. (°)	21.51	0.008	21.494	21.526
v_{ini} (km/s)	17.71	0.001	17.704	17.71
R.A. (°)	221.42	0.01	221.396	221.440
Decl. (°)	–16.63	0.01	-16.650	-16.614
v_g (km/s)	14.03	0.002	14.025	14.031
a (AU)	2.22	0.0008	2.2138	2.2169
e	0.6164	0.0001	0.6162	0.6166
i (°)	0.25	0.004	0.2411	0.2551
ω (°)	55.896	0.022	55.854	55.935
Ω (°)	244.043	0.018	244.01	244.08
q (AU)	0.8498	0.00007	0.8497	0.8500

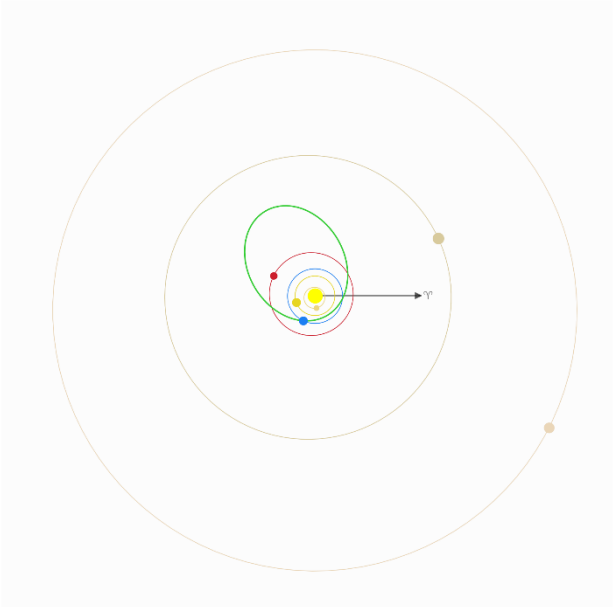

Figure 11 – The orbit in the Solar System for the fireball on 2023, May 27, $01^h09^m07^s$ UTC.

References

King A. J., Daly L., Rowe J., Joy K. H., Greenwood R. C., Devillepoix H. A., Suttle M. D., Chan Q. H., Russell S. S., Bates H. C. and Bryson J. F. (2022). "The Winchcombe meteorite, a unique and pristine witness from the outer solar system". *Science Advances*, **8**(46), p.eabq3925.

Southworth R. B. and Hawkins G. S. (1963). "Statistics of meteor streams". *Smithsonian Contributions to Astrophysics*, **7**, 261–285.

Vida D., Gural P. S., Brown P. G., Campbell-Brown M. and Wiegert P. (2020). "Estimating trajectories of meteors: an observational Monte Carlo approach–I. Theory". *Monthly Notices of the Royal Astronomical Society*, **491**, 2688–2705.

Vida D., Šegon D., Gural P. S., Brown P. G., McIntyre M. J., Dijkema T. J., Pavletić L., Kukić P., Mazur M. J., Eschman P., Roggemans P., Merlak A., Zubrović D. (2021). "The Global Meteor Network – Methodology and first results". *Monthly Notices of the Royal Astronomical Society*, **506**, 5046–5074.

June 2023 report CAMS-BeNeLux

Carl Johannink

Am Ollenkamp 4, 48599 Gronau, Germany
c.johannink@t-online.de

A summary of the activity of the CAMS-BeNeLux network during the month of June 2023 is presented. This month was good for 10725 multi-station meteors resulting in 2889 orbits.

1 Introduction

In June the sporadic meteor activity is slowly rising. On the other hand, no major shower is present in this month and astronomical twilight is lasting all night from BeNeLux latitudes. So, in all, meteor rates are low, and it is no surprise that the total amount of orbits in June after 11 years of CAMS activity is one of the lowest of all months.

2 June 2023 statistics

The weather in June was perfect: warm and sunny. In fact, June was the sunniest and warmest month of June since the start of the measurements in the Netherlands in 1901.

With regard to all months in a year, it was the sunniest month after July 2018 and May 1989. So, it should be no surprise that we could collect orbits in every single night this month.

In 17 nights, we could collect more than 100 orbits. This is a new record for June. The best results in June so far, looking at this limit, were obtained in June 2020 (12 nights with more than 100 orbits).

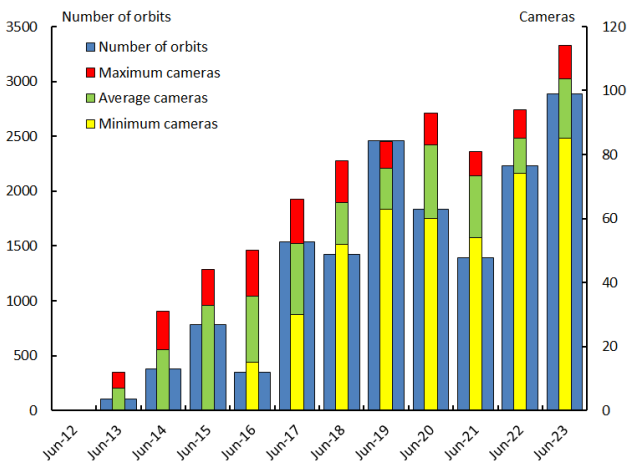

Figure 1 – Comparing June 2023 to previous months of June in the CAMS-BeNeLux history. The blue bars represent the number of orbits, the red bars the maximum number of cameras capturing in a single night, the green bars the average number of cameras capturing per night and the yellow bars the minimum number of cameras.

CAMS BeNeLux collected 10725 multi-station meteors this month, resulting in a total of 2889 orbits. And yes, this too is a new record for this month. 60.5% of all orbits were captured by more than two stations, a bit more than in the last months as a result from the good conditions in the BeNeLux.

On average 103.7 cameras were active this month. This number is much higher than last year, since the number of stations grow significantly compared to last year. At least 85 cameras were active in a single night this month. But these numbers are lower than last month, because observations at several stations were confronted this month with technical problems during several days.

We hope that most of the problems are solved next month.

Table 1 – June 2023 compared to previous months of June.

Year	Nights	Orbits	Stations	Max. Cams	Min. Cams	Mean Cams
2012	0	0	4	0	–	0.0
2013	16	102	9	12	–	7.0
2014	23	379	13	31	–	19.0
2015	20	779	15	44	–	32.9
2016	18	345	17	50	15	35.7
2017	26	1536	19	66	30	52.1
2018	28	1425	21	78	52	64.9
2019	28	2457	20	84	63	75.6
2020	27	1834	24	93	60	83.1
2021	22	1389	26	81	54	73.3
2022	30	2228	30	94	74	85.2
2023	30	2889	35	114	85	103.7
Total	268	15363				

3 Conclusion

Compared to other months of June this year gave a record number of orbits, due to very good weather conditions.

Acknowledgement

Many thanks to all participants in the CAMS-BeNeLux network for their dedicated efforts. The CAMS-BeNeLux team was operated by the following volunteers during the month of June 2023:

Hans Betlem (Woold, Netherlands, Watec 3071, 3072, 3073, 3074, 3075, 3076, 3077 and 3078), *Felix Bettonvil* (Utrecht, Netherlands, Watec 376), *Jean-Marie Biets* (Wilderen, Belgium, Watec 379, 380 and 381), *Ludger Boergerding* (Holdorf, Germany, RMS 3801), *Günther Boerjan* (Assenede, Belgium, RMS 3823), *Martin Breukers* (Hengelo, Netherlands, Watec 320, 321, 322, 323, 324, 325, 326 and 327, RMS 319, 328 and 329), *Seppe Canonaco* (Genk, RMS 3818 and 3819), *Pierre de Ponthiere* (Lesve, Belgium, RMS 3816 and 3826), *Bart Dessoy* (Zoersel, Belgium, Watec 397, 398, 804, 805, 806, 3888 and RMS 3827), *Tammo Jan Dijkema* (Dwingeloo, Netherlands, RMS 3199), *Isabelle Ansseau*, *Jean-Paul Dumoulin*, *Dominique Guiot* and *Christian Wanlin* (Grapfontaine, Belgium, Watec 814 and 815, RMS 3814 and 3817), *Uwe Glässner* (Langenfeld, Germany, RMS 3800), *Luc Gobin* (Mechelen, Belgium, Watec 3890, 3891, 3892 and 3893), *Tioga Gulon* (Nancy, France, Watec 3900 and 3901), *Robert Haas* (Alphen aan de Rijn, Netherlands, Watec 3160, 3161, 3162, 3163, 3164, 3165, 3166 and 3167), *Robert Haas* (Texel, Netherlands, Watec 811, 812 and 813), *Kees Habraken* (Kattendijke, Netherlands, RMS 3780, 3781, 3782 and 3783), *Klaas Jobse* (Oostkapelle, Netherlands, Watec 3030, 3031, 3032, 3033, 3034, 3035, 3036 and 3037), *Carl Johannink* (Gronau, Germany, Watec 3100, 3101, 3102), *Reinhard Kühn* (Flatzby, Germany, RMS 3802), *Hervé Lamy* (Dourbes, Belgium, Watec 394 and 395, RMS 3825 and 3841), *Hervé Lamy* (Humain, Belgium, RMS 3821 and 3828), *Hervé Lamy* (Ukkel, Belgium, Watec 393 and 817), *Hartmut Leiting* (Solingen, Germany, RMS 3806), *Koen Miskotte* (Ermelo, Netherlands, Watec 3051, 3052, 3053 and 3054), *Pierre-Yves Péchart* (Hagnicourt, France, RMS 3902, 3903, 3904 and 3905), *Eduardo Fernandez del Peloso* (Ludwigshafen, Germany, RMS 3805), *Tim Polfliet* (Gent, Belgium, Watec 396, RMS 3820 and 3840), *Steve Rau* (Oostende, Belgium, RMS 3822), *Steve Rau* (Zillebeke, Belgium, Watec 3850 and 3852, RMS 3851 and 3853), *Paul and Adriana Roggemans* (Mechelen, Belgium, RMS 3830 and 3831, Watec 3832, 3833, 3834, 3835, 3836 and 3837), *Jim Rowe* (Eastbourne, Great Britain, RMS 3829), *Philippe Schaack* (Roodt-sur-Syre, Luxemburg, RMS 3952), *Hans Schremmer* (Niederkruechten, Germany, Watec 803), *Erwin van Ballegoij* (Heesh, Netherlands Watec 3148 and 3149), *Andy Washington* (Clapton, England, RMS 3702).

July 2023 report CAMS-BeNeLux

Carl Johannink

Am Ollenkamp 4, 48599 Gronau, Germany
c.johannink@t-online.de

A summary of the activity of the CAMS-BeNeLux network during the month of July 2023 is presented. This month was good for 13808 multi-station meteors resulting in 3966 orbits.

1 Introduction

In July the sporadic meteor activity is rising. Some major showers as the Capricornids and the Southern delta Aquariids are present mainly towards the end of this month and astronomical twilight is no longer lasting all night at BeNeLux latitudes. So, in all, meteor rates are increasing.

2 JuLy 2023 statistics

The weather in July was very unsettled: especially the eastern parts of the BeNeLux had to deal with much rain: around 50% more than the normal amount for this month. Despite the unfavorable weather, we could collect more than 100 orbits in 18 nights. One night more than in June, but compared to for instance July 2022 it is not a record as then we had 24 nights with more than 100 orbits.

CAMS-BeNeLux collected 13808 multi-station meteors this month, resulting in a total of 3966 orbits. This is the fourth best result for this month since the start of our network in 2012, mainly because of the large number of cameras meanwhile involved in our network.

It happened very regularly this month, that some stations had clouds during a part of the night, but due to the large number of cameras, many meteors were nevertheless captured simultaneously.

Skies were completely overcast on July 27–28. This was the third night this year, after January 24 and March 6, that not a single meteor was capture by any of our cameras.

58.9% of all orbits were captured by more than two stations, a bit less than in the last months as a result of the unsettled weather in the BeNeLux.

This month, we could welcome *Horst Meyerdierks*, located in Germany in Osterholz Scharmbeck near Bremen, as a new station (CAMS number 3807) in our network.

On average 102 cameras were active this month. This number is a bit lower than last month. Main reason is that some operators of RMS cameras struggled with technical problems. All problems were solved within a few nights, so at least 89 cameras were still active in a single night this month.

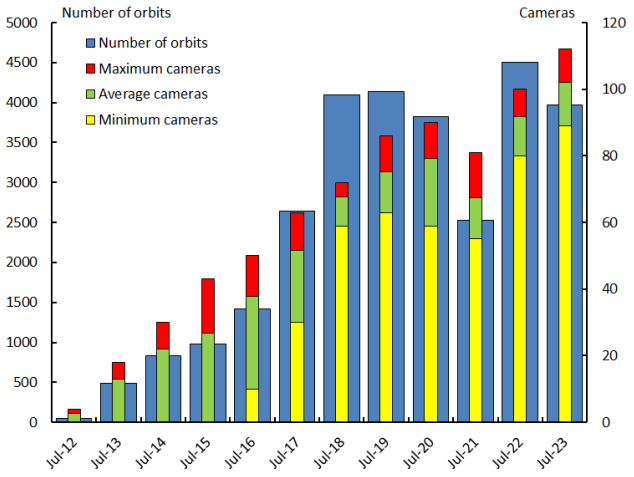

Figure 1 – Comparing July 2023 to previous months of July in the CAMS-BeNeLux history. The blue bars represent the number of orbits, the red bars the maximum number of cameras capturing in a single night, the green bars the average number of cameras capturing per night and the yellow bars the minimum number of cameras.

Table 1 – July 2023 compared to previous months of July.

Year	Nights	Orbits	Stations	Max. Cams	Min. Cams	Mean Cams
2012	7	49	4	4		2.6
2013	22	484	10	18		12.9
2014	19	830	14	30		22.0
2015	28	976	15	43		26.7
2016	28	1420	18	50	10	37.9
2017	27	2644	20	63	30	51.6
2018	30	4098	19	72	59	67.7
2019	30	4139	21	86	63	75.2
2020	28	3823	24	90	59	79.1
2021	28	2525	27	81	55	67.3
2022	31	4499	30	100	80	91.7
2023	30	3966	36	112	89	102.1
Total	308	29453				

3 Conclusion

Compared to other months of July, this year resulted in a good number of orbits, despite unfavorable weather conditions.

Acknowledgement

Many thanks to all participants in the CAMS-BeNeLux network for their dedicated efforts. The CAMS-BeNeLux team was operated by the following volunteers during the month of July 2023:

Hans Betlem (Woold, Netherlands, Watec 3071, 3072, 3073, 3074, 3075, 3076, 3077 and 3078), *Felix Bettonvil* (Utrecht, Netherlands, Watec 376), *Jean-Marie Biets* (Wilderen, Belgium, Watec 379, 380 and 381), *Ludger Boergerding* (Holdorf, Germany, RMS 3801), *Günther Boerjan* (Assenede, Belgium, RMS 3823), *Martin Breukers* (Hengelo, Netherlands, Watec 320, 321, 322, 323, 324, 325, 326 and 327, RMS 319, 328 and 329), *Seppe Canonaco* (Genk, RMS 3818 and 3819), *Pierre de Ponthiere* (Lesve, Belgium, RMS 3816 and 3826), *Bart Dessoy* (Zoersel, Belgium, Watec 397, 398, 804, 805, 806, 3888 and RMS 3827), *Tammo Jan Dijkema* (Dwingeloo, Netherlands, RMS 3199), *Isabelle Ansseau*, *Jean-Paul Dumoulin*, *Dominique Guiot* and *Christian Wanlin* (Grapfontaine, Belgium, Watec 814 and 815, RMS 3814 and 3817), *Uwe Glässner* (Langenfeld, Germany, RMS 3800), *Luc Gobin* (Mechelen, Belgium, Watec 3890, 3891, 3892 and 3893), *Tioga Gulon* (Nancy, France, Watec 3900 and 3901), *Robert Haas* (Alphen aan de Rijn, Netherlands, Watec 3160, 3161, 3162, 3163, 3164, 3165, 3166 and 3167), *Robert Haas* (Texel, Netherlands, Watec 811 and 812), *Kees Habraken* (Kattendijke, Netherlands, RMS 3780, 3781, 3782 and 3783), *Klaas Jobse* (Oostkapelle, Netherlands, Watec 3030, 3031, 3032, 3033, 3034, 3035, 3036 and 3037), *Carl Johannink* (Gronau, Germany, Watec 3100, 3101, 3102), *Reinhard Kühn* (Flatzby, Germany, RMS 3802), *Hervé Lamy* (Dourbes, Belgium, Watec 394 and 395, RMS 3825 and 3841), *Hervé Lamy* (Humain, Belgium, RMS 3821 and 3828), *Hervé Lamy* (Ukkel, Belgium, Watec 393 and 817), *Hartmut Leiting* (Solingen, Germany, RMS 3806), *Horst Meyerdierks* (Osterholz-Scharmbeck, Germany, RMS 3807), *Koen Miskotte* (Ermelo, Netherlands, Watec 3051, 3052, 3053 and 3054), *Pierre-Yves Péchart* (Hagnicourt, France, RMS 3902, 3903, 3904 and 3905), *Eduardo Fernandez del Peloso* (Ludwigshafen, Germany, RMS 3805), *Tim Polfliet* (Gent, Belgium, Watec 396, RMS 3820 and 3840), *Steve Rau* (Oostende, Belgium, RMS 3822), *Steve Rau* (Zillebeke, Belgium, Watec 3850 and 3852, RMS 3851 and 3853), *Paul and Adriana Roggemans* (Mechelen, Belgium, RMS 3830 and 3831, Watec 3832, 3833, 3834, 3835, 3836 and 3837), *Jim Rowe* (Eastbourne, Great Britain, RMS 3829), *Philippe Schaack* (Roodt-sur-Syre, Luxemburg, RMS 3952), *Hans Schremmer* (Niederkruechten, Germany, Watec 803), *Erwin van Ballegoij* (Heesh, Netherlands Watec 3148 and 3149), *Andy Washington* (Clapton, England, RMS 3702).

Radio meteors June 2023

Felix Verbelen

Vereniging voor Sterrenkunde & Volkssterrenwacht MIRA, Grimbergen, Belgium
felix.verbelen@skynet.be

An overview of the radio observations during June 2023 is given.

1 Introduction

The graphs show both the daily totals (*Figure 1 and 2*) and the hourly numbers (*Figure 3 and 4*) of "all" reflections counted automatically, and of manually counted "overdense" reflections, overdense reflections longer than 10 seconds and longer than 1 minute, as observed here at Kampenhout (BE) on the frequency of our VVS-beacon (49.99 MHz) during the month of June 2023.

The hourly numbers, for echoes shorter than 1 minute, are weighted averages derived from:

$$N(h) = \frac{n(h-1)}{4} + \frac{n(h)}{2} + \frac{n(h+1)}{4}$$

However, due to technical problems with the beacon, data are missing from June 6 at 19^h17^m UT till June 11 at 15^h15^m UT. As already pointed out in our previous monthly report, the registrations showed abnormal jumps, the cause of which remained uncertain. Eventually it became clear that the cause lay with the beacon. Thanks to the people of AstroLab-Iris (Ypres), the repairs were carried out expertly and quickly and our beacon now functions again as it did in the past 18 years.

Lightning activity was recorded on only 3 days: on 18 and 22 June the number of lightnings was quite low, but on June 20th between 12^h and 13^h UT a violent thunderstorm raged in the vicinity of the beacon and caused hundreds of short reflections (*Figure 5*).

Solar outbursts produced strong noise almost daily. Most of them were type III at our frequency of observation, and thus relatively short-lived (*Figures 6 & 7*). Due to the problems with the beacon, it is difficult to make a global evaluation of the meteor activity, but the counts of the overdense reflections in particular show interesting shower activity.

During the period that registrations were carried out, 6 reflections longer than 1 minute were observed. A selection of these is included along with some interesting "epsilons" (*Figures 8 to 20*). Many more of these are available on request.

In addition to the usual graphs, you will also find the raw counts in cvs-format[18] from which the graphs are derived. The table contains the following columns: day of the month, hour of the day, day + decimals, solar longitude (epoch J2000), counts of "all" reflections, overdense reflections, reflections longer than 10 seconds and reflections longer than 1 minute, the numbers being the observed reflections of the past hour.

[18] https://www.meteornews.net/wp-content/uploads/2023/07/202306_49990_FV_rawcounts.csv

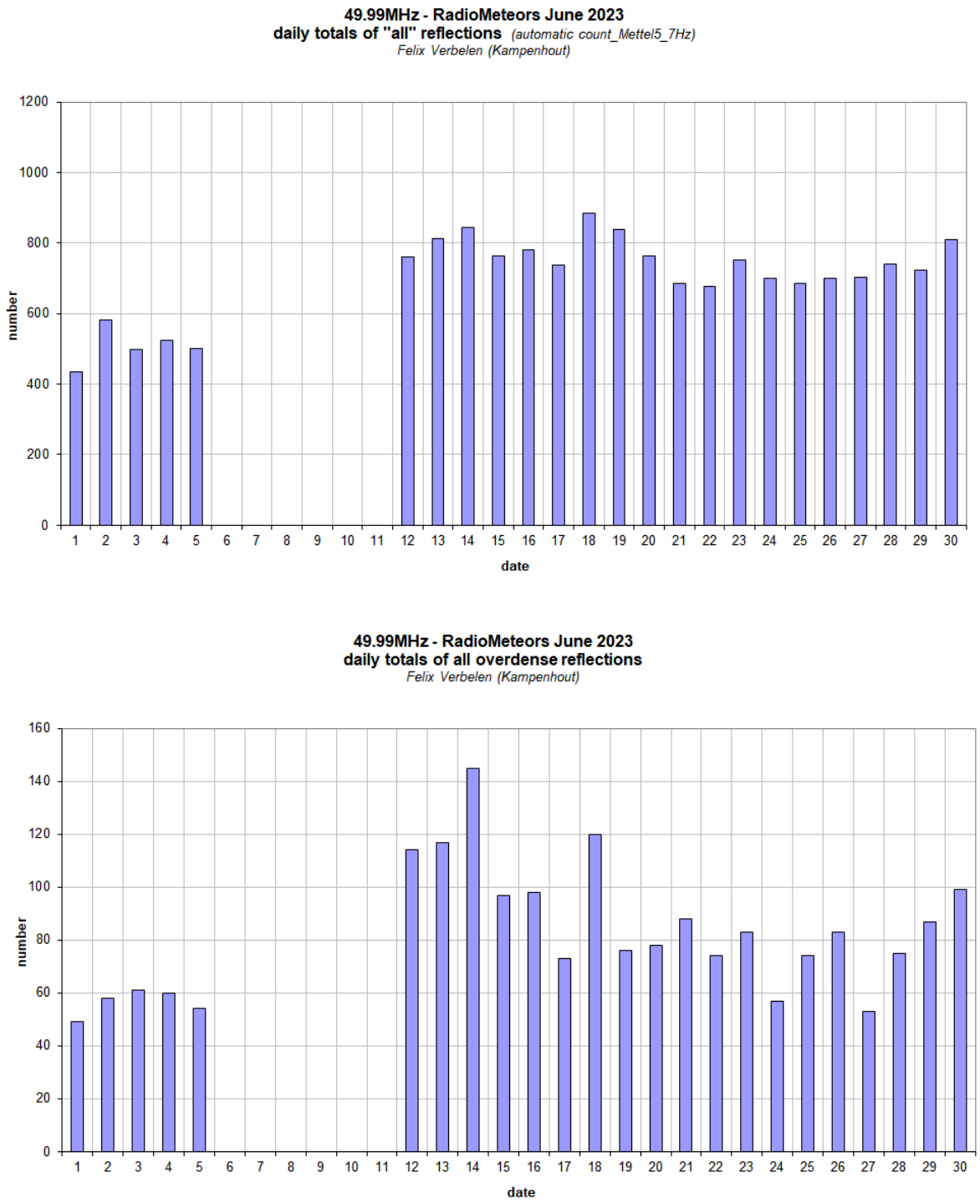

Figure 1 – The daily totals of "all" reflections counted automatically, and of manually counted "overdense" reflections, as observed here at Kampenhout (BE) on the frequency of our VVS-beacon (49.99 MHz) during June 2023.

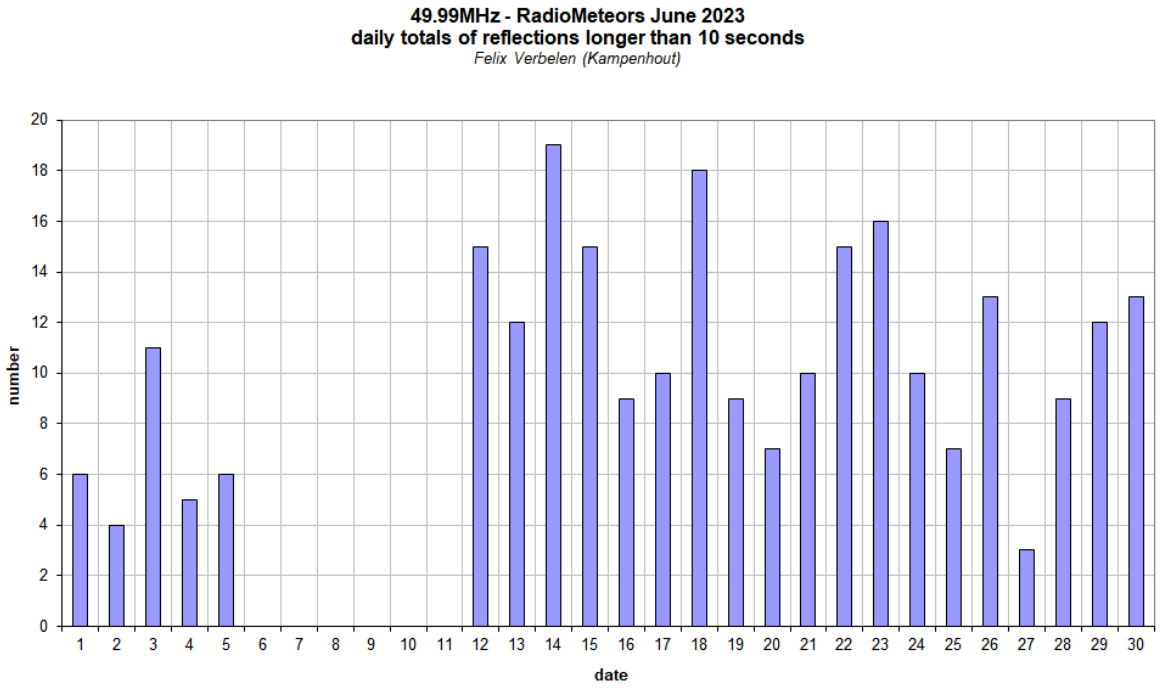

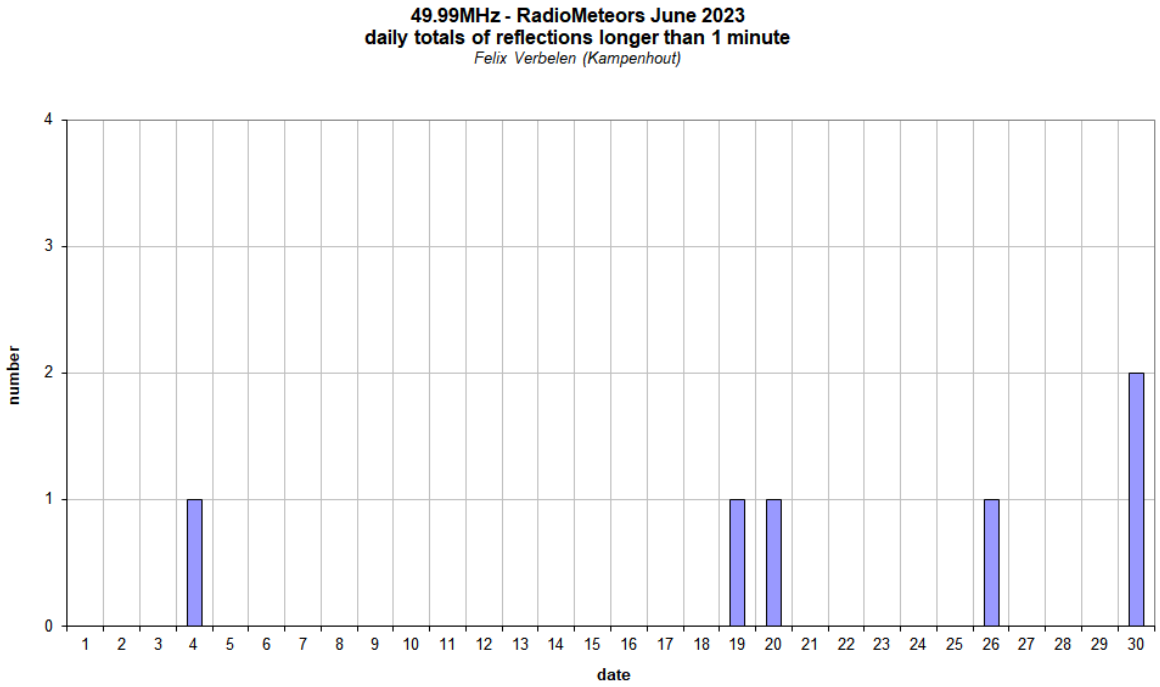

Figure 2 – The daily totals of overdense reflections longer than 10 seconds and longer than 1 minute, as observed here at Kampenhout (BE) on the frequency of our VVS-beacon (49.99 MHz) during June 2023.

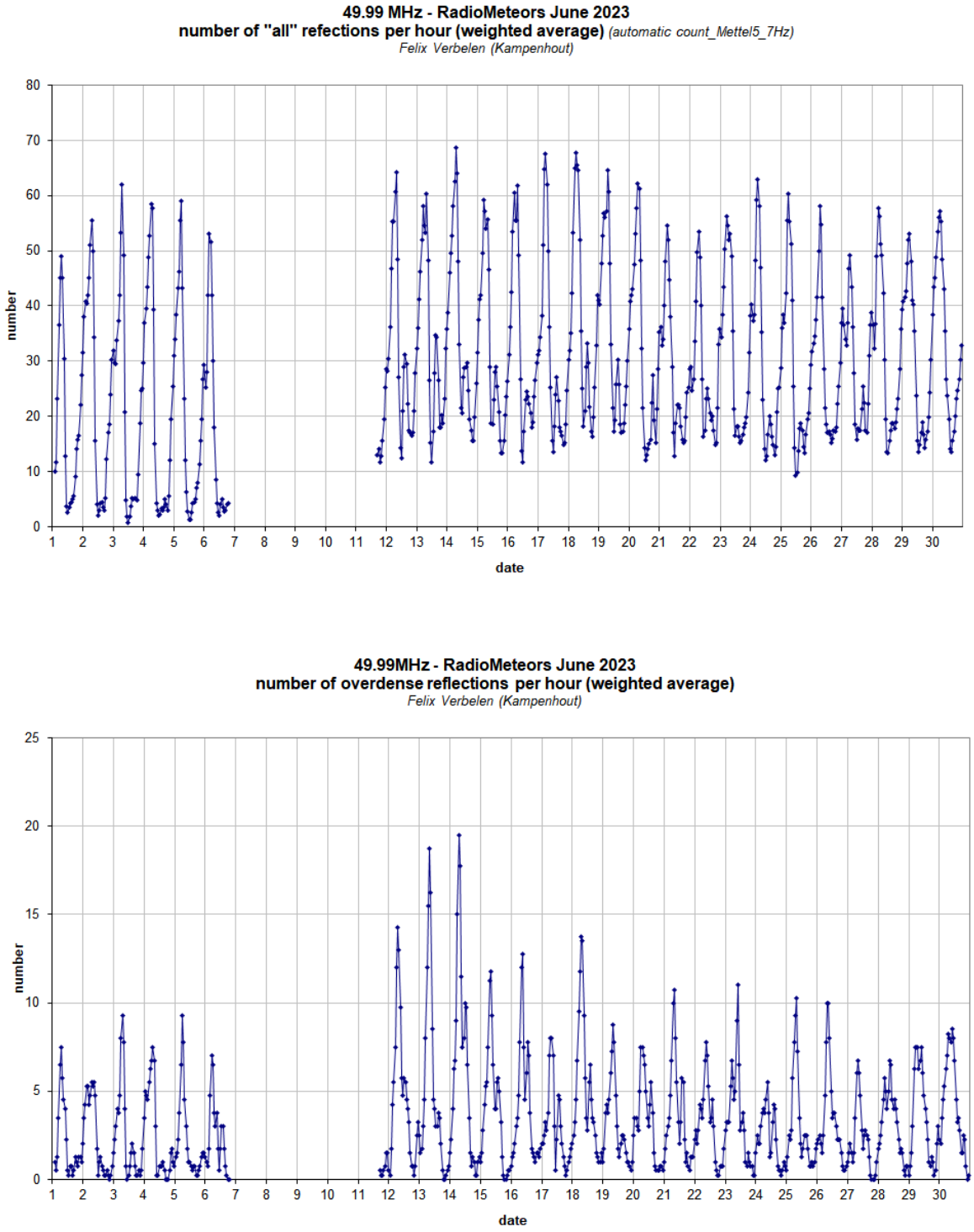

Figure 3 – The hourly numbers of "all" reflections counted automatically, and of manually counted "overdense" reflections, as observed here at Kampenhout (BE) on the frequency of our VVS-beacon (49.99 MHz) during June 2023.

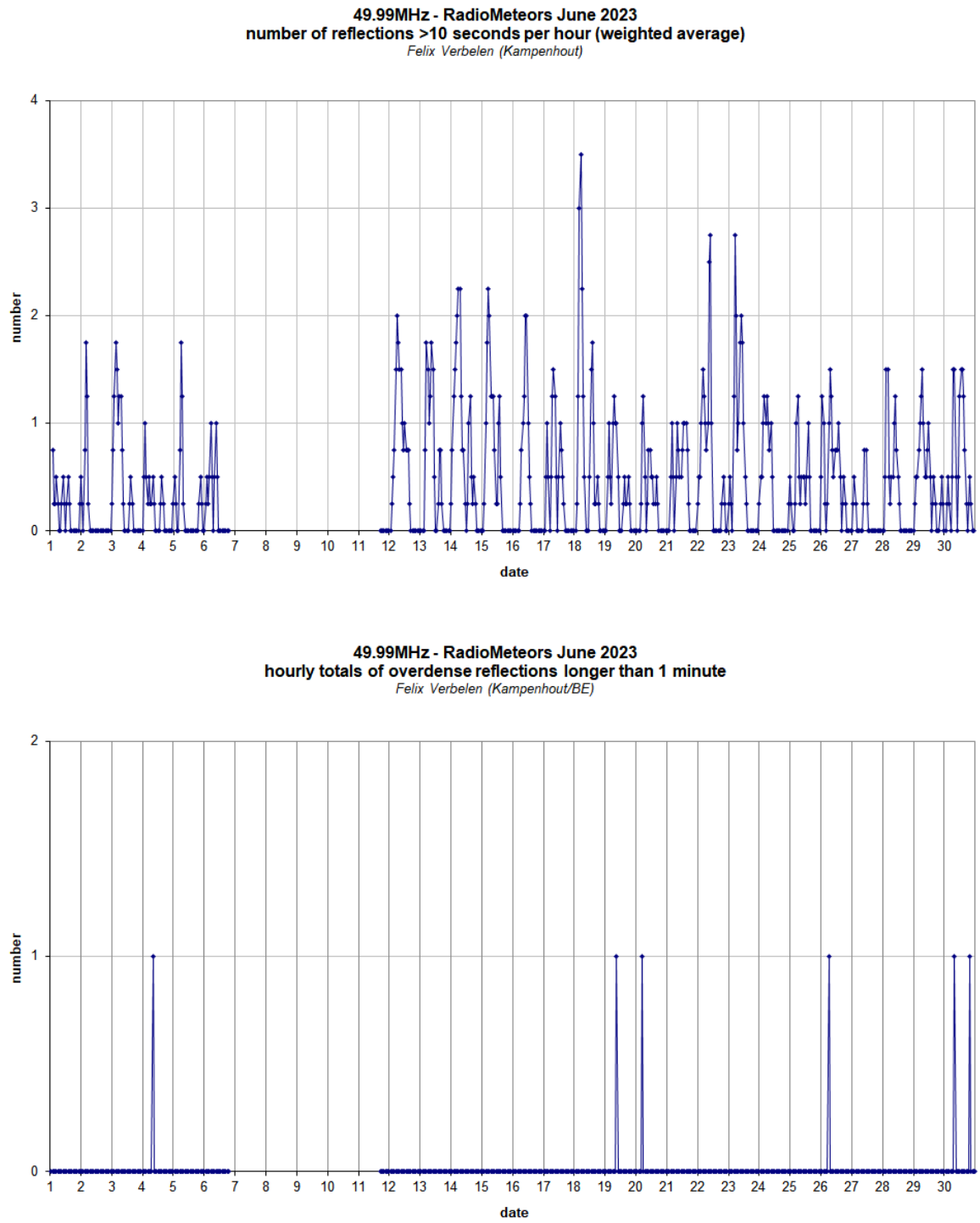

Figure 4 – The hourly numbers of overdense reflections longer than 10 seconds and longer than 1 minute, as observed here at Kampenhout (BE) on the frequency of our VVS-beacon (49.99 MHz) during June 2023.

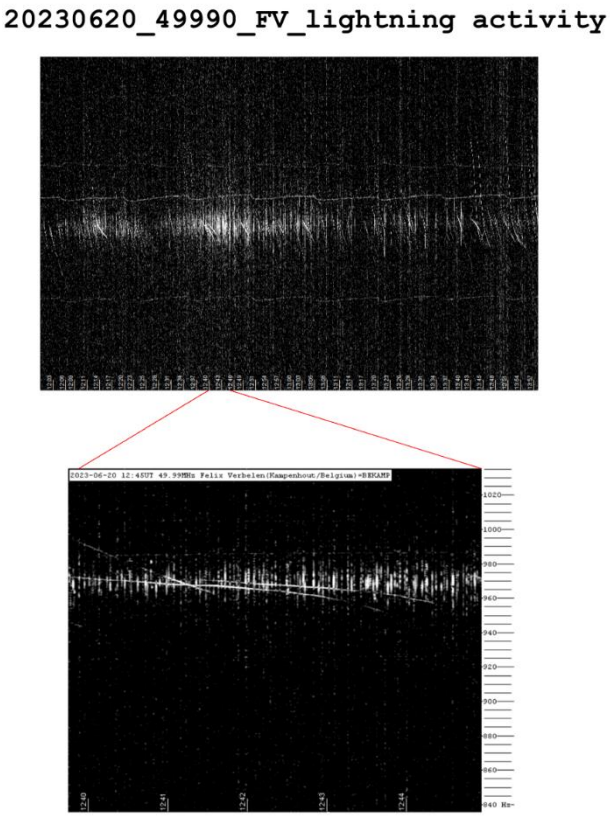

Figure 5 – Lightning on 20 June 2023.

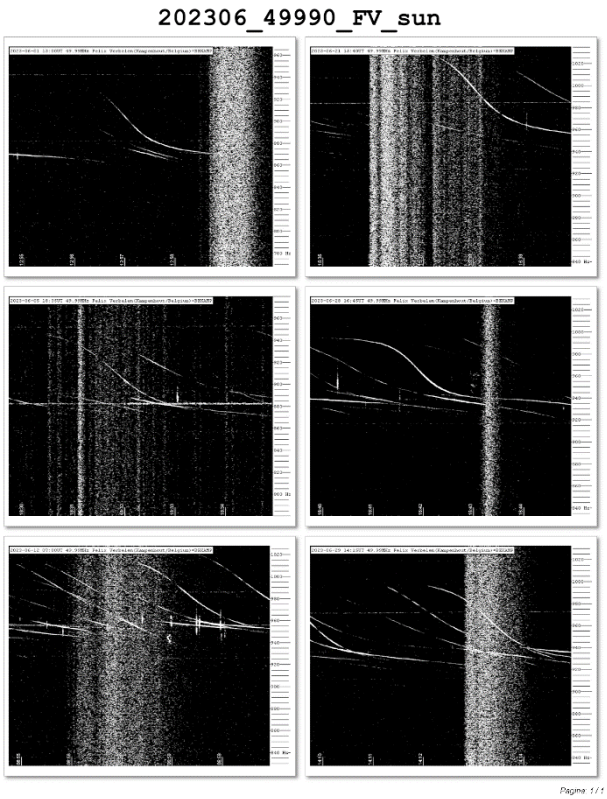

Figure 6 – Solar noise outburst in June 2023.

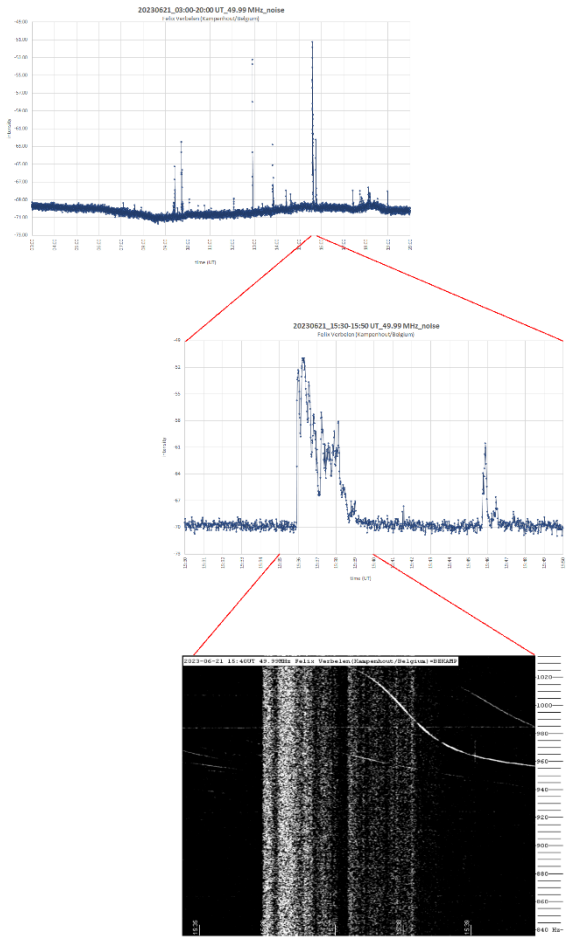

Figure 7 – Solar noise outburst 21 June 2023.

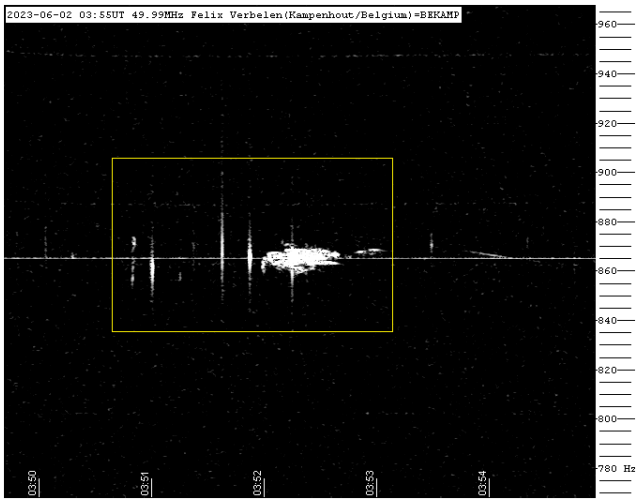

Figure 8 – Meteor echo 2 June 2023, $03^{h}55^{m}$ UT.

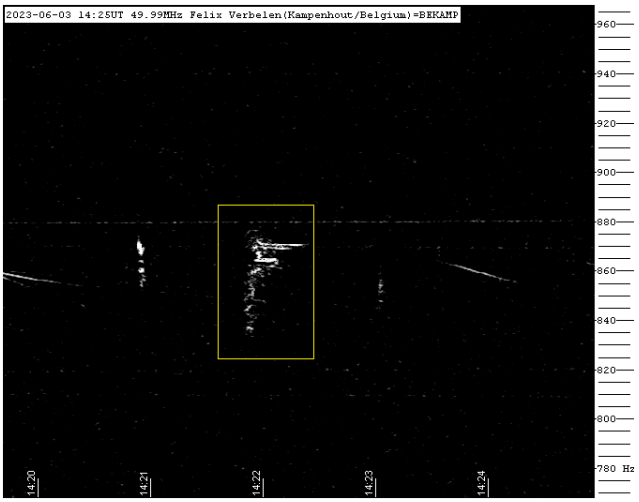

Figure 9 – Meteor echo 3 June 2023, 14^h25^m UT.

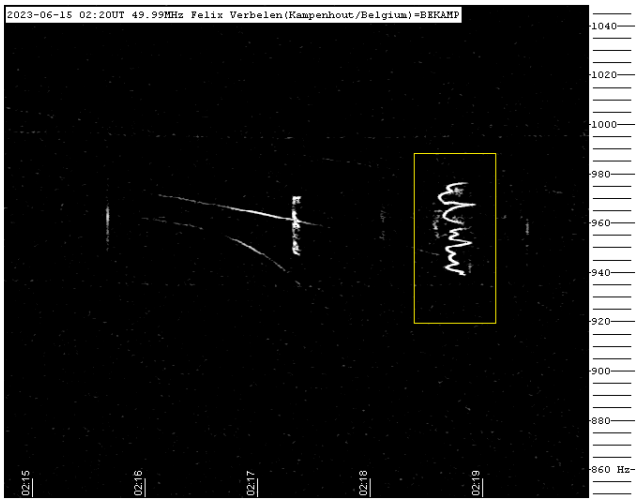

Figure 12 – Meteor echo 15 June 2023, 2^h20^m UT.

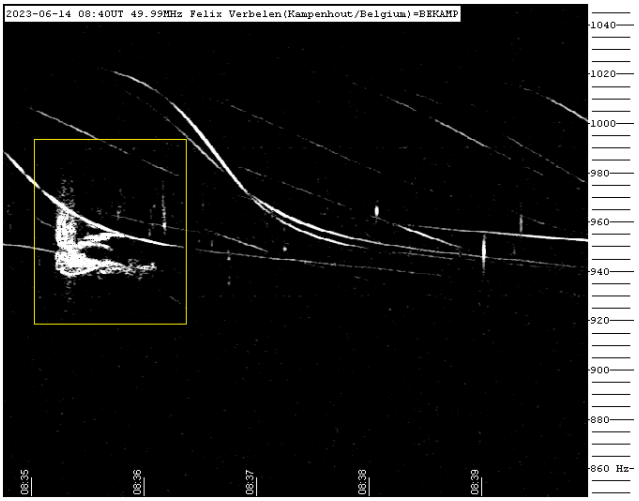

Figure 10 – Meteor echo 14 June 2023, 08^h40^m UT.

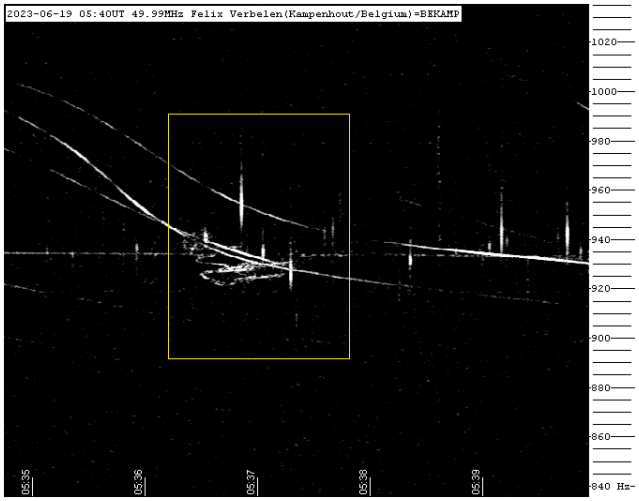

Figure 13 – Meteor echo 19 June 2023, 5^h40^m UT.

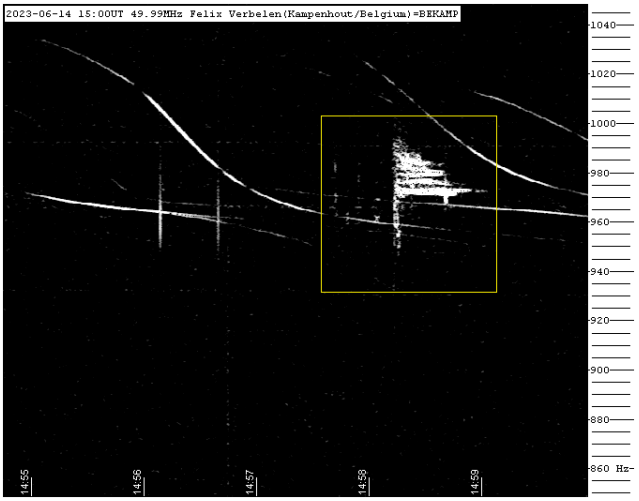

Figure 11 – Meteor echo 14 June 2023, 15^h00^m UT.

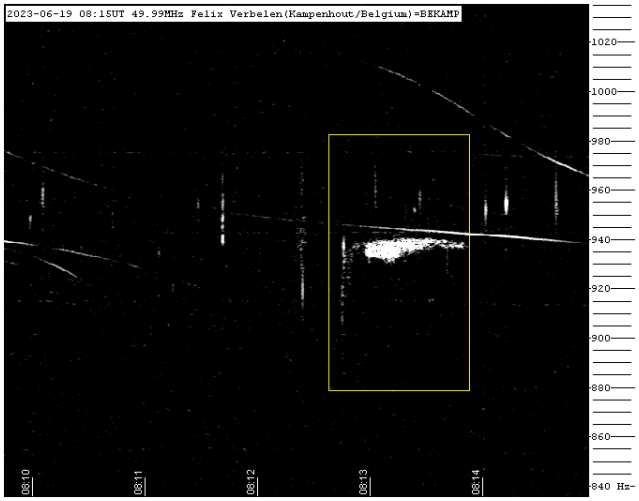

Figure 14 – Meteor echo 19 June 2023, 8^h15^m UT.

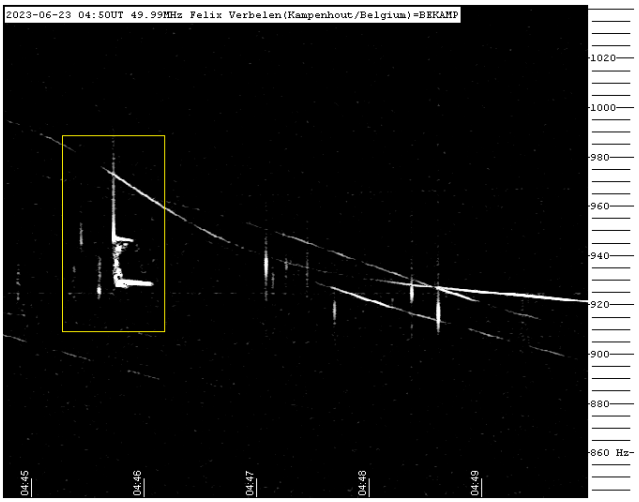

Figure 15 – Meteor echo 23 June 2023, 4^h50^m UT.

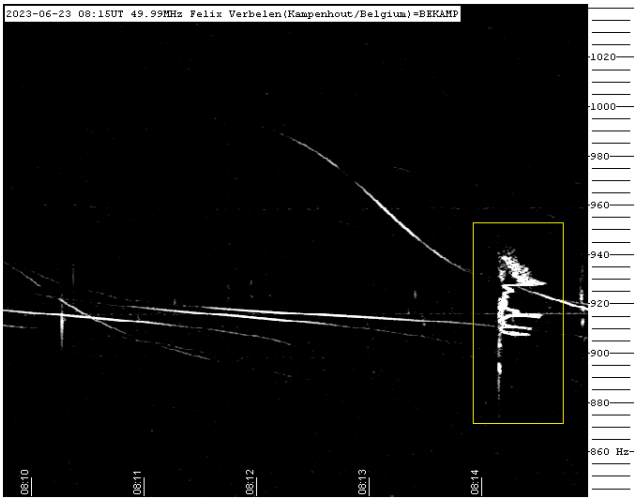

Figure 16 – Meteor echo 23 June 2023, 8^h15^m UT.

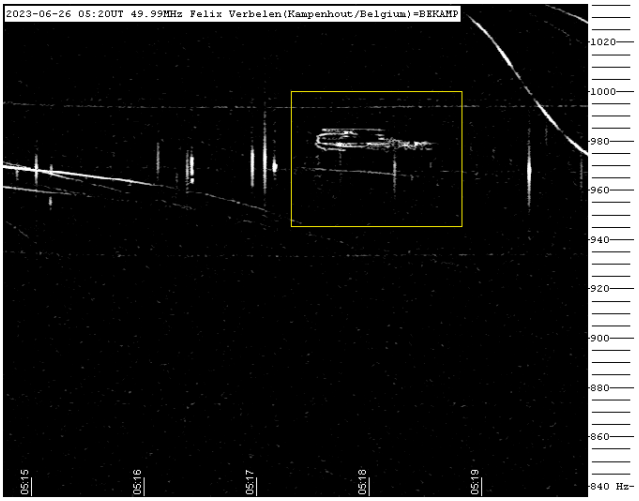

Figure 17 – Meteor echo 26 June 2023, 5^h20^m UT.

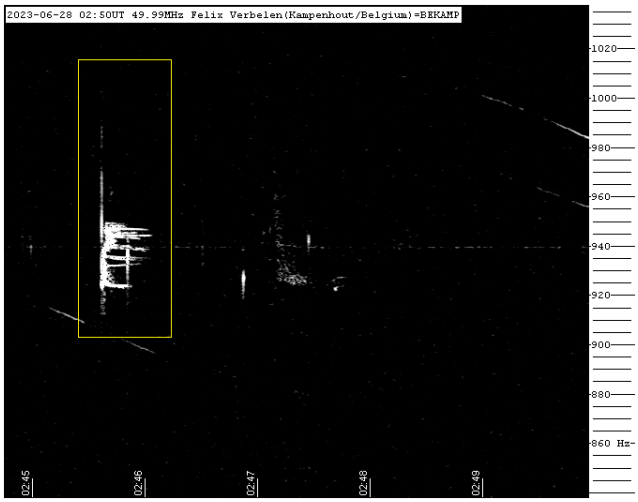

Figure 18 – Meteor echo 28 June 2023, 2^h50^m UT.

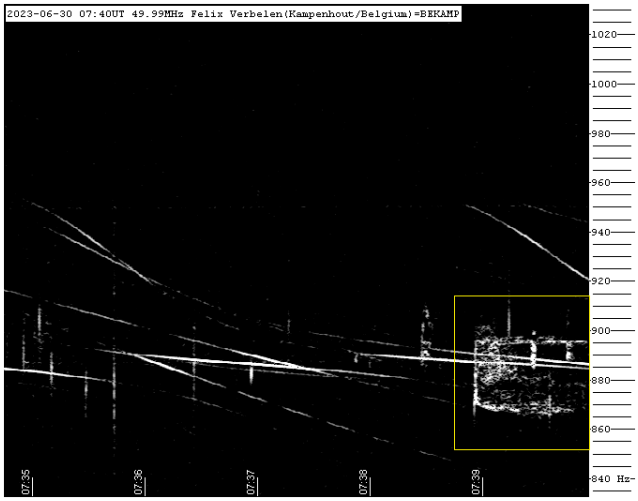

Figure 19 – Meteor echo 30 June 2023, 7^h40^m UT.

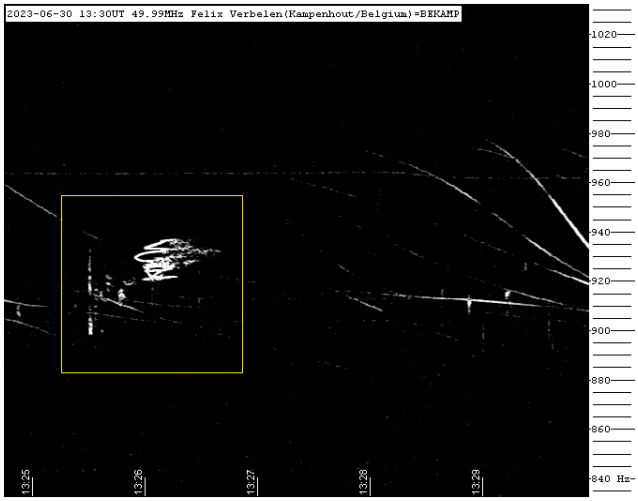

Figure 20 – Meteor echo 30 June 2023, 13^h30^m UT.

Radio meteors July 2023

Felix Verbelen

Vereniging voor Sterrenkunde & Volkssterrenwacht MIRA, Grimbergen, Belgium
felix.verbelen@skynet.be

An overview of the radio observations during July 2023 is given.

1 Introduction

The graphs show both the daily totals (*Figure 1 and 2*) and the hourly numbers (*Figure 3 and 4*) of "all" reflections counted automatically, and of manually counted "overdense" reflections, overdense reflections longer than 10 seconds and longer than 1 minute, as observed here at Kampenhout (BE) on the frequency of our VVS-beacon (49.99 MHz) during the month of July 2023.

The hourly numbers, for echoes shorter than 1 minute, are weighted averages derived from:

$$N(h) = \frac{n(h-1)}{4} + \frac{n(h)}{2} + \frac{n(h+1)}{4}$$

While local interference and unidentified noise remained low, on 11 days lighting activity was recorded here and solar activity produced strong noise almost daily. Some examples are attached (*Figure 5*).

General meteor activity was quite high, with some nice showers and a marked increase towards the end of the month.

Over the entire month, 8 reflections longer than 1 minute were observed. A selection of these is included along with some other interesting "epsilons" (*Figures 6 to 17*). Many more of these are available on request.

In addition to the usual graphs, you will also find the raw counts in cvs-format[19] from which the graphs are derived. The table contains the following columns: day of the month, hour of the day, day + decimals, solar longitude (epoch J2000), counts of "all" reflections, overdense reflections, reflections longer than 10 seconds and reflections longer than 1 minute, the numbers being the observed reflections of the past hour.

[19] https://www.meteornews.net/wp-content/uploads/2023/08/202307_49990_FV_rawcounts.csv

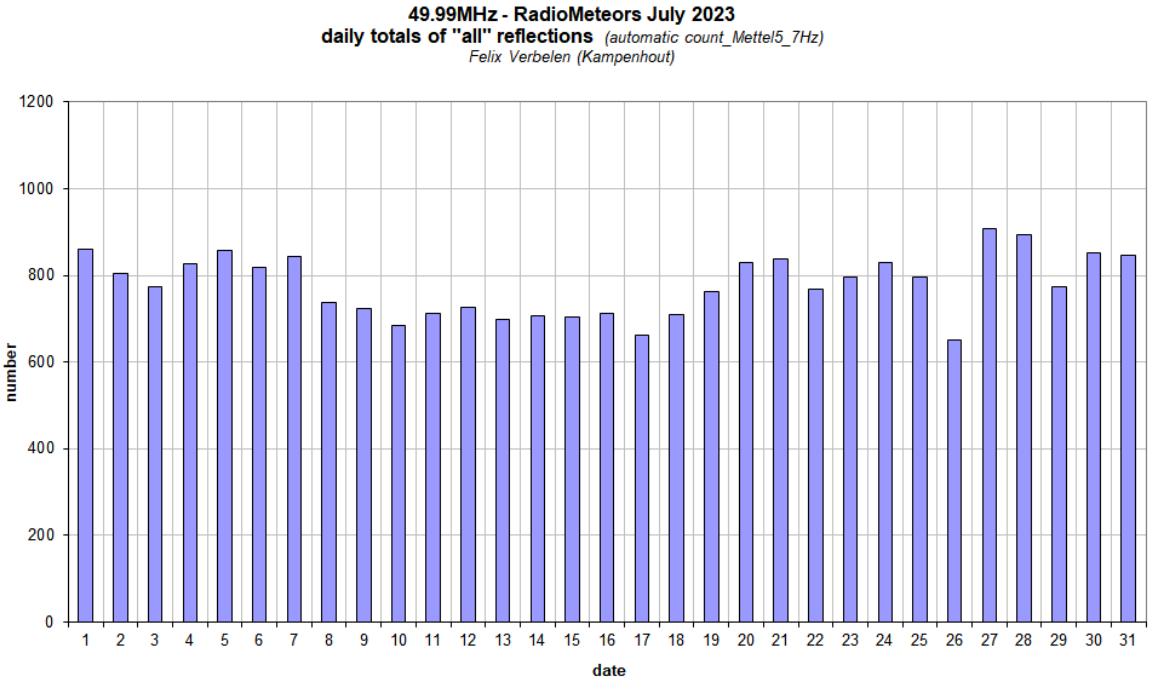

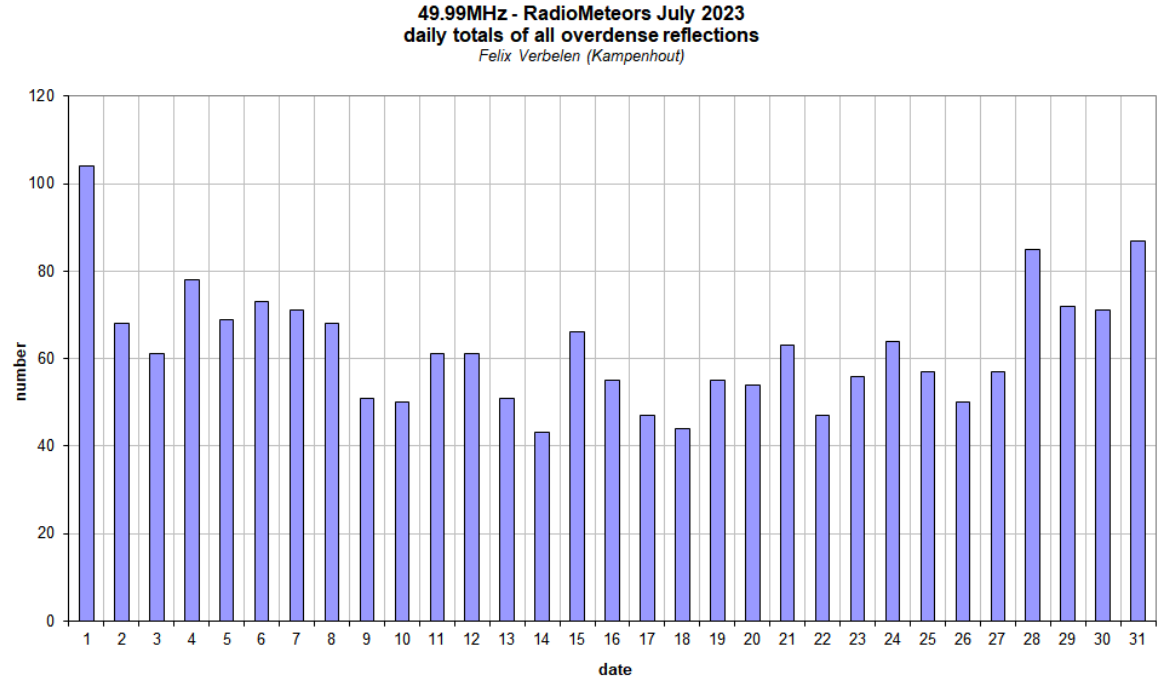

Figure 1 – The daily totals of "all" reflections counted automatically, and of manually counted "overdense" reflections, as observed here at Kampenhout (BE) on the frequency of our VVS-beacon (49.99 MHz) during July 2023.

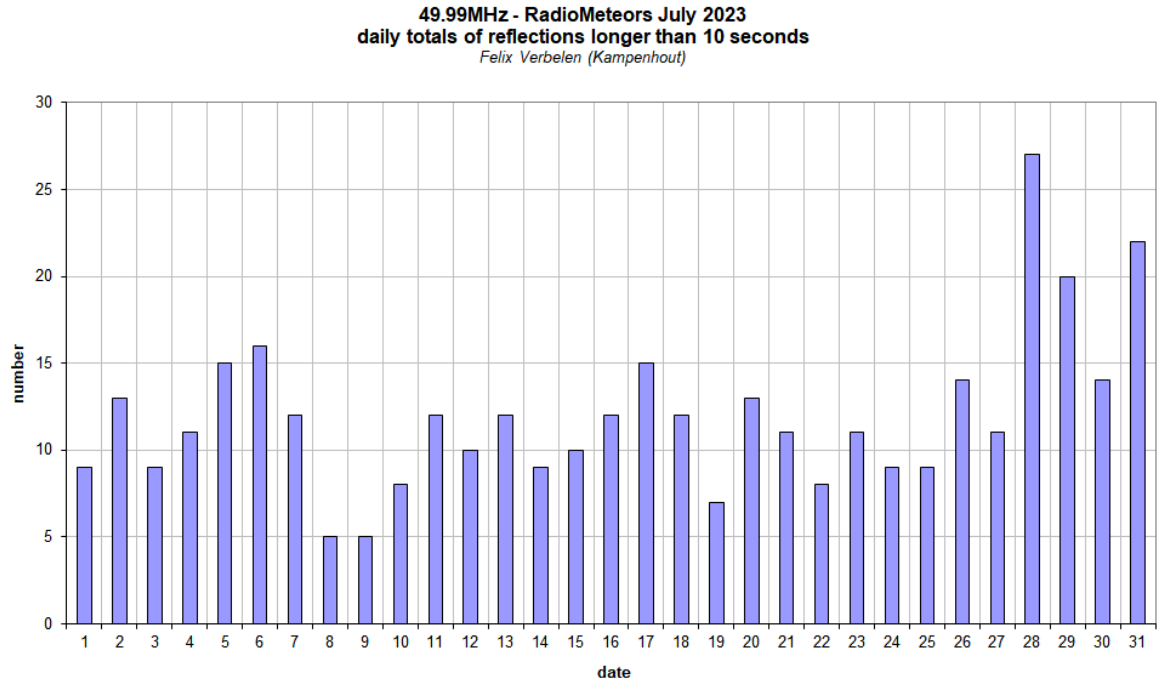

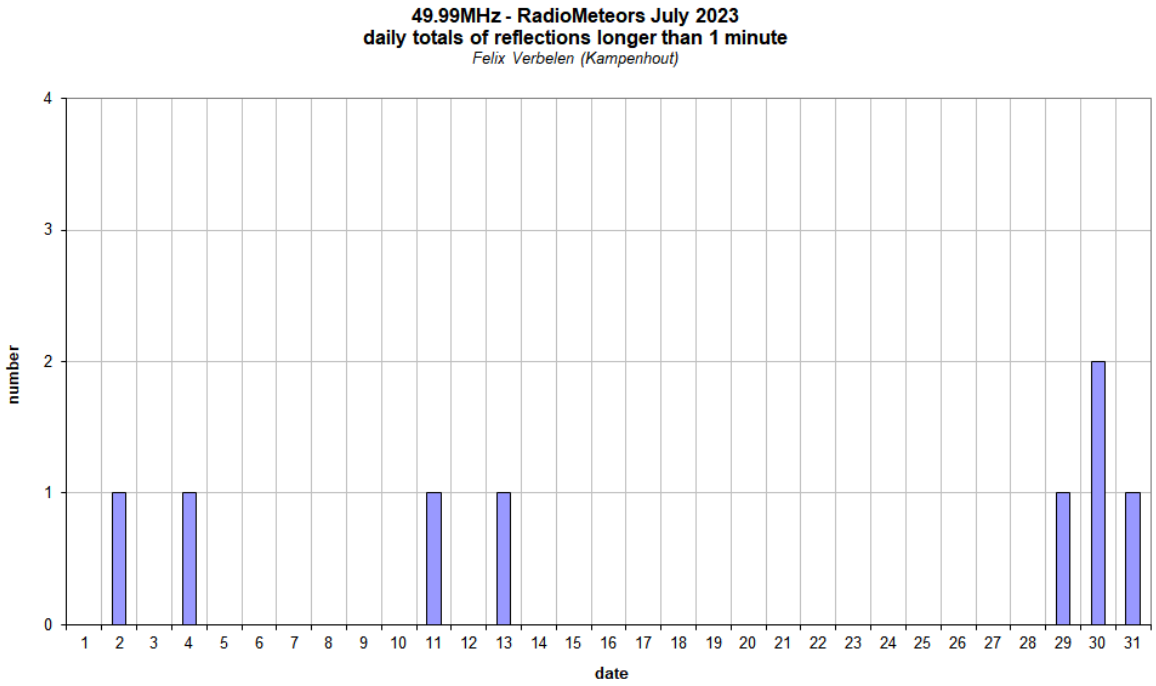

Figure 2 – The daily totals of overdense reflections longer than 10 seconds and longer than 1 minute, as observed here at Kampenhout (BE) on the frequency of our VVS-beacon (49.99 MHz) during July 2023.

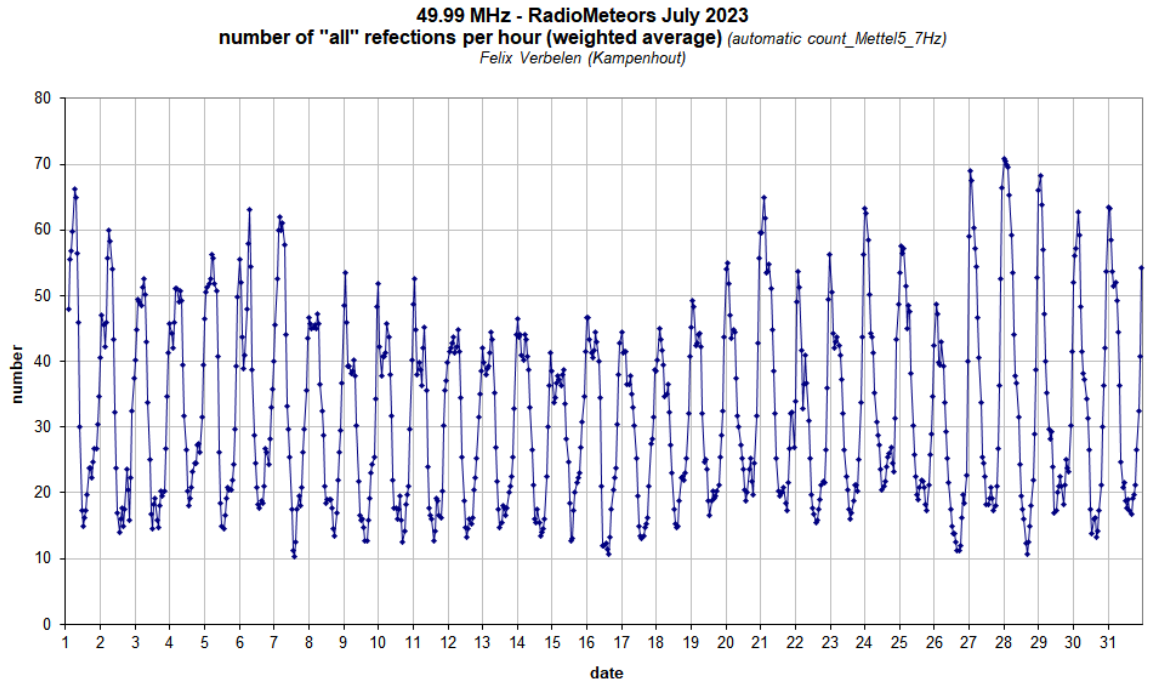

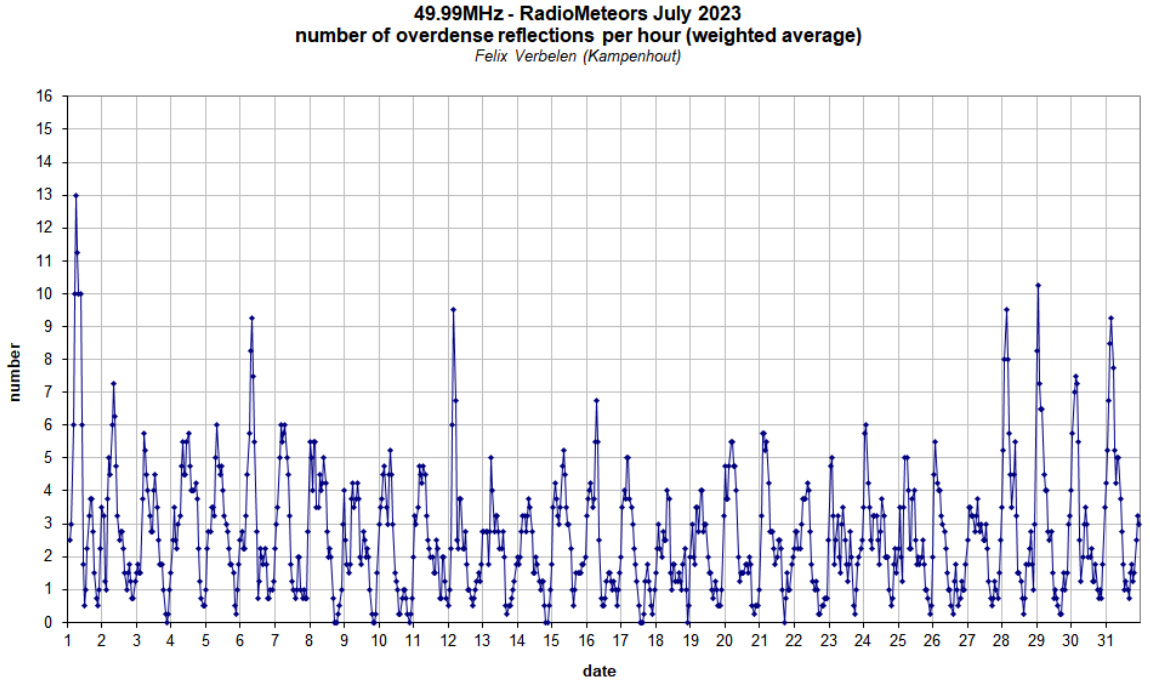

Figure 3 – The hourly numbers of "all" reflections counted automatically, and of manually counted "overdense" reflections, as observed here at Kampenhout (BE) on the frequency of our VVS-beacon (49.99 MHz) during July 2023.

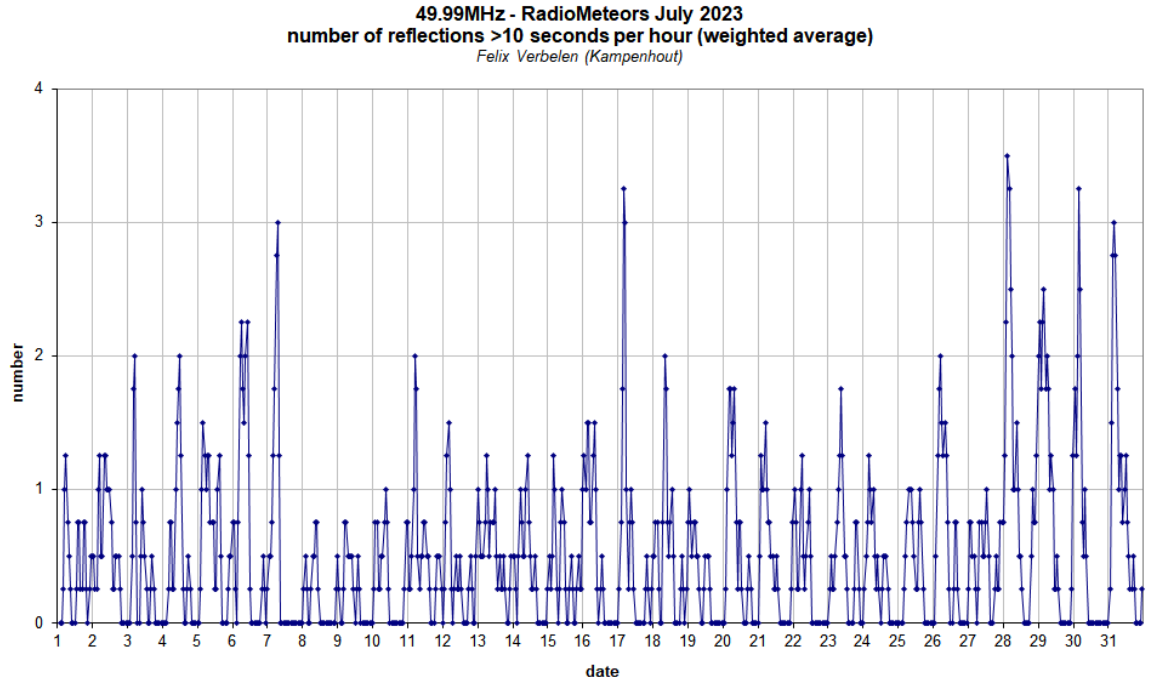

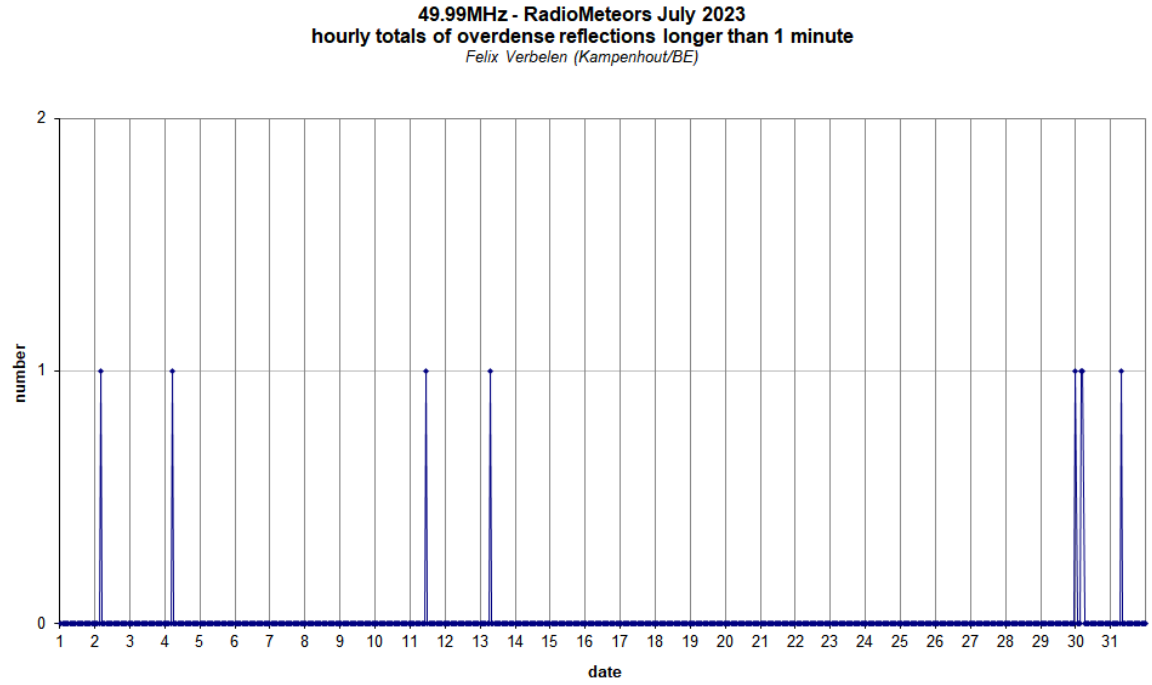

Figure 4 – The hourly numbers of overdense reflections longer than 10 seconds and longer than 1 minute, as observed here at Kampenhout (BE) on the frequency of our VVS-beacon (49.99 MHz) during July 2023.

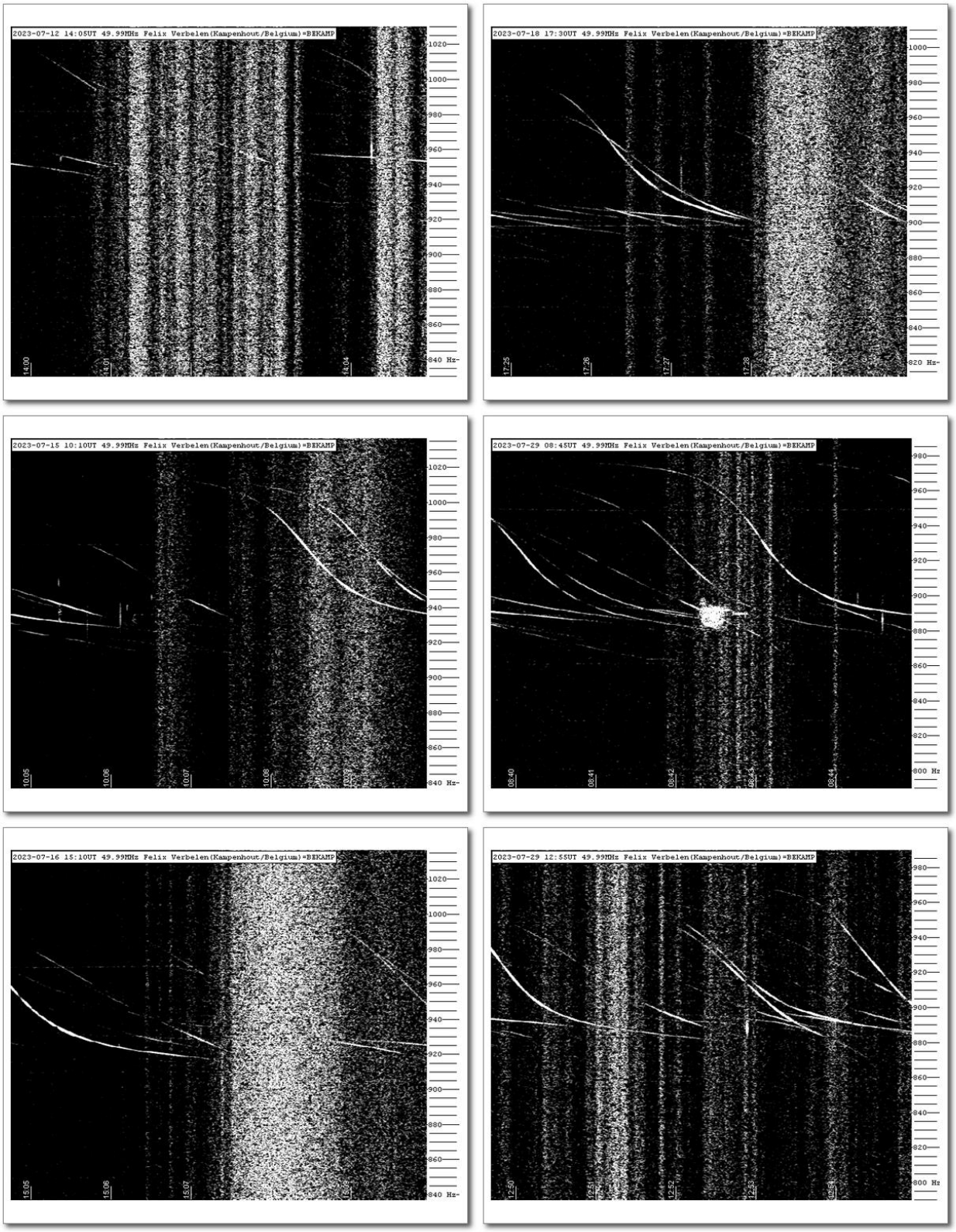

Figure 5 – Solar noise outbursts in July 2023.

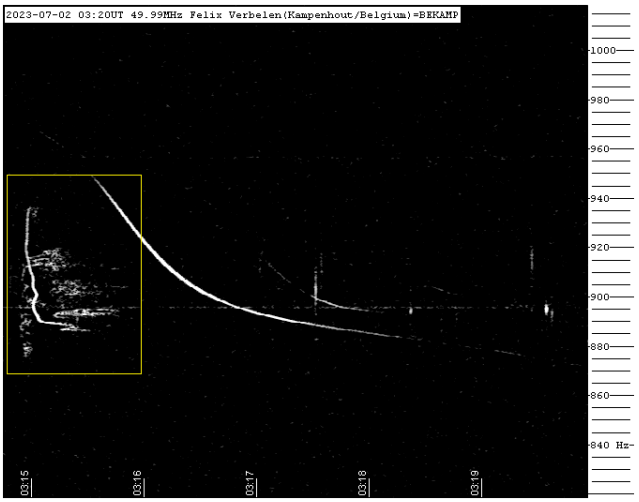

Figure 6 – Meteor echo 2 July 2023, 3^h20^m UT.

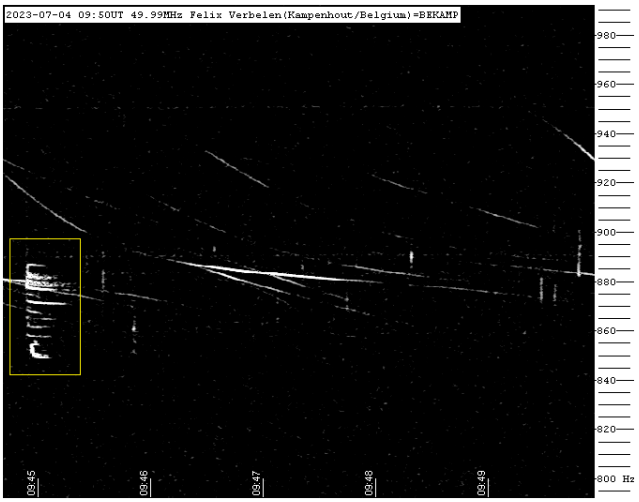

Figure 7 – Meteor echo 4 July 2023, 9^h50^m UT.

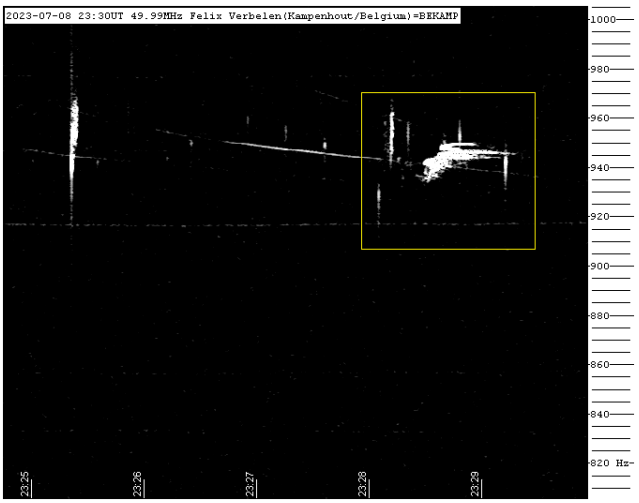

Figure 8 – Meteor echo 8 July 2023, 23^h30^m UT.

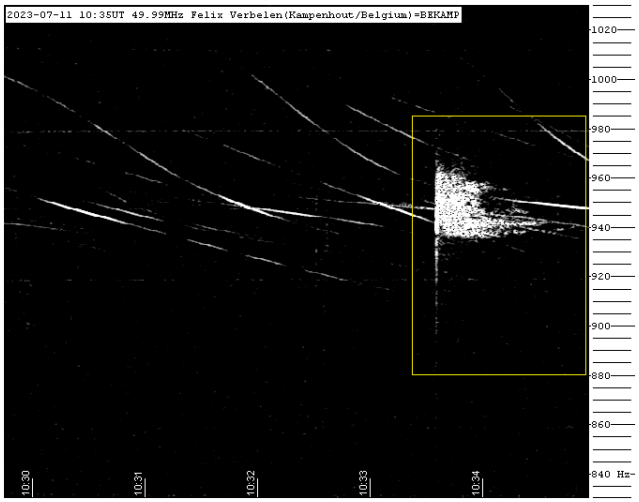

Figure 9 – Meteor echo 11 July 2023, 10^h35^m UT.

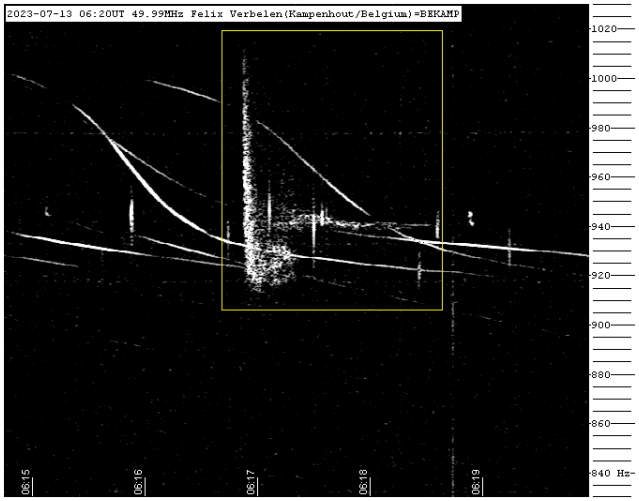

Figure 10 – Meteor echo 13 July 2023, 6^h20^m UT.

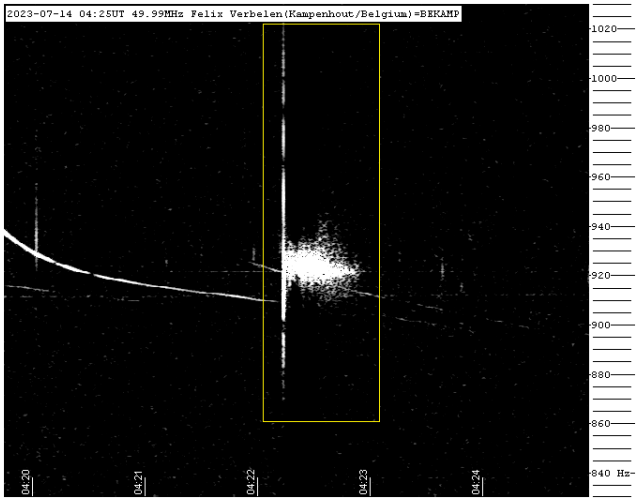

Figure 11 – Meteor echo 14 July 2023, 4^h25^m UT.

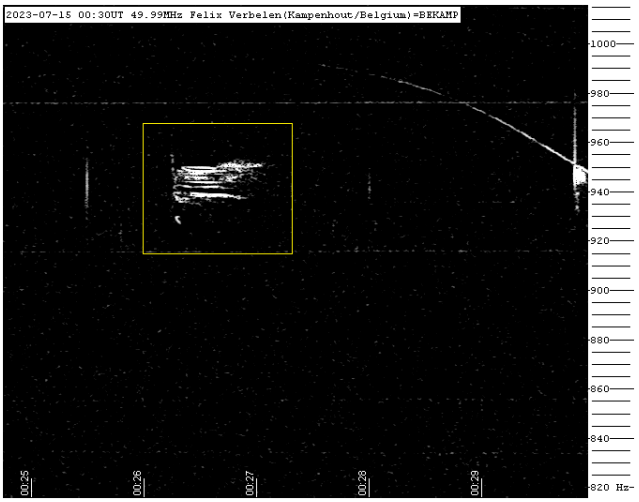

Figure 12 – Meteor echo 15 July 2023, 0^h30^m UT.

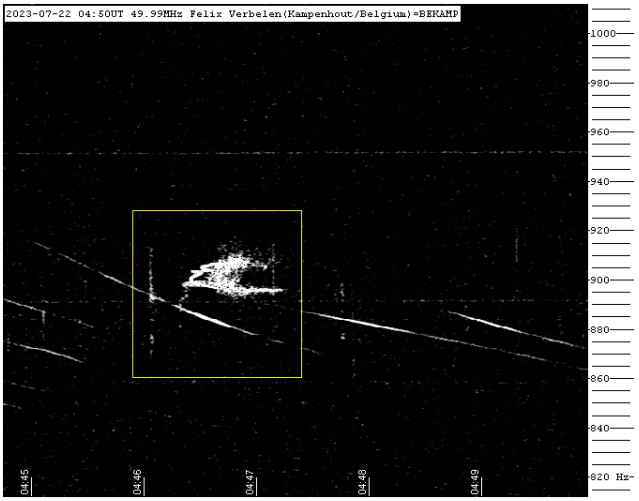

Figure 13 – Meteor echo 22 July 2023, 4^h50^m UT.

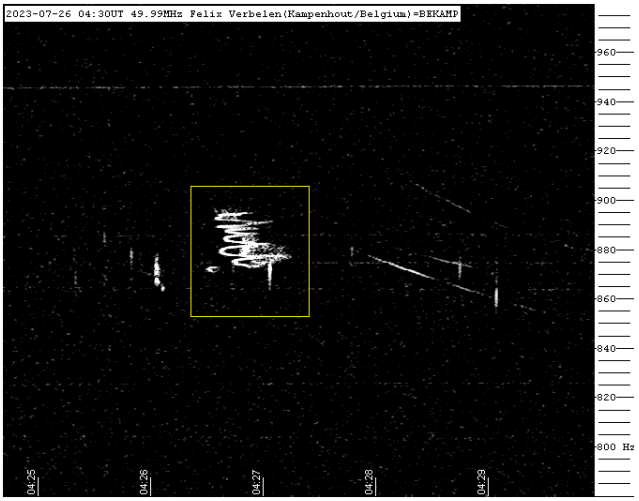

Figure 14 – Meteor echo 26 July 2023, 4^h30^m UT.

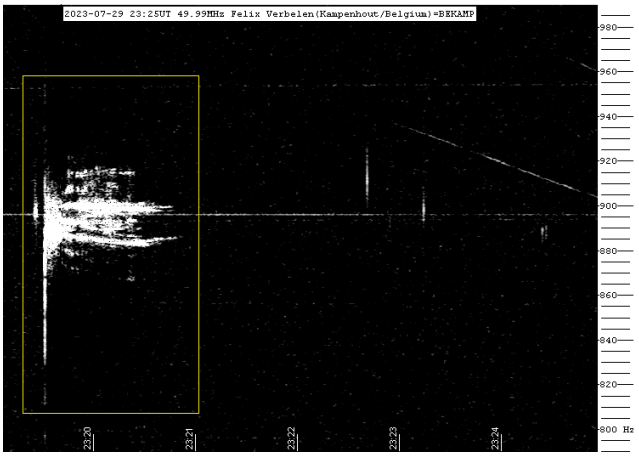

Figure 15 – Meteor echo 29 July 2023, 23^h25^m UT.

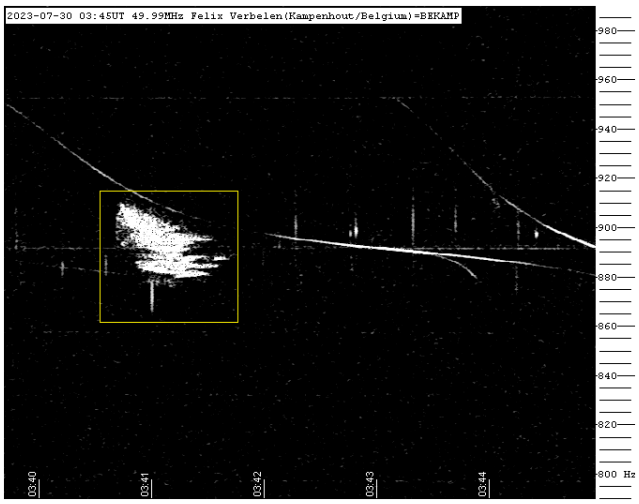

Figure 16 – Meteor echo 30 July 2023, 3^h45^m UT.

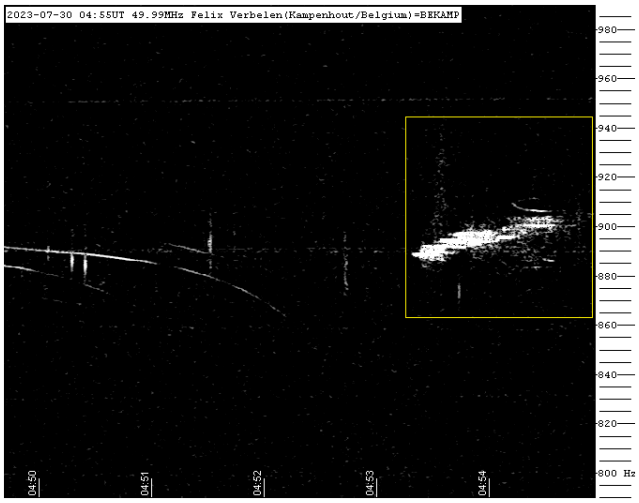

Figure 17 – Meteor echo 30 July 2023, 4^h55^m UT.

The mission of MeteorNews is to offer fast meteor news to a global audience, a swift exchange of information in all fields of active amateur meteor work without editing constraints. MeteorNews is freely available without any fees.

You are welcome to contribute to MeteorNews on a regular or casual basis, if you wish to. Anyone can become an author or editor, send an email to us. For more info read: https://meteornews.net/writing-content-for-emeteornews/

MeteorNews account manager: Richard Kacerek <rickzkm@gmail.com>.

The running costs for website hosting are covered by a team of sponsors. We want to thank the 2022-2023 sponsors: Anonymous (3x), Mikhail Bidnichenko, Gaetano Brando, TomB, Trevor C, Nigel Cunnington, Richard Glassner, Kevin Heider, Paul Hyde, K. Jamrogowicx, Dave Jones, Richard Kacerek, Richard Lancaster, Joseph Lemaire, Mark McIntyre, Hiroshi Ogawa, Paul Mohan, Stan Nelson, Lubos Neslusan, BillR, Whitham D. Reeve, John Schlin, Ann Schroyens and Denis Vida.

Contributing to this issue:

- de Ponthiere P.
- Dijkema T. J.
- Dörr J.
- Glässner U.
- Gloudemans R.
- Greaves J.
- Habraken K.
- Johannink C.
- Kacerek R.
- Koseki M.
- Lamy H.
- Masson J.
- Miskotte K.
- Ogawa H.
- Rau S.
- Roggemans P.
- Šegon D.
- Sugimoto H.
- Verbelen F.
- Vida D.

ISSN 2570-4745 Online publication https://meteornews.net

Listed and archived with ADS Abstract Service: https://ui.adsabs.harvard.edu/search/q=eMetN

MeteorNews Publisher:

Valašské Meziříčí Observatory, Vsetínská 78, 75701 Valašské Meziříčí, Czech Republic